

University of Montana

## ScholarWorks at University of Montana

---

Graduate Student Theses, Dissertations, &  
Professional Papers

Graduate School

---

2004

### The host inflammatory response to a xenograft arterial bypass in a rabbit model

Albert C. Grobe  
*The University of Montana*

Follow this and additional works at: <https://scholarworks.umt.edu/etd>

**Let us know how access to this document benefits you.**

---

#### Recommended Citation

Grobe, Albert C., "The host inflammatory response to a xenograft arterial bypass in a rabbit model" (2004). *Graduate Student Theses, Dissertations, & Professional Papers*. 9511.  
<https://scholarworks.umt.edu/etd/9511>

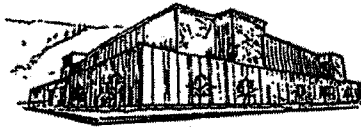
This Dissertation is brought to you for free and open access by the Graduate School at ScholarWorks at University of Montana. It has been accepted for inclusion in Graduate Student Theses, Dissertations, & Professional Papers by an authorized administrator of ScholarWorks at University of Montana. For more information, please contact [scholarworks@mso.umt.edu](mailto:scholarworks@mso.umt.edu).

# NOTE TO USERS

This reproduction is the best copy available.

**UMI**<sup>®</sup>





**Maureen and Mike  
MANSFIELD LIBRARY**

The University of  
**Montana**

---

Permission is granted by the author to reproduce this material in its entirety,  
provided that this material is used for scholarly purposes and is properly  
cited in published works and reports.

**\*\*Please check "Yes" or "No" and provide signature\*\***

Yes, I grant permission

No, I do not grant permission

Author's Signature:

Date:

08/31/04

Any copying for commercial purposes or financial gain may be undertaken  
only with the author's explicit consent.

---



The Host Inflammatory Response to a Xenograft Arterial Bypass in a Rabbit Model

By

Albert C. Grobe

B.A. The University of Montana, 1990

M.S. The University of Montana, 1995

presented in partial fulfillment of the requirements

for the degree of

Doctorate of Philosophy

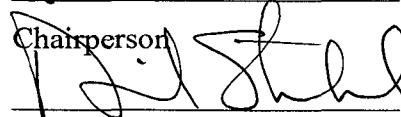
The University of Montana

August 2004

Approved by:



Chairperson



Dean, Graduate School

8/30/04

Date

UMI Number: 3139039

### INFORMATION TO USERS

The quality of this reproduction is dependent upon the quality of the copy submitted. Broken or indistinct print, colored or poor quality illustrations and photographs, print bleed-through, substandard margins, and improper alignment can adversely affect reproduction.

In the unlikely event that the author did not send a complete manuscript and there are missing pages, these will be noted. Also, if unauthorized copyright material had to be removed, a note will indicate the deletion.

**UMI**<sup>®</sup>

---

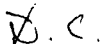
UMI Microform 3139039

Copyright 2004 by ProQuest Information and Learning Company.

All rights reserved. This microform edition is protected against unauthorized copying under Title 17, United States Code.

ProQuest Information and Learning Company  
300 North Zeeb Road  
P.O. Box 1346  
Ann Arbor, MI 48106-1346

The Host Inflammatory Response to a Xenograft Arterial Bypass in a Rabbit Model

Director: David T. Cheung, Ph.D. 

Cardiovascular disease is the leading cause of death in the United States. In a six year period, 12.9 million people were diagnosed with coronary heart disease with 515,204 deaths. When non-invasive treatments are insufficient, coronary bypass surgery is necessary. Many graft options are available but not all are suitable as coronary bypass grafts.

This study was designed to evaluate the effect of the host inflammatory response toward the Corograft™ xenograft conduit material implanted in the arterial circulation. The rabbit model developed is useful for the evaluation of small-diameter biological grafts when implanted into the abdominal aorta, and the inflammatory response could be increased via hypercholesterolemia or decreased via anti-inflammatory drug treatments.

Normal diet rabbits survive the surgery, maintain patent grafts for up to 6 months which are recolonized by host cells. Hypercholesterolemic rabbits had an elevated post-operative mortality and aneurysm formation was seen in several rabbits, which was attributed to hypercholesterolemia. Macrophages are increased, and can secrete matrix degrading enzymes, leading to an increased inflammatory response leading to observed aneurysm formation.

These grafts elicit a chronic-type inflammatory response allowing this model to be used to study the effect of anti-inflammatory drugs. Grafts from drug-treatment samples were partially recolonized by host cells and no aneurysm development was seen in any of these samples. Both Indomethacin and Etidronate reduced overall macrophage numbers compared to saline controls while the humoral response was not reduced.

These data suggest that macrophages, as part of an inflammatory response, may play a role in vascular graft failure, and anti-inflammatory treatments reduce the host response toward the graft material. This indicates that anti-inflammatory treatments after bypass grafting could be important in the long-term survival of grafts in the clinical setting. These data could also lead to further modifications of the original graft material during production, leading to a product with superior resistance to inflammatory degradation.



## Table of Contents

	Page
<b>Title Page</b>	i
<b>Abstract</b>	ii
<b>Table of Contents</b>	iii
<b>List of Abbreviations</b>	vii
<b>List of Tables</b>	x
<b>List of Illustrations</b>	xi
<b>Acknowledgments</b>	xiii
<b>Background</b>	
Cardiovascular and Coronary Heart Disease	1
Coronary Graft Options: Advantages, Disadvantages and Limitations	2
Vascular grafts: Clinical and Experimental	5
General Conclusions on Graft Options	9
Xenograft Developed at IHI (Corograft™)	10
<b>Chapter I Development of the Animal model</b>	
<b>Introduction</b>	
Choice of Animal Model	12
Rabbit Model	13
Surgical Model - Location of Implantation	13
Specific Aim	14
Rationale	14
Experimental design	15
<b>Materials and Methods</b>	
Animal Source and Care	16
Preoperative Preparation	16
Surgical Protocol	17
<b>Results</b>	
Pilot group	20

	Page
<b>Discussion</b>	
Rabbit Model	23
Abdominal Aorta	23
Hypothermia and Cross-Clamp Time	24
Anastomosis	26
Graft Length	27
Graft Performance: Corograft™ vs. Other Graft Options	27
Conclusions	29
<b>Literature Cited</b>	30
<b>Chapter II The effect of an increased inflammatory response on graft survival</b>	
<b>Introduction</b>	
Inflammation	38
Modes of Graft Failure	39
Intimal Hyperplasia	39
Atherosclerosis	41
Aneurysms	42
The Role of Inflammation in Vascular Diseases	43
Models of Human Disease	44
Increasing Inflammation via Hypercholesterolemia	44
Specific Aim	46
Rationale	46
Experimental Design	47
<b>Materials and Methods</b>	
Animal Source and Care	48
Preoperative Preparation	48
Surgical Protocol	49
Sacrifice	51
Macroscopic Examination	51
Histology	52
Immunohistology	52
Macrophage Counts	53
Zymography	54
ELISA for Humoral Response	55
<b>Results</b>	
Post-Operative Survival and Graft <b>Patency</b>	57
Normal diet samples macroscopic	58
Un-Implanted Graft Histology	58
Histology of Explanted Samples from Normal diet Rabbits	65
Cholesterol-diet samples macroscopic	83
Cholesterol diet Macroscopic Aneurysm samples	90
Cholesterol-diet Histology	90

	<b>Page</b>
Macrophage Counts	93
Zymography	101
Humoral ELISA	101
<b>Discussion</b>	
Effects of Atherosclerosis	112
Normal diet rabbits	113
Cholesterol diet rabbits	113
The effects of hypercholesterolemia on the graft	114
Graft durability in an atherosclerotic rabbit model	115
Conclusions	116
<b>Appendix</b>	118
<b>Literature Cited</b>	122
<b>Chapter III The effect of a decreased inflammatory response on graft survival</b>	
<b>Introduction</b>	
Inflammation	133
Indomethacin	134
Etidronate	135
Specific Aim	136
Rationale	136
Experimental Design	137
<b>Materials and Methods</b>	
Animal Source and Care	138
Drug Administration	138
Preoperative Preparation	139
Surgical Protocol	139
Sacrifice	142
Macroscopic Examination	142
Histology	142
Immunohistology	143
Macrophage Counts	144
Zymography	144
ELISA for Humoral Response	145
<b>Results</b>	
Post-Operative Survival	147
Drug Treated Groups Macroscopic	147
Histology	147
Macrophage Counts	174
Zymography	174
Humoral ELISA	181

	Page
<b>Discussion</b>	
Reduce Inflammation: Effect of Anti-Inflammatory Drugs	192
Indomethacin	193
Etidronate	193
Zymography	194
Humoral response	194
Conclusions	195
<b>Appendix</b>	197
<b>Literature Cited</b>	205

## List of Abbreviations

AAA	Abdominal Aortic Aneurysm
ATP	Adenosine Triphosphate
AV-Fistula	Arterio-Venous Fistula
BID	Twice Daily
BSA	Bovine Serum Albumin
CABG	Coronary Artery Bypass Grafting
CHD	Coronary Heart Disease
COX	Cyclooxygenase
CVD	Cardiovascular Disease
ECM	Extracellular Matrix
ELISA	Enzyme Linked Immunosorbent Assay
ePTFE	Expanded PTFE
EtOH	Ethanol, Ethyl Alcohol
Fem-Pops	Femoral-Popliteal Graft
H <sub>2</sub> O <sub>2</sub>	Hydrogen Peroxide
H <sub>2</sub> SO <sub>4</sub>	Sulfuric Acid
HRP	Horseradish Peroxidase
ICAM-1	Intercellular Adhesion Molecule 1
ID	Internal Diameter
IL-1	Interleukin 1
IL-2R	Interleukin 2 Receptor
LAD	Left Anterior Descending, Coronary Artery

LDL	Low Density Lipoprotein
MCP-1	Monocyte Chemotactic Protein 1
MIP	Macrophage Inflammatory Protein
MMP	Matrix Metalloproteinase/Metalloprotease
MT-MMP	Membrane-Type Matrix Metalloproteinase
MW	Molecular Weight
NO	Nitric Oxide
NSAID	Non-Steroidal Anti-Inflammatory Drug
OPD	1,2-phenylenediamine dihydrochloride, HRP substrate
PAI	Plasminogen Activator Inhibitor
PET	Polyethylene Terephthalate, Dacron <sup>®</sup>
PGE2	Prostaglandin E2
pro-uPA	Pro-Urokinase-type Plasminogen Activator
PTCA	Percutaneous Transluminal Coronary Angioplasty
PTFE	Polytetrafluoroethylene, Teflon <sup>®</sup>
RAM 11	Rabbit Alveolar Macrophage, Rabbit-specific Macrophage Antibody
SC	Subcutaneous
SDS-PAGE	Sodium Dodecyl Sulfate-Polyacrylamide Gel Electrophoresis
SMC	Smooth Muscle Cell
TGF $\beta$	Transforming Growth Factor $\beta$
TIMP	Tissue Inhibitor of Metalloproteinase
TNF $\alpha$	Tumor Necrosis Factor $\alpha$
TTV	Thrombotic Threshold Velocity

uPA	Urokinase-type Plasminogen Activator
uPA-r	Urokinase Plasminogen Activator Receptor
VCAM-1	Vascular Cell Adhesion Molecule 1
VWF	von Willebrand Factor, an endothelial cell marker

## List of Tables

		Page
Table 1	Mean Flow	4
Table 2	Valid Animals	22
Table 3	Macrophage Counts - Diet	103
Table 4	ELISA of 2, 4 and 6 Month Samples - Diet	107
Table 5	Compiled Results of 2, 4 and 6 Month Samples - Diet	111
Table 6	Surgery and Sacrifice Data - Diet	119
Table 7	Sacrifice - Diet	121
Table 8	Macrophage Counts - Drug Treatment	183
Table 9	ELISA - Drug Treatment	187
Table 10	Compiled Results - Drug Treatment	191
Table 11	Surgery and Sacrifice Data – Drug Treatment	201
Table 12	Sacrifice - Drug Treatment	203



## List of Illustrations

		Page
Figure 1-1	2Mo Macroscopic	60
Figure 1-2	4Mo Macroscopic	62
Figure 1-3	6Mo Macroscopic	64
Figure 2	Corograft Histology	67
Figure 3-1	2Mo Histology - H&E	70
Figure 3-2	2Mo Histology – Actin	72
Figure 3-3	2Mo Histology – Trichrome	74
Figure 4-1	4Mo Histology - H&E	78
Figure 4-2	4Mo Histology – Actin	80
Figure 4-3	4Mo Histology – Trichrome	82
Figure 5-1	6Mo Histology - H&E	85
Figure 5-2	6Mo Histology – Actin	87
Figure 5-3	6Mo Histology – Trichrome	89
Figure 6	Cholesterol Diet and Aneurysm Samples Macroscopic	92
Figure 7-1	H&E, Actin and Trichrome of 2 Month Cholesterol Diet Graft	95
Figure 7-2	Aneurysm Histology	97
Figure 7-3	Normal and Atherosclerotic Aorta	100
Figure 8	Zymograms of 2, 4 and 6 Month Samples - Diet	105
Figure 9	Humoral ELISA of 2, 4 and 6 Month Samples - Diet	109
Figure 10	Saline Macroscopic	149
Figure 11	Indomethacin Macroscopic	152
Figure 12	Etidronate macroscopic	155
Figure 13-1	Saline - H&E	160
Figure 13-2	Saline - Actin	162
Figure 13-2	Saline - Trichrome	164
Figure 14-1	Indomethacin - H&E	167
Figure 14-2	Indomethacin - Actin	169
Figure 14-3	Indomethacin - Trichrome	171
Figure 15-1	Etidronate - H&E	176

Figure 15-2	Etidronate - Actin	178
Figure 15-3	Etidronate - Trichrome	180
Figure 16	Zymograms of Normal, Indomethacin and Etidronate samples	185
Figure 17	ELISA of Control, Indomethacin and Etidronate Samples	189
Figure 18	Indomethacin Effects on Inflammation	197
Figure 19	Bisphosphonate Action	199

## Acknowledgements

I would like to express my deepest gratitude to my advisor, mentor and friend, Dr. David Cheung. Without his confidence, guidance and perseverance this undertaking would never have happened. My heartfelt thanks also go to my other committee members, Dr. Carlos M.G. Duran, Dr. Mike Minnick, Dr. George Card and Dr. Mary Poss who helped me along the way. Thank you to Dr. Ralph Judd for organizing my comprehensive exams. Special thanks to The International Heart Institute Foundation for support during this research project.

To my family who supported this effort, who always heard “I’m almost done, just one more semester”, this is a tribute to you. Especially to my father and mother, who by example showed me how valuable learning was. To my many friends who listened and supported me in my efforts, I couldn’t have done it without you. Special thanks to Anna, Jory, Dale, Ron, Jack, Sue & Charlie, Ann, Barb & Bill, Grandma Loretta, Mom Sperry, The Larry’s, and Mindy. Thanks also go to the people who helped me carry out this project, Filip, Jerome, Wolfgang, Matthew and Leslie.

This work is in memory of my greatest friend, Buck. Thank you for all you did!

## The Road Not Taken

-Robert Frost-

Two roads diverged in a yellow wood,  
And sorry I could not travel both  
And still be one traveler, long I stood  
And looked down one as far as I could  
To where it bent in the undergrowth;

Then took the other, as just as fair,  
And having perhaps the better claim,  
Because it was grassy and wanted wear;  
Though the passing there  
Had worn them really about the same,  
And both that morning equally lay

In leaves no step had trodden black.  
Oh, I kept the first for another day!  
Yet knowing how way leads on to way,  
I doubted if I should ever come back.

I shall be telling this with a sigh  
Somewhere ages and ages hence:  
Two roads diverged in a wood, and I –  
I took the one less traveled by,  
And that has made all the difference.

## **Background**

### **Cardiovascular and Coronary Heart Disease**

Cardiovascular disease (CVD) has been the primary cause of death in the United States since 1900 and has killed more people than the next five causes of death combined (cancer, chronic lower respiratory diseases, accidents, diabetes, influenza and pneumonia) <sup>1</sup>. Between 1988 and 1994, an estimated 62 million people in the United States were diagnosed with some form of cardiovascular disease, and of these 12.9 million people were diagnosed with coronary heart disease (CHD) with 515,204 deaths attributed to CHD <sup>1</sup>. This corresponds to an average total (direct and indirect) cost of \$21.7 billion per year for coronary heart disease. In 2000 alone, interventions to treat CHD included 519,000 coronary artery bypass grafting (CABG) surgeries performed in 314,000 patients; 561,000 percutaneous transluminal coronary angioplasty (PTCA) interventions in 547,000 patients; 456,000 stenting procedures; and 2,401,000 other procedures which include valve replacements, open heart surgeries, pacemakers, endarterectomies, defibrillators, and cardiac catheterizations <sup>1</sup>.

A variety of factors contribute to the development of CVD, including but not limited to: diet, health status, genetic predisposition, level of activity, smoking, and obesity. If the condition is not advanced to the point of needing surgical intervention, patients can be treated with medications, encouraged to quit smoking, exercise more, and educated in ways to improve their diet and control diabetes. If medication, diet and exercise are insufficient in controlling the progression of the disease, then more aggressive treatments are available. Depending on the severity of the condition, catheter-based coronary revascularization therapies such as percutaneous transluminal coronary

angioplasty, coronary arthroectomy, laser coronary angioplasty, and coronary stenting have proven to be highly effective in a selected population, but restenosis has been a common complication with these procedures <sup>2</sup>.

In cases where further intervention is necessary by-pass surgery (also CABG or Coronary Artery Bypass Grafting) is performed. During coronary artery bypass grafting, a blockage or stenosis within the coronary artery(s) is bypassed using an autologous small-diameter arterial or venous conduit. This serves to immediately improve blood flow to under-perfused areas of the heart, relieve angina, and prevent myocardial infarction.

### **Coronary Graft Options: Advantages, Disadvantages and Limitations**

Vascular grafts represent a significant percentage of all the medical device implantations performed worldwide <sup>3</sup>, and have clinical applications in peripheral vascular surgery, arterio-venous shunt construction and coronary artery revascularizations. The choice of conduit is important for the outcome of a coronary artery bypass graft surgery (CABG), and graft patency is associated with an uneventful post-operative recovery and long-term patient survival <sup>2</sup>. The determination of patency is based upon conduit type (arterial or venous) and the location of the graft insertion (which coronary artery) into the coronary circulation, but regardless of location and graft type, a high average flow has been used as an indication of a viable patent graft <sup>4</sup> (**Table 1: Mean Flow**).

**Table 1:** Flow readings were recorded during coronary artery bypass surgeries using a Transonic Flow Probe. The normal flow readings shown are for 85% of all measured cases, and normal flow is given for each graft type and position. Normal coronary flow (left and right) is approximately 4% of the cardiac output, or about 225ml/min for a 5L/min cardiac output <sup>5</sup> and is split between the right and left coronary branches.

**Table 1: Mean Flow of Arterial and Venous Bypass Grafts**

<b>Mean Flow Readings through Grafts during Surgery*</b>			
<b>Graft Location</b>	<b>Normal Flow</b>	<b>Questionable flow</b>	<b>Obstructed</b>
LIMA to LAD	>27 ml/min	27 to 5 ml/min	Flow less than 5 ml/min
RIMA to RCA	>26 ml/min	26 to 5 ml/min	
SVG to RCA	>29 ml/min	29 to 5 ml/min	
SVG to DIAG	>21 ml/min	21 to 5 ml/min	
SVG to OM1/OM2	>29 ml/min	29 to 5 ml/min	
SVG to PDA	>24 ml/min	24 to 5 ml/min	
SVG to CX	>48 ml/min	48 to 5 ml/min	

\*Adapted from Transonic Systems, 2002<sup>4</sup>

The Left and/or Right Internal Mammary Arteries are dissected from the chest wall and directly grafted to a coronary artery. Saphenous Vein Grafts are harvested from the leg, reversed and grafted from the ascending aorta (proximal) to the coronary artery (distal).

LIMA - Left Internal Mammary Artery, RIMA - Right Internal Mammary Artery, SVG - Saphenous Vein Graft, DIAG - Diagonal, OM - Oblique Marginal, PDA - Posterior Descending Artery, CX - Circumflex Artery, LAD - Left Anterior Descending, RCA - Right Coronary Artery

## **Vascular grafts: Clinical and Experimental**

The available graft options, either autologous or non-autologous, possess one or more of the characteristics described for an 'ideal' graft<sup>6,7</sup>. These include biocompatibility, lack of chemical reactivity, low thrombogenicity, porosity, cost, sterility and no leaching of processing chemicals. The ideal physical characteristics for grafts include: infection resistance, flexibility, resistance to kinking and compression, stretch, size range, tensile and shear strength, resistance to arterial pressure, and compliance. While several types of grafts are available, autologous grafts are the first choice. Problems arise when patients return for a re-operation for failed grafts or have pre-existing vascular disease<sup>8</sup>, and no autologous conduits are available which is the case for 15% of patients returning for a re-operation<sup>2</sup>. In these cases, suitable autologous conduits may not be available, and other options must be explored. These options will be described in the following paragraphs.

### **Autologous Grafts**

Autologous conduits can be either venous (Greater and lesser saphenous veins, cephalic and basilic veins)<sup>2</sup> or arterial (Internal thoracic, right gastroepiploic, inferior epigastric, radial, splenic, gastroduodenal, left gastric, and intercostal)<sup>2,9</sup>. These vessels are harvested as part of the revascularization procedure and can be an additional source of morbidity with associated risks and complications. The internal thoracic artery (ITA, also internal mammary artery or IMA) and greater saphenous veins are the first and second choices for small diameter conduits used in revascularizations<sup>2,10</sup>. The other choices are less commonly used.



The ITA has a 90% patency at 10 years when grafted to the left anterior descending artery (LAD) compared with a 40-50% patency for venous grafts<sup>2,11</sup>. An estimated 10-15% of all vein grafts occlude within the first year, after which the failure rate is estimated at 1-2% for years 1-6 years, and 4% per year for years 6-10<sup>12</sup>. Of these, 30% of vein grafts require re-intervention within two years due to significant stenosis due to intimal hyperplasia<sup>13</sup>. Within 10 years, 30-40% of the re-vascularizations performed using autologous conduits are occluded due to atherosclerosis or stenosis secondary to atherosclerosis, and of the remaining 60-70% only half are free of significant amounts of stenosis<sup>12</sup>.

Intimal hyperplasia is the most common cause of graft failure when autologous vein is used for peripheral or coronary bypass surgeries, accounting for 30 to 50% of all graft failures<sup>9,14-17</sup>. The majority of vein grafts placed in the arterial circulation develop intimal hyperplasia within 6 weeks of implantation, which has been attributed to vessel wall ischemia and stress<sup>18,19</sup>. These factors contribute to endothelial dysfunction, an important early step in the development of intimal hyperplasia<sup>17,18,20,21</sup> and atherosclerosis<sup>22</sup>. Experimentally, autologous venous conduits have been shown to be more susceptible to accelerated atherosclerosis and intimal thickening than arterial grafts<sup>23</sup>.

### **Non-Autologous Grafts**

**Synthetic Grafts:** Commercially available synthetic grafts include polytetrafluoroethylene (PTFE), expanded PTFE (ePTFE, Teflon<sup>™</sup>), polyethylene terephthalate (PET, Dacron<sup>™</sup>), and polyurethanes. Synthetic conduits are attractive due

to their physical characteristics and lack of immunogenicity<sup>2</sup>. Grafts with an internal diameter of 6mm or greater have worked well under clinical conditions<sup>3,6,24,25</sup>, while grafts with an internal diameter of 6mm or less have met with a high failure rate due to thrombosis, or thrombosis secondary to intimal hyperplasia<sup>8,25</sup>.

PTFE grafts have a satisfactory short-term performance but are susceptible to infection and intimal hyperplasia<sup>2</sup>. These conduits become re-endothelialized on the pannus ingrowth from the anastomosis while thrombus forms in the more central portions of the grafts and can become occluded due to pannus sloughing or intimal hyperplasia at the anastomotic junction<sup>10</sup>. PTFE patency rates in the coronary position vary from 59% between 1 to 26 months, 64% at one year, and 14% at 45 months, but these grafts rarely remain patent in the coronary position<sup>10</sup>.

ePTFE is not very hemocompatible/wettable and is not considered suitable for applications needing a small diameter graft of 4mm or less<sup>3</sup>. One patient is documented in literature with a patent 4mm ePTFE aortocoronary graft at 12 years<sup>26</sup>. This patient had unsuitable greater saphenous veins and internal mammary arteries.

Dacron grafts have been successful in the coronary position when used as short interposition grafts in areas of high flow (ascending aorta and proximal end of the coronary artery)<sup>10</sup>.

Polyurethane grafts implanted into animals as peripheral grafts resist thrombosis and showed a rapid cellular ingrowth with a reduced incidence of intimal hyperplasia at the anastomosis<sup>27,28</sup>. However, when 7 different brands of polyurethane grafts were used in clinical applications (peripheral implantation or Arterio-venous (AV) fistulae for hemodialysis access), these grafts had a high rate of thrombosis, were prone to infection

and the patency in the femoro-popliteal position varied from 47-59% at 6 months, and as AV fistulae from 73% at 6 months to 45-64% at 1 year<sup>27</sup>. Aria™ grafts (Thoralon® polyurethane with silicone) were implanted into 27 patients for compassionate use between 1993-96, and at 1 year five patients had died of causes unrelated to the graft while the remaining 22 patients were alive and asymptomatic<sup>29</sup>. No polyurethane grafts are currently approved for human use.

**Biological Grafts:** Detergent/enzymatically extracted grafts of human or animal origin<sup>30-34</sup> have met with some success in animal models<sup>35,36</sup>, but are not generally available for clinical implantation into humans. Fixed xenogenic grafts such as dialdehyde-tanned bovine internal thoracic artery have been used, but this graft was deemed unsuitable having a 16% patency rate at 10 months<sup>37</sup>.

Umbilical vein conduits (both cryopreserved and glutaraldehyde-fixed) are potentially an ideal non-autologous conduit source as they are easily obtained and are able to withstand arterial pressure and stress due to their circumferential elasticity, however they are potentially immunogenic, prone to intimal dissection, and only have a 50% short-term patency rate which limits their use<sup>2</sup>. Umbilical vessels fixed in glutaraldehyde have found clinical applications in lower limb revascularization but long term patency is poor and they are susceptible to aneurysmatic degeneration<sup>38</sup>.

Greater saphenous vein (GSV) grafts are easily obtained (cryopreserved and glutaraldehyde-fixed) but immunogenicity is a problem and the cryopreserved grafts have a high failure rate due to a deteriorated intima. Patency data indicates these grafts should be used with caution and only in cases where no autologous grafts are available<sup>2</sup>. GSV homografts (12 of 38) had a patency rate of 31.5% at 1 year. Cryopreserved GSV (61

grafts in 28 patients) had a 65% patency rate at 2 weeks, while at 12 months none of the 13 grafts examined were normal. In another study, cryopreserved GSV patency at 7.5 months was 41% in 19 patients <sup>2</sup>.

**Biodegradable Polymer Grafts:** Biodegradable grafts <sup>39-41</sup> have been used under experimental conditions with some success, but are not yet a viable clinical option.

These grafts consist of a biodegradable scaffold which, depending on the composition/ratio of the components, can be 'programmed' to degrade within a defined period of time. The most common polymers used as scaffold material are poly L-lactic acid (PLLA), polyglycolic acid (PGA), poly DL-lactic-co-glycolic acid (PLGA), and poly-4-hydroxybutyrate (P4HB) <sup>42</sup>. These grafts are usually seeded with cells *in vitro* prior to implantation <sup>6</sup>.

### **General Conclusions on Graft Options**

“An excellent substitute conduit for coronary bypass operations that can be taken ‘off the shelf’ is certainly the dream of every practicing cardiac surgeon” <sup>2</sup>. Since 1942, significant efforts have been made to develop alternative grafts for vascular applications but have met with limited success <sup>3</sup>. Graft options other than autologous conduits are experimental, have unsatisfactory patency rates, or both. The major issues linked to vascular graft failure include immediate and long-term patency, lack of complete re-endothelialization, aneurysmic degeneration, and intimal hyperplasia. The available information leads one to conclude that a satisfactory small-diameter blood vessel replacement has not yet been found.

## **Xenograft Developed at IHI (Corograft™)**

The Corograft™ conduits used in this study were obtained from Philogenesis (Monrovia, CA), the company responsible for the commercial production and distribution of the conduit material developed at IHI. The conduits used in this study are bovine arterial grafts treated by the L-Hydro™ method to reduce antigenicity. The L-Hydro™ treatment for biological transplantable tissues (Patent pending) consists of two steps: the first step combines a mild extraction of antigens without the use of detergents or digestive enzymes and the masking of unextracted antigens by a polyglycol in conjunction with a mild chemical oxidation under physical conditions that protect the extracellular components (such as collagen and elastin), and as a second step the incorporation of a common anti-inflammatory agent (equivalent to aspirin) and an anti-thrombotic agent (equivalent to heparin). The conduits are then lyophilized prior to being gas-phase sterilized (D-Hydro™).

These conduits have been implanted in a sheep model into both a peripheral (carotid) and coronary position and compared to autologous venous conduits. When implanted as a coronary bypass (ascending or descending aorta to LAD), Corograft™ conduits (less than 4mm ID and more than 10cm in length) showed excellent patency rates at five or more months. When examined histologically, the implants were readily recolonized by host cells *in vivo* and showed a complete endothelial-like covering of the lumen with smooth muscle cells in the media of the arterial graft wall. When implanted in the carotid artery of sheep, complete endothelialization occurred within 3 months post-operatively. No evidence of thrombosis, stenosis or aneurysm was seen in these studies.

These conduits have several advantages including biocompatibility, off-the-shelf availability, absence of toxic cross-linking agents (glutaraldehyde or formaldehyde), room temperature storage, simplified shipping, and no co-morbidity associated with autologous vessel harvest. The graft material is easy to handle and use, can be tailored to the particular application, and takes a suture well without tearing. These technologies have been applied to valves with promising results<sup>43</sup>. Although the Corograft™ implant studies in sheep have shown promising results, the exact role the anti-inflammatory strategy in the treatment of the graft has not been established. The optimum dosage for the anti-inflammatory agents used has also not been determined.

In order to study the role of the host inflammatory response to a xenograft arterial bypass, three questions needed to be answered: 1) Which animal models and graft materials are most appropriate, so that the graft remains patent for an extended period of time? 2) If the original hypothesis that inflammation contributes significantly to the failure of a xenograft implants is true, can we choose a model to study the role of increased inflammation on the implant? 3) Can we find alternate ways of decreasing the inflammatory response toward the graft? Three sets of experiments were designed to answer of these questions: 1) a rabbit model with a xenograft implanted in the abdominal aorta was studied, 2) inflammation was enhanced by diet-induced hypercholesterolemia to see if this accelerated the failure of the graft, and 3) inflammation was suppressed by the administration of anti-inflammatory agents to see if graft durability could be improved. Each of these experiments will be addressed in separate chapters.

## Chapter I

### Development of the Animal model

#### Introduction

#### Choice of Animal Model

Many issues must be taken into consideration when choosing an animal model for vascular graft testing. These may include length and size of the graft which will dictate the anatomical locations available for implantation. Composition and size of the graft (e.g. biological vs. synthetic) may also play an important role in site selection (e.g. aorta vs. femoral vs. coronary) as well as animal model used (large vs. small). The coagulation and fibrinolytic characteristics of the individual models must be considered and compared to the human system. Other issues may include availability, human perception (e.g. using a dog model vs. sheep model), housing and nutritional requirements, body size, etc. Animal models used in the past to evaluate vascular grafts include calf, primate, pig, sheep, dog, rabbit, rat, and mouse, each with its' own advantages and disadvantages.

Another important consideration in evaluating models for vascular grafts is the dynamics of re-endothelialization. The majority of the animal models will spontaneously re-endothelialize (with exception of the dog), which is in direct contrast with the human system<sup>44</sup>. Re-endothelialization in humans is usually limited to a distance of ~ 1 cm from the anastomosis and appears to correspond to the maximal distance of pannus ingrowth/anastomotic hyperplasia.

## **Rabbit Model**

The rabbit model has been used extensively for the *in vivo* evaluation of small-bore (less than 6mm) vascular grafts<sup>45-49</sup>. The thrombogenic properties of rabbit blood are similar to that of humans<sup>48,50</sup>, as are the thromboplastic and fibrinolytic properties of rabbit arteries<sup>50,51</sup>, making the rabbit an ideal model for experimental small-diameter vascular graft studies. Furthermore, the ease of animal handling, size and cost effectiveness make this model attractive. Their low cost makes them economical in studies requiring a larger sample size and their small size allows for easy handling and boarding. The main disadvantage is their smaller size, necessitating magnification during surgery and the use of microsurgical techniques and instruments.

## **Surgical Model - Location of Implantation**

The location of graft implantation depends on the graft to be tested, size of the graft, and other issues such as arterial vs. venous conditions (high vs. low flow). Common sites of arterial implantation in the various animal models include the carotid arteries, as a coronary bypass, the thoracic aorta, the abdominal aorta, as well as the iliac and femoral arteries. In a rabbit model, several sites have been used for graft implantation studies; the carotid artery, the iliac artery, the femoral artery, thoracic aorta, and the abdominal aorta.

Many studies have used the rabbit model to evaluate small diameter grafts, but the grafts were placed into the carotid position. The carotid position in rabbits has been used in the past to evaluate the behavior of autologous vein grafts under both normal and atherosclerotic conditions<sup>15,23,52-54</sup>. However, this position is not suitable for the



evaluation of a 2-3mm vascular graft due to the size mismatch between the carotid artery and the graft. In the rabbit the thoracic and abdominal aortae fall into this size category.

Therefore, the abdominal aorta was chosen in this study because the graft would be under arterial pressure, the diameter of the aorta more closely matches the diameter of a human coronary artery, and the flow is similar to bypass graft flow conditions. The site is also easy to access (compare to the thoracic aorta), the surgery is less invasive than the thoracic position, does not require active ventilation, and several studies had been done implanting vascular grafts into this position<sup>46,48,49,55,56</sup>. In the course of the study, modifications in the surgical protocol were made to increase operative and post-operative survival as well as decreasing the incidence of post-operative paralysis, a common occurrence in surgery on the abdominal aorta.

**Specific Aim: To develop an animal model in which the Corograft™ conduit can be implanted, remain patent long-term, and allow for the study of the host inflammatory response toward the graft material under varied conditions.**

### **Rationale**

With an increasing number of bypass grafts and re-operations being performed each year, there is an urgent need to develop an alternative to the currently available coronary graft options. Autologous conduits as well as synthetic and biological options explored to this point have all fallen short of the optimal outcome, a disease-free, fully-integrated conduit. The key role of inflammation in the failure of both autologous and non-autologous options is finally being acknowledged, though much work still needs to

be done to address this issue. To these ends, a model was developed in which the graft material could be implanted and the inflammatory response could be increased or decreased as desired.

### **Experimental design**

The pilot group consisted of 11 rabbits in which the surgical protocol was optimized by the addition of an end-to-end anastomosis, systemic hypothermia and supplemented Lactated Ringers solution. This protocol was then used to implant the graft into an additional 54 rabbits in two experimental groups, 26 rabbits in diet group and 28 in the drug groups. In the diet group, the graft performance was evaluated out to 6 months and to 2 months in the drug groups.

## Materials and Methods

### Animal Source and Care

Female New Zealand White rabbits (weighing ~3-4kg) were purchased from Western Oregon Rabbit Company (Philomath, OR, USA) and allowed to acclimate for at least 7-14 days before initiating any procedures. Rabbits had access to normal rabbit chow and water *ad libitum* through out the duration of the study. Average room temperature was 63°F (17-18°C), with a 12hr day/night cycle and 10-12 air changes/hr. All animals appeared clinically normal throughout the quarantine period and no other pathogen testing was done.

All animals were cared for in accordance with the "*Principles of Laboratory Animal Care*" formulated by the National Society of Medical Research and the "*Guide for the Care and Use of Laboratory Animals*" prepared by the Institute of Animal Resources, National Research council, and published by the National Academy Press, revised 1996. The use of the animals for this project was reviewed and approved by the Institutional Animal Care and Use Committee (IACUC) of The University of Montana. The submitted protocol also included criteria for analgesia and euthanasia.

### Preoperative Preparation

Rabbits were sedated with an intramuscular dose of ketamine (50mg/kg), the abdominal region shaved, and the rabbit placed in a dorsal recumbent position on a heating pad (heating pad was off during the hypothermic phase of the surgery). Anesthesia was induced and maintained with 1.5-2% Isoflurane/Oxygen mixture administered via a ventilator/anesthesia delivery system (North American Drager,

Telford, PA, USA or Isotec 4, Surgivet/Anesco Veterinary Surgical Products, Waukesha, WI, USA), and the level of isoflurane was adjusted as needed to keep the animal sufficiently anesthetized, as evaluated by ear pinch or any evidence of discomfort. The chest cavity was not opened allowing for passive, spontaneous ventilation by the animal<sup>56,57</sup>. The core temperature was monitored with a rectal temperature probe and electrocardiographic leads were attached so the heart rate could be monitored. Icepacks were placed around and between the hind-legs and along the lower flanks. An intravenous cannula (22 gauge) was introduced into the marginal ear vein and cold (4°C) supplemented Lactated Ringer's Solution was given initiating the hypothermic phase of the surgery. The supplemented Lactated Ringer's solution contained per liter: 20ml sodium bicarbonate (84mg/ml and 50mEq/50ml, American Pharmaceutical Partners, Inc. Los Angeles, CA, USA), 50ml of 20% mannitol solution and 0.5ml dexamethasone sodium phosphate (4mg/ml, American Regent Laboratories, Shirley, NY, USA).

### **Surgical Protocol**

After sterile draping, a midline laparotomy was performed. The skin was retracted with traction sutures and the intestines were displaced to the right side and wrapped in laparotomy sponges moistened with cold sterile saline. Isolation of the abdominal aorta from the surrounding tissues from below the left renal artery to the iliac bifurcation was performed meticulously to avoid accidental injury to the inferior vena cava and its branches. Care was taken to identify all aortic branches along the entire circumference. If feasible, anastomotic sites were planned to avoid cutting of the large dorsal aortic branches. Once all dissection was completed, one ml of heparin was

administered i.v. (1000 USP units/ml, American Pharmaceutical Partners, Inc., Los Angeles, CA, USA) and if necessary, further cooling of the animal was achieved by using sterile saline slush applied directly into the abdominal cavity and to the laparotomy sponge covering the intestines.

When the rectal temperature of the animal reached 34.5°C, the ice packs and the saline slush were removed as the temperature continued to drop without additional cooling. The cold supplemented Lactated Ringer's solution was exchanged for warm (37°C). Also, warm packs were placed next to the rabbit under the sterile draping and the heating pad under the rabbit was switched on to start the re-warming phase of the procedure initiating the re-warming period of the surgery.

Dorsal aortic branches within the previously prepared aortic segment were clipped and cut. The aorta was occluded proximally and distally with micro-surgical vascular clamps (MORIA 200/A, Angled, 30mm. Fine Science Tools, Inc. Foster City, CA, USA) placed below the left renal artery and above the inferior mesenteric artery. And keeping in mind the elastic recoil of the vessel, the aorta was cut approximately 1cm from each clamp to avoid space issues.

All animals had a Corograft™ (~3-4mm ID x ~4cm minimum) previously re-hydrated in heparinized saline, implanted into the infrarenal abdominal aorta. An end-to-end anastomosis (distal then proximal) was performed with a continuous single 8/0 Prolene suture (Polypropylene, Ethicon, Inc., Somerville, NJ, USA). Before tying the suture for the proximal anastomosis, the distal vascular clamp was removed to flush air from the graft by filling the graft with blood to avoid an air embolism. After tying the

suture, the proximal vascular clamp was removed and additional 8/0 Prolene suture used (as needed) to control anastomotic or graft bleeding.

The intestines were returned to the abdominal cavity and repeatedly lavaged with warm sterile saline to achieve appropriate re-warming of the animal. When the rectal temperature of the rabbit reached 36.5°C to 37.5°C, the saline was removed and the laparotomy closed in two layers with 3/0 Vicryl (Polygalactin 910, Ethicon, Inc., Somerville, NJ, USA). The supplemented Lactated Ringer's solution was discontinued, with a total amount of 100-150ml having been administered for both the cold and warm solutions. When the animal was re-warmed to physiological temperature (101-104°F/38-40°C) and movement was seen in the hind-limbs, the animal was returned to its' cage.

Rabbits received 0.2ml flunixin meglumine (50mg/ml, Equileve®, Phoenix Scientific, Inc., St. Joseph, MO, USA) i.m. as an analgesic immediately after surgery, and 0.2ml i.m. flunixin meglumine BID for 4 days post-operatively. All rabbits were monitored for neurologic or ischemic complications of the hind limbs throughout the study. No antibiotic prophylaxis, platelet aggregation inhibitors nor anticoagulants were used postoperatively.

## Results

### Pilot group

The pilot group consisted of 11 rabbits in which the surgical, anesthesia, and hypothermia techniques were optimized. Initially, the graft material was implanted into the carotid position in 3 rabbits, but this was discontinued. All subsequent rabbits had the conduit implanted into the abdominal position. The graft was implanted into the abdominal position without hypothermia in four rabbits, all of which died during surgery. One died due to excessive cross-clamp time, the other due to anesthetic complications, the remaining two rabbits due to unknown causes. Two rabbits underwent surgery with systemic hypothermia, but died during the procedure. Of the two that survived the surgery, one died the following day and the other was euthanized at 22 days.

Incorporation of systemic hypothermia, modified Lactated Ringers solution and short cross-clamp time resulted in greater graft patency. All grafts implanted into normal rabbits were patent at surgery (13 of 13), and ten were patent at sacrifice at 2 (n=3), 4 (n=4) and 6 months (n=3). Of the additional three, one rabbit died at 5+ months due to intestinal ischemia and two rabbits were euthanized due to post-operative complications and were excluded from the study. For the cholesterol-diet rabbits all 13 grafts were patent at surgery, and with the exception of the 2 month sample, the grafts harvested from the cholesterol-diet rabbits were post-mortem samples and patency could not be assessed. In the drug treatment groups, 28 of 28 grafts were patent at surgery and 15 at sacrifice. The additional 13 rabbits died or were sacrificed due to peri-operative or post-operative complications unrelated to graft patency. Of these, 2 rabbits developed paraplegia. These results are summarized in table 2.

**Table 2:** Except for three rabbits in the pilot group which had the graft implanted in the carotid position, all other rabbits had the 3-4mm diameter x 4cm Corograft™ xenograft conduit implanted into the abdominal aorta distal to the kidneys but proximal to the iliac bifurcation. The **Pilot Group** includes rabbits used to develop the surgical model in which the operative variables (hypothermic and cross-clamp time) were optimized. The **Normal Diet** group includes all rabbits fed a normal rabbit chow, while the **Cholesterol Diet** group includes all rabbits fed commercially available rabbit chow supplemented with 1% cholesterol. The **Drug Treated** group includes rabbits in which saline, Indomethacin or Etidronate were administered subcutaneously during the duration of the study. The total number of rabbits implanted with a graft in each group are listed in the # **Operated** column. The total number of rabbits included in each group are listed in the # **Valid** column, and represent animals sacrificed when scheduled. The remainder of the animals were excluded due to death, operative or post-operative complications unrelated to the graft.



**Table 2: Valid Animals**

<b>Group</b>	<b># Operated</b>	<b># Valid</b>	<b># Excluded</b>
Pilot Study	11	NA	NA
Normal Diet	13	10	3
Cholesterol Diet	13	1	12
Drug Treated	28	15	13
Total	<b>65</b>	<b>26</b>	<b>28</b>

NA - Not Applicable

## Discussion

The implantation of small-diameter vascular grafts, either of human or synthetic origin, is performed daily in current medical practice and the number of vascular grafts implanted each year numbers over one million throughout the world. In the USA alone, 571,000 coronary artery bypass grafts were performed in 1999<sup>58</sup>. Autologous arteries and veins still represent the best treatment options, however pre-existing vascular diseases or previous cardiovascular procedures emphasize the need for a safe, durable and long-term alternative graft of an acceptable diameter.

### Rabbit Model

This project was started due to an observation that the Corograft<sup>TM</sup> conduit had not been tested in a disease model, and that the long-term outcome of this graft under conditions of atherosclerosis would provide valuable information. This study would have been prohibitively expensive in the sheep model used at the time to evaluate these grafts *in vivo*. After reviewing the available literature the rabbit was chosen as a model due to the amount of information in the literature using this model to evaluate small diameter grafts (less than 6mm) and that inflammation could be increased or decreased in order to further evaluate the role of inflammation on the host response toward the Corograft<sup>TM</sup> in later portions of this study.

### Abdominal Aorta

Initially, the graft material was implanted into the carotid position, but this was discontinued for several reasons. There was a large size mismatch between the carotid

artery (~1-2mm) and the graft material available at the time (3-4mm). The carotid position was difficult to access due to limited space, and close proximity of the jugular vein made it difficult to isolate the carotid without damage to the vein. Also, there was no way to monitor the patency of the graft material during the long term study. This approach was discontinued and the alternate implantation site of the abdominal aorta used instead.

The abdominal aorta was chosen as it approximates the size and arterial conditions of a human coronary artery (superior to implantation into the carotid position of rabbits). The blood flow through the abdominal aorta proximal to the iliac bifurcation for a rabbit is  $65.1 \pm 3.2 \text{ ml/min}$ <sup>59</sup> compared to ~225ml/min (split between the left and right coronary arteries) through the coronary circulation in humans<sup>5</sup>. This flow falls into the normal flow range of a coronary graft from either an internal thoracic or the ascending aorta to any coronary artery branch<sup>4</sup>. An additional advantage of this model is that if the graft occludes post-operatively, hind-limb paralysis results and serves as an indicator of patency throughout the study. This is a separate issue from spinal chord ischemia which can occur as a complication associated with surgery involving the thoracic and abdominal aorta, and also results in hind-limb paralysis in the rabbit model

57

### **Hypothermia and Cross-Clamp Time**

The basic surgical protocol put forth by Nordestgaard *et al.*<sup>49</sup> was explored as a model of graft implantation into the abdominal aorta of rabbits. Initially, several cases of postoperative paraplegia in rabbits implanted with a Corograft<sup>™</sup> conduit led us to explore

reasons for these complications and a literature review indicated that normothermic ischemic injury of the spinal chord had been previously shown to result in paraplegia<sup>48,57,60</sup>. This led to the application of controlled mild systemic hypothermia (32-34°C) to this surgical model. Mild hypothermia offers significant protection from ischemic spinal chord injury resulting in increased recovery of motor function<sup>48,57,60</sup> and reduces metabolic demands during the ischemic period<sup>60</sup>.

However hypothermia alone might be insufficient to avoid paraplegia when the cross-clamp time was in excess of 20 minutes<sup>57</sup>. For this reason the supplemented Lactated Ringers solution was incorporated into the methodology. This was based in part on a study by Ueno *et.al.*<sup>60</sup> in which they occluded the abdominal aorta of rabbits for 45 minutes and also infused Lactated Ringers solution alone or containing methylprednisolone (MP), MP+Mannitol, or MP+mannitol+vitamins E and C, and found no incidence of paraplegia in the group in which the complete solution was administered. The Lactated Ringers solution used in this study was supplemented with sodium bicarbonate, mannitol and dexamethasone sodium phosphate in an effort to further reduce the incidence of paralysis due to spinal ischemia. This solution is similar to cardioplegia formulations used during bypass surgery to protect the heart from ischemic damage and would control metabolic acidosis (sodium bicarbonate), ischemic cellular swelling (mannitol) and ischemia-reperfusion injury induced inflammation (dexamethasone).

The pilot group indicated that a cross-clamp time in excess of 30 minutes under normothermic or mild hypothermic conditions contributed to a high rate of postoperative paralysis in rabbits regardless of graft patency. This observation was supported by the study of Tolwani *et.al.*<sup>48</sup>, where mild hypothermia and a mean cross-clamp time of 30

minutes or less resulted in a 3% incidence of paraplegia, while without hypothermia the incidence of paraplegia was 100%. This observation is also supported by Nordestgaards' study where grafted rabbits had a high incidence of paralysis which could possibly be attributed to their cross-clamp time. Their cross-clamp time varied from 20-50 minutes under normothermic conditions and of 42 rabbits implanted with 2 and 3mm grafts, 18 developed paralysis during their study (42%).

### **Anastomosis**

An end-to-side type of anastomosis was initially performed which would simulate grafting in humans bypassing an occlusion or stenosis in a coronary artery, with the intention of sparing the spinal aortic branches from the abdominal aorta by ligating the aorta between the anastomoses. Due to the technical performance of an end-to-side anastomosis, a longer cross-clamping time and the possibility of anastomotic occlusion by thrombus extension from the point of the tied native aorta, this approach was discontinued. Instead, an end-to-end anastomosis was performed and every possible effort was made to position the graft to avoid the clipping and cutting of large spinal branches. A continuous suture pattern was chosen over an interrupted pattern in order to minimize the cross-clamp time. An interrupted suture pattern is more commonly used with smaller grafts under conditions where there is a possibility of producing a stenosis at the anastomosis.

## **Graft Length**

The general criteria used by cardiac surgeons to evaluate an experimental vascular graft for possible use as a coronary bypass in humans are: 4mm diameter by 4cm length with at least 4 months patency (Personal Communication, Dr. C. M. G. Duran). When testing grafts in a rabbit model many published studies implanted grafts of ~1cm which appears insufficient to adequately evaluate re-endothelialization, which in humans can reach 1cm at each anastomosis due to pannus ingrowth. For this reason the graft length implanted in this study was 3-4mm in diameter by ~4cm in length in which patency was confirmed out to 6 months.

## **Graft Performance: Corograft™ vs. Other Graft Options**

Of the 58 rabbits implanted with a graft in the abdominal position, all grafts were patent at surgery, giving a 100% immediate patency. Of the 26 valid animals (normal diet n=11, cholesterol diet n=1, drug groups n=15), one possible case of thrombosis (5mo death) gives a patency rate of 96%. Six rabbits of 58 developed paraplegia during this study in the immediate post-operative period, giving a paraplegia rate of 10.3%. The grafts were examined in all cases of post-operative paralysis, and none of the grafts were thrombosed, suggesting that ischemic injury to the spinal chord might be the cause. Patency could not be assessed due to post-mortem clotting for grafts removed from rabbits found dead, but one death at 5 months due to intestinal ischemia might have been due to thrombosis.

By comparison, Nordestgaard *et.al.*<sup>49</sup> implanted polytetrafluoroethylene conduits (2 or 3mm by 1cm) into the abdominal position of rabbits with a patency rate of 24% for

2mm grafts and 72% for 3mm grafts. Of the 17 rabbits with 2mm grafts, 12 were killed or died within the first 7 days due to graft thrombosis, while 4 of the 5 survivors had patent grafts at the end of 3 months. Of the 25 rabbits they grafted with 3mm grafts, 19 grafts were patent at 1 week and 18 were patent at 3 months. Lee *et.al.* implanted 3mm x 35mm PTFE grafts into the abdominal aorta <sup>47</sup> under normothermic conditions. The grafts were harvested at 7 and 42 days (5 each). They had no instances of thrombosis in their study and no cross-clamp information was given.

The patency of PTFE (2mm x 15mm) in the carotid position of rabbits is excellent at 2 weeks (89%), after which patency declines to 86% at 16 weeks, and ~68% at 32 weeks compared to 100% patency for autologous grafts <sup>61</sup>. Sparks *et.al.* implanted PTFE grafts (2mm x 10mm) into the carotid position and evaluated patency at 7, 14 and 21 days (each n=5). Patency was 40% at 7 and 14 days with a patency of 20 % at 21 days <sup>62</sup>. When PTFE or polyurethane grafts (1.5mm x 10mm) grafts were implanted into the carotid position of rabbits by van der Lei *et.al.*, no improvements in patency or thrombosis resistance were seen <sup>50</sup>. All polyurethane and PTFE grafts (each 4 of 4) were patent at 1 hour, 2 of 4 were patent at 1 day, 1 of 4 at 1 week, while none were patent at 2, 3 and 6 weeks (each 6 of 6). By comparison, all arterial autografts were patent to 2 weeks (not done at 3 and 6 weeks).

The differences in patency seen in these published studies could be attributed to among other things surgical technique, but they serve to illustrate that the patency of non-autologous small diameter grafts in the rabbit model is less than optimal. However, a true assessment of patency for these studies may be difficult to determine as only successfully grafted animals may have been included in the published study. By

comparison, the graft used in this study shows excellent patency and thrombosis resistance, indicating that performance of this graft material is superior to previously published studies where non-autologous grafts were implanted into the circulation of rabbits.

## **Conclusions**

Hypothermia in conjunction with the supplemented Lactated Ringers solution and strictly observing a cross-clamp time of 30 minutes or less effectively reduced the incidence of post-operative paraplegia in this study and contributed to the success of this model<sup>63</sup>. In addition, the surgical protocol is straight forward in its' approach and gives excellent results allowing for a greater percentage of valid animals, allowing for refinement of the study approach and a reduction in the total number of animals needed for a given study. When compared to similar studies in which a vascular graft was implanted into the abdominal aorta or carotid artery position of rabbits, the graft implanted in this study had a 100% immediate patency rate in all study groups using a 3-4mm diameter graft with a 4cm length. The longer term patency and thrombosis resistance of the Corograft<sup>™</sup> is excellent, and exceeds published studies. However, in all cases one must remember the rabbit is an animal model and that any findings must eventually be verified in humans.



## Literature Cited

1. AHA. Heart Disease and Stroke Statistics - 2003 Update. In. Dallas, TX: American Heart Association; 2002.
2. Canver CC. Conduit options in coronary artery bypass surgery. *Chest*. 1995;108:1150-5.
3. Zdrahala RJ. Small caliber vascular grafts. Part I: state of the art. *J Biomater Appl*. 1996;10:309-29.
4. Transonic Systems I. Flow-based Coronary Graft Flow Assessment during CABG. In: Eymann S, ed.: Cornelis J. Drost; 2002.
5. Downey JM. Hemodynamics. In: Johnson LR, ed. *Essential Medical Physiology*. 2nd ed. Philadelphia: Lippincott-Raven Publishers; 1998:149-164.
6. Greenwald SE, Berry CL. Improving vascular grafts: the importance of mechanical and haemodynamic properties. *J Pathol*. 2000;190:292-9.
7. Abbott WM, Callow A, Moore W, Rutherford R, Veith F, Weinberg S. Evaluation and performance standards for arterial prostheses. *J Vasc Surg*. 1993;17:746-56.
8. Burkel WE. The challenge of small diameter vascular grafts. *Med Prog Technol*. 1988;14:165-75.
9. Cox JL, Chiasson DA, Gotlieb AI. Stranger in a strange land: the pathogenesis of saphenous vein graft stenosis with emphasis on structural and functional differences between veins and arteries. *Prog Cardiovasc Dis*. 1991;34:45-68.
10. Tomizawa Y. Vascular prostheses for aortocoronary bypass grafting: a review. *Artif Organs*. 1995;19:39-45.

11. Motwani JG, Topol EJ. Aortocoronary saphenous vein graft disease: pathogenesis, predisposition, and prevention. *Circulation*. 1998;97:916-31.
12. Shuhaiber JH, Evans AN, Massad MG, Geha AS. Mechanisms and future directions for prevention of vein graft failure in coronary bypass surgery. *Eur J Cardiothorac Surg*. 2002;22:387-96.
13. Davies MG, Hagen PO. Pathophysiology of vein graft failure: a review. *Eur J Vasc Endovasc Surg*. 1995;9:7-18.
14. Faries PL, Marin ML, Veith FJ, Ramirez JA, Suggs WD, Parsons RE, Sanchez LA, Lyon RT. Immunolocalization and temporal distribution of cytokine expression during the development of vein graft intimal hyperplasia in an experimental model. *J Vasc Surg*. 1996;24:463-71.
15. Massey MF, Davies MG, Svendsen E, Klyachkin ML, Schwartz LB, Barber L, McCann RL, Hagen PO. Reduction of experimental vein graft intimal hyperplasia by ketanserin. *J Surg Res*. 1993;54:530-8.
16. Chaux A, Ruan XM, Fishbein MC, Sandhu M, Matloff JM. Influence of vein valves in the development of arteriosclerosis in venoarterial grafts in the rabbit. *J Thorac Cardiovasc Surg*. 1995;110:1381-9; discussion 1389-90.
17. Davies MG, Klyachkin ML, Dalen H, Massey MF, Svendsen E, Hagen PO. The integrity of experimental vein graft endothelium--implications on the etiology of early graft failure. *Eur J Vasc Surg*. 1993;7:156-65.
18. Loscalzo J. Vascular matrix and vein graft failure. Is the message in the medium? *Circulation*. 2000;101:221-3.

19. Michiels C, Arnould T, Janssens D, Bajou K, Geron I, Remacle J. Interactions between endothelial cells and smooth muscle cells after their activation by hypoxia. A possible etiology for venous disease. *Int Angiol.* 1996;15:124-30.
20. Fortunato JE, Glagov S, Bassiouny HS. Biomechanical factors as regulators of biological responses to vascular grafts. *Semin Vasc Surg.* 1999;12:27-37.
21. Clowes AW, Gown AM, Hanson SR, Reidy MA. Mechanisms of arterial graft failure. 1. Role of cellular proliferation in early healing of PTFE prostheses. *Am J Pathol.* 1985;118:43-54.
22. Boyle EM, Jr., Lille ST, Allaire E, Clowes AW, Verrier ED. Endothelial cell injury in cardiovascular surgery: atherosclerosis. *Ann Thorac Surg.* 1997;63:885-94.
23. Zwolak RM, Kirkman TR, Clowes AW. Atherosclerosis in rabbit vein grafts. *Arteriosclerosis.* 1989;9:374-9.
24. Pasquinelli G, Freyrie A, Preda P, Curti T, D'Addato M, Laschi R. Healing of prosthetic arterial grafts. *Scanning Microsc.* 1990;4:351-62.
25. White RA. The effect of porosity and biomaterial on the healing and long-term mechanical properties of vascular prostheses. *ASAIO Trans.* 1988;34:95-100.
26. McLarty AJ, Phillips MR, Holmes DR, Jr., Schaff HV. Aortocoronary bypass grafting with expanded polytetrafluoroethylene: 12-year patency. *Ann Thorac Surg.* 1998;65:1442-4.
27. Tiwari A, Salacinski H, Seifalian AM, Hamilton G. New prostheses for use in bypass grafts with special emphasis on polyurethanes. *Cardiovasc Surg.* 2002;10:191-7.

28. Underwood CJ, Tait WF, Charlesworth D. Design considerations for a small bore vascular prosthesis. *Int J Artif Organs*. 1988;11:272-6.
29. Farrar DJ. Development of a prosthetic coronary artery bypass graft. *Heart Surg Forum*. 2000;3:36-40.
30. Vesely I, Noseworthy R, Pringle G. The hybrid xenograft/autograft bioprosthetic heart valve: in vivo evaluation of tissue extraction. *Ann Thorac Surg*. 1995;60:S359-64.
31. Wilson GJ, Courtman DW, Klement P, Lee JM, Yeger H. Acellular matrix: a biomaterials approach for coronary artery bypass and heart valve replacement. *Ann Thorac Surg*. 1995;60:S353-8.
32. Malone JM, Brendel K, Duhamel RC, Reinert RL. Detergent-extracted small-diameter vascular prostheses. *J Vasc Surg*. 1984;1:181-91.
33. Allaire E, Guettier C, Bruneval P, Plissonnier D, Michel JB. Cell-free arterial grafts: morphologic characteristics of aortic isografts, allografts, and xenografts in rats. *J Vasc Surg*. 1994;19:446-56.
34. Walter M, Erasmi H. A new vascular prosthesis of bovine origin. *Thorac Cardiovasc Surg*. 1992;40:38-41.
35. Clarke DR, Lust RM, Sun YS, Black KS, Ollerenshaw JD. Transformation of Nonvascular Acellular Tissue Matrices Into Durable Vascular Conduits. *Annals of Thoracic Surgery*. 2001;71:S433-436.
36. Elkins RC, Dawson PE, Goldstein S, Walsh SP, Black KS. Decellularized human valve allografts. *Ann Thorac Surg*. 2001;71:S428-32.

37. Mitchell IM, Essop AR, Scott PJ, Martin PG, Gupta NK, Saunders NR, Nair RU, Williams GJ. Bovine internal mammary artery as a conduit for coronary revascularization: long-term results. *Ann Thorac Surg.* 1993;55:120-2.
38. Wagner E, Guidoin R, Marois M, Mantovani D, Roy R, Ricci M, Marois Y, King MW, Gill F, Awad JA. Histopathologic findings in synthetic and biologic explanted grafts used in peripheral arterial reconstruction. *Asaio J.* 1994;40:M279-83.
39. Shum-Tim D, Stock U, Hrkach J, Shinoka T, Lien J, Moses MA, Stamp A, Taylor G, Moran AM, Landis W, Langer R, Vacanti JP, Mayer JE, Jr. Tissue engineering of autologous aorta using a new biodegradable polymer. *Ann Thorac Surg.* 1999;68:2298-304; discussion 2305.
40. Niklason LE, Gao J, Abbott WM, Hirschi KK, Houser S, Marini R, Langer R. Functional arteries grown in vitro. *Science.* 1999;284:489-93.
41. Greisler HP. Arterial regeneration over absorbable prostheses. *Arch Surg.* 1982;117:1425-31.
42. MacNeill BD, Pomerantseva I, Low HC, Oesterle SN, Vacanti JP. Toward a new blood vessel. *Vasc Med.* 2002;7:241-6.
43. Cheung DT, Weber PA, Grobe AC, Shomura Y, Choo SJ, Luo HH, Marchion DC, Duran CM. A New Method for the Preservation of Aortic Valve Homografts. *J Heart Valve Dis.* 2001;10:728-735; discussion 734-5.
44. Simon P, Kasimir MT, Seebacher G, Weigel G, Ullrich R, Salzer-Muhar U, Rieder E, Wolner E. Early Failure of the tissue engineered porcine heart valve

- SYNERGRAFT in pediatric patients. *European Journal of Cardio-thoracic Surgery*. 2003;23:1002-1006.
45. Baumann DS, Doblus M, Daugherty A, Sicard G, Schonfeld G. The role of cholesterol accumulation in prosthetic vascular graft anastomotic intimal hyperplasia. *J Vasc Surg*. 1994;19:435-45.
  46. Greisler HP, Klosak JJ, Endean ED, McGurrin JF, Garfield JD, Kim DU. Effects of hypercholesterolemia on healing of vascular grafts. *J Invest Surg*. 1991;4:299-312.
  47. Lee ES, Caldwell MP, Tretinyak AS, Santilli SM. Supplemental oxygen controls cellular proliferation and anastomotic intimal hyperplasia at a vascular graft-to-artery anastomosis in the rabbit. *J Vasc Surg*. 2001;33:608-13.
  48. Tolwani RJ, Yamamoto K, Waggie K, Green S, Otto G, Takahashi K, Rubinstein YD, Pratt RE. Hypothermia reduces neurologic deficits associated with placement of a vascular prosthesis in the abdominal aorta of rabbits. *Lab Anim Sci*. 1998;48:282-7.
  49. Nordestgaard AG, Buckels JA, Wilson SE. A laboratory model for the evaluation of thromboembolic complications of small diameter vascular prostheses. *Br J Exp Pathol*. 1986;67:839-49.
  50. van der Lei B, Robinson PH, Bartels HL, Wildevuur CR. Microarterial grafting into the carotid artery of the rabbit: some considerations concerning species-dependent thrombogenicity. *Br J Plast Surg*. 1989;42:59-64.
  51. Astrup T, Buluk K. Thromboplastic and Fibrinolytic Activities in Vessels of Animals. *Circulation Research*. 1963;13:253-260.

52. Zhang WD, Bai HZ, Sawa Y, Yamakawa T, Kadoba K, Taniguchi K, Masuda J, Ogata J, Shirakura R, Matsuda H. Association of smooth muscle cell phenotypic modulation with extracellular matrix alterations during neointima formation in rabbit vein grafts. *J Vasc Surg.* 1999;30:169-83.
53. Klyachkin ML, Davies MG, Svendsen E, Kim JH, Massey MF, Barber L, McCann RL, Hagen PO. Hypercholesterolemia and experimental vein grafts: accelerated development of intimal hyperplasia and an increase in abnormal vasomotor function. *J Surg Res.* 1993;54:451-68.
54. Davies MG, Huynh TT, Fulton GJ, Barber L, Svendsen E, Hagen PO. Early morphology of accelerated vein graft atheroma in experimental vein grafts. *Ann Vasc Surg.* 1999;13:378-85.
55. Lee ES, Bauer GE, Caldwell MP, Santilli SM. Association of artery wall hypoxia and cellular proliferation at a vascular anastomosis. *J Surg Res.* 2000;91:32-7.
56. Kreitmann B, Riberi A, Zeranska M, Novakovitch G, Metras D. Growth potential of aortic autografts and allografts: effects of cryopreservation and immunosuppression in an experimental model. *Eur J Cardiothorac Surg.* 1997;11:943-52.
57. Kazama S, Miyoshi Y, Nie M, Imai H, Lin ZB, Kurata A, Machii M. Protection of the Spinal Cord with Pentobarbital and Hypothermia. *Ann Thorac Surg.* 2001;71:1591-5.
58. AHA. American Heart Association. 2002 Heart and Stroke Statistical Update. In. Dallas, TX: American Heart Association; 2001.

59. Brooks VL, Kane CM, Welch LS. Regional conductance changes during hemorrhage in pregnant and nonpregnant conscious rabbits. *Am J Physiol.* 1999;277:R675-81.
60. Ueno T, Furukawa K, Katayama Y, Suda H, Itoh T. Spinal Cord Protection: Development of a Paraplegia-Preventive Solution. *Ann Thorac Surg.* 1994;58:116-20.
61. Cassel WS, Mason RA, Campbell R, Newton GB, Hui JC, Giron F. An animal model for small-diameter arterial grafts. *J Invest Surg.* 1989;2:181-6.
62. Sparks SR, Tripathy U, Broudy A, Bergan JJ, Kumins NH, Owens EL. Small-caliber mesothelial cell-layered polytetrafluoroethylene vascular grafts in New Zealand white rabbits. *Ann Vasc Surg.* 2002;16:73-6.
63. Pekar F, Grobe AC, Weber PA, Cheung DT, Duran CM. Improving Results of Small-Bore Vascular Graft Testing in Rabbits: A Technical Primer. *Contemporary Topics in Laboratory Animal Science.* 2004;43:25-27.



## Chapter II

### The effect of an increased inflammatory response on graft survival

#### Introduction

##### Inflammation

Within several minutes of injury, the vessels in the area of injury vasodilate (heat and redness) and become permeable, leaking fluid (edema) and leukocytes into the injured tissue. This leads to the activation of the clotting, kinin, and fibrinolytic cascades. Within several hours, neutrophils bind to the activated endothelium, extravasate into the surrounding tissues, and actively phagocytize invading organisms and release other inflammatory mediators, including MIP-1a and -1b (Macrophage Inflammatory Protein), which are responsible for attracting monocyte/macrophages into the area. Once present the macrophages are also responsible for phagocytosis and the release of further inflammatory mediators affecting coagulation, vascular permeability, and leucocyte chemotaxis. Eventually the offending stimulus is phagocytized or removed and the inflammatory response resolves. If the stimulus is not removed, the inflammatory response may proceed into a chronic inflammatory reaction.

Chronic inflammation can follow acute inflammation or can develop independently. Chronic inflammation may be a result of persistence of an infectious microorganism (e.g. tuberculosis), the presence of foreign bodies (e.g. surgical implants) or insoluble particles (e.g. silicosis), a persistent hypersensitive state (e.g. non-infective-allergic contact dermatitis, autoimmune-rheumatoid arthritis), or due to an unknown cause (e.g. Crohn's disease)<sup>1</sup>. Chronic inflammation is characterized by the presence of

an inflammatory infiltrate (macrophages, lymphocytes and plasma cells, not usually neutrophils), the formation of granulation tissue, fibrosis, and abnormal tissue remodeling. The presence of macrophage giant cells, generated by the fusion of activated macrophages, is indicative of an on-going chronic inflammatory reaction, and the type of giant cell present can serve as a preliminary indicator of the type of offending stimulus.

### **Modes of Graft Failure**

Implanted grafts are susceptible to failure via several mechanisms including thrombosis, intimal hyperplasia, atherosclerosis, and aneurysm. The primary cause of graft failure is thrombosis<sup>2,3</sup>. Thrombosis can also occur secondary to intimal hyperplasia and atherosclerosis as both are responsible for grafts stenosis which can result in thrombosis via the reduction of flow<sup>3</sup>. Thrombosis can also be a result of atherosclerotic plaque rupture, as the lipid core of an advanced plaque contains a large amount of tissue factor that can initiate the coagulation cascade leading to thrombus formation<sup>4</sup>. Grafts can also fail by aneurysmatic degeneration<sup>2</sup>.

### **Intimal Hyperplasia**

First described in 1906 by Carrel and Guthrie<sup>5</sup>, intimal hyperplasia can develop as a result of mechanical, chemical or immunological injury to a vessel or when vein grafts or prosthetic grafts are used<sup>6</sup> in clinical applications. Intimal hyperplasia is characterized by neointimal thickenings composed of smooth muscle cells and extracellular matrix which develop between the internal elastic lamina and endothelium (artery) or the endothelium and medial smooth muscle layer (vein). This is accomplished

by the proliferation of resident vascular smooth muscle cells and may also involve the migration of cells from surrounding tissue <sup>7</sup>.

While intimal hyperplasia is typically addressed as a pathological manifestation, derangement of the normal healing response or as a response to an insult, it does occur under normal conditions. It is responsible for the closure of the ductus arteriosus, the arterio-venous shunt bypassing the fetal lungs during gestation, allowing normal circulation and oxygenation of blood post-natally. It also occurs as a part of the normal aging process and is seen as diffuse thickenings in the vasculature or at sites of turbulence in the flow of blood at points where vessels branch (often referred to as adaptive intimal thickenings).

Intimal hyperplasia appears to be linked to an inflammatory response as an infiltration of mononuclear cells and T cells is a common finding. Cytokines from these inflammatory cells may be responsible for initiating and supporting the proliferation and migration of smooth muscle cells and the deposition of extracellular matrix. Research has shown a strong correlation between the severity of the inflammatory response and the ultimate severity of the hyperplasia, and reducing the inflammatory response like-wise reduces intimal hyperplasia <sup>8-10</sup>. Intimal hyperplasia may also play a role in the development of atherosclerosis <sup>7,11-13</sup> while hypercholesterolemia increases the development of intimal hyperplasia <sup>14-16</sup>. This process also contributes to the failure of vascularized organ transplants and venous conduits used as bypass grafts <sup>7</sup>.

## **Atherosclerosis**

Atherosclerosis is primarily a disease of the large arteries and is the most significant cause of heart disease and strokes in westernized societies, accounting for 50% of all deaths<sup>17</sup>. Risk factors associated with the development of atherosclerosis include high levels of lipoproteins, genetic predisposition, sedentary life-style, obesity, and smoking<sup>18-20</sup>. This condition is characterized by the progressive accumulation of lipid-laden macrophage-derived foam cells in the arterial wall, proliferation of smooth muscle cells and foam cells, and the abnormal deposition of extracellular matrix. The apoptosis of foam cells releases the intracellular oxidized lipids into the surrounding tissue that ultimately results in the formation of a necrotic lipid pool. These atherosclerotic plaques in latter stages of the disease can encroach on the lumen of the vessel causing a progressive stenosis. Both the rupture of a plaque releasing the necrotic lipid core or the development of an advanced stenosis can lead to thrombosis of the affected vessel. Atherosclerosis also affects vascular grafts (both artery and vein) and can lead to graft failure directly (by the rupture of an advanced lesion resulting in thrombosis) or indirectly (due to plaque formation causing a stenosis which reduces flow, leading to thrombosis).

Macrophages play an important role in the development and progression of atherosclerosis<sup>12,21,22</sup> which can also be considered a chronic inflammatory response<sup>23-28</sup>. The lesions produced during the evolution of atherosclerosis are dominated by macrophages, and the severity of the disease appears to be linked to the prominence of these cells. Activated T cells are also a significant component of atherosclerotic lesions, and the presence of T cells and macrophages suggests that a cell-mediated inflammatory

response may play a role in atherosclerosis, with the macrophages functioning as antigen presenting cells for T cells<sup>29</sup>. Using a rat model of diet-induced atherosclerosis, T cell infiltration was most significant within two weeks of initiating the hypercholesterolemic diet, making up 60%, 29% and 34% of the infiltrating cells in lesions of the superior thoracic, inferior thoracic and abdominal aorta, respectively<sup>26</sup>. The secretory products of macrophages and T cells have been implicated in the cellular responses that occur throughout lesion formation<sup>17,30</sup>. For example, Interferon  $\beta$  from activated T cells causes smooth muscle cell apoptosis, inhibits collagen synthesis by smooth muscle cells, and increases MMP release from foam cells, all which contribute to a reduction in the amount of extracellular matrix and increased matrix degradation seen in atherosclerosis<sup>31</sup>.

### **Aneurysms**

Aneurysm development has also been characterized as a chronic-type inflammatory response<sup>32-34</sup>. Four major factors have been implicated in the formation of an aneurysmatic lesion: degradation of aortic wall tissue, inflammation and immune response, wall stress, and predisposing genetic factors<sup>34</sup> however the initiating stimulus for aneurysm formation is yet unclear. The formation of an aneurysm<sup>35-37</sup> is characterized by dilation of the affected vessel, remodeling of the vessel wall with destruction of elastin and abnormal deposition of collagen, and an extensive chronic inflammatory infiltrate of macrophages and T cells<sup>38,39</sup> with associated elevated production of matrix metalloproteases (MMPs)<sup>38,39</sup>.

The inflammatory infiltrate is thought to play a causative role in aneurysm formation by stimulating the secretion of MMPs and by releasing cytokines that induce

the production of MMPs by activated *in situ* mesenchymal cells and phagocytic cells<sup>40</sup>. The dilation is often attributed to the loss of elastic tissue due to breakdown of this component by matrix metalloproteases (MMPs) which are increased in human aneurysm tissue<sup>35,36,38,39</sup> and animal models of aneurysm<sup>40</sup>. Models of aneurysm formation have shown that attenuating the inflammatory response inhibits further dilation while increasing inflammation augments the development<sup>38</sup>. Elevated plasma levels of MMPs are also seen in patients with abdominal aortic aneurysms and appear to correlate with elevated tissue levels of MMP in affected tissue<sup>36</sup>.

### **The Role of Inflammation in Vascular Diseases**

Inflammation has been linked to the development of vascular conditions such as intimal hyperplasia<sup>7,41</sup>, atherosclerosis<sup>23-28</sup> and aneurysm<sup>32-34</sup>. In these conditions there is a response involving resident and inflammatory cells, matrix metalloproteases (MMPs) and the extracellular matrix, resulting in abnormal matrix remodeling with thinning (aneurysm)<sup>35-39</sup> or excessive/abnormal deposition (atherosclerosis and intimal hyperplasia)<sup>17,27,29</sup>.

Levels of inflammatory markers (especially C-reactive protein (CRP), but also IL6, TNF $\alpha$  and adhesion molecules) have been used as indicators of cardiovascular disease and levels correlate well with the severity of the disease and may also be predictive of future events<sup>42-44</sup>. CRP level were elevated in Intimal Hyperplasia<sup>45</sup>, Atherosclerosis<sup>43,46,47</sup>, Aneurysm<sup>48,49</sup>, indicating an ongoing inflammatory response in each of these conditions. CRP levels have also been linked to thrombosis<sup>50,51</sup>.

Jabs *et.al.* <sup>45</sup> examined samples of normal and diseased vessels as well as diseased coronary bypass grafts for the presence of CRP. Their results showed the presence of CRP protein in 82% of diseased coronary arteries and in 100% of the diseased bypass grafts. These observations implicate inflammation in the failure of grafts implanted into the circulation.

Since intimal hyperplasia, atherosclerosis, aneurysm and thrombosis have been linked to the failure of vascular grafts implanted into the circulation, and in each condition an important marker of inflammation is elevated, leading to the hypothesis that **inflammation plays a key role in vascular graft failure.**

### **Models of Human Disease**

Many animal models have been adapted to approximate human vascular disease and have been used with great success (e.g. Atherosclerosis; diet-induced without injury <sup>52,53</sup>, with injury for advanced lesion formation by balloon or catheter denuding <sup>54,55</sup>; Aneurysm formation; CaCl<sub>2</sub> application <sup>33</sup>, Elastase perfusion model <sup>56-58</sup>; Intimal Hyperplasia; Grafting <sup>59-61</sup>, Injury <sup>55,62</sup>). However, one must always remember that they are an artificially created condition that does not spontaneously/normally occur in the particular model. Physical and physiological parameters of the model must be carefully evaluated and compared to the human system they are to represent.

### **Increasing Inflammation via Hypercholesterolemia**

Inflammation has been linked to the development of atherosclerosis <sup>23-28</sup> and previous work with animal models has shown that inflammation and the development of

atherosclerosis are linked <sup>28</sup>. This is supported by observations that endothelial cells become activated and express adhesion molecules which allow for the binding and transmigration of monocytes, and these areas of activated endothelial cells correspond to areas of developing atheroma. Once in the vessel media, these macrophages differentiate into foam cells and contribute to the development of a chronic-type inflammatory response <sup>26-28</sup> leading to complex lesions involving endothelial cells, macrophages, T cells, and smooth muscle cells. In atherosclerosis, macrophage-derived foam cells are the main component of lesions and are involved in the development and progression of the disease <sup>12,21,22,63</sup>.

Published studies suggest that the production of MMPs as well as MMP activity are increased by atherosclerosis. In a study by Galis *et.al.* <sup>64</sup>, foam cells isolated from rabbit atheroma were shown to produce MMPs constitutively when compared to alveolar macrophages isolated from the same animal. Both stimulated and unstimulated foam cells synthesized and released MMPs *in vitro* while alveolar macrophages did not, and stimulation caused the foam cells to release additional MMPs <sup>64</sup>. Hypercholesterolemia has been shown to cause the increased secretion of MMP-2 and -9 in the aortas of cholesterol-fed rabbits <sup>33,65</sup> which has been associated with the formation of abdominal aortic aneurysms. MMP-2 production and binding to the aortic matrix has been shown to be increased in abdominal aneurysm formation in human samples <sup>66</sup> and circulating levels of MMP-9 have been associated with abdominal aortic aneurysms <sup>67</sup>. Also partially digested fragments of ECM have been shown to induce an inflammatory response by calling in lymphocytes, monocytes and PMNs <sup>40</sup>.



Atherosclerosis is considered the primary cause of aneurysm development in humans as atherosclerotic changes were seen in aneurysm tissue, there was an association between aneurysm diameter and adventitial inflammation, and hypercholesterolemia plays an important role in monocyte/macrophage chemotaxis and activation<sup>33</sup>. In humans, injury to the media caused by atherosclerosis, hypertension, smoking, genetic factors, etc. that damaged the elastic components of the vessel, in conjunction with alterations in the elasticity of the aorta due to pulse pressure, were considered critical for aneurysmal dilation<sup>33</sup>. In a study by Freestone *et.al.*<sup>33</sup>, both hypercholesterolemia and adventitial inflammation both played a role in aneurysm development in rabbit vessels.

**Specific Aim: To evaluate the role of increased inflammation via an atherogenic diet on the xenogenic graft material.**

### **Rationale**

Previous studies have shown that feeding rabbits a diet supplemented with cholesterol leads to the development of atherosclerosis<sup>52-54,68-70</sup> that is similar to atherosclerosis in humans<sup>71,72</sup>. Since hyperlipidemia has been linked to the accelerated development of atherosclerosis in prosthetic and vein grafts<sup>14,16,73,74</sup>, and atherosclerosis is considered an inflammatory disease<sup>28</sup>, it was hypothesized that by inducing atherosclerosis via a hypercholesterolemic diet in the rabbit model described in the previous section, the severity of inflammation could be increased towards the Corograft<sup>TM</sup> conduit and the effect of increased inflammation on the vascular graft could be assessed.

## **Experimental Design**

In this portion of the study, 26 rabbits were divided into two groups. Thirteen rabbits were fed a commercially available rabbit chow and thirteen were fed rabbit chow containing 1% cholesterol for 3 months prior to surgery. Blood samples were collected on a weekly basis and the serum cholesterol levels analyzed. Rabbits fed a cholesterol diet had serum cholesterol levels well above normal, while normal diet rabbits showed no increase. After 3 months of the diet, grafts were implanted into the abdominal aorta and the rabbits continued on the respective diets. The grafts were harvested at 2, 4 and 6 months and analyzed by histology and immunohistology. Also, zymograms for MMP activity and a Humoral ELISA were performed on surgery and sacrifice serum samples. As atherosclerosis is considered an inflammatory disease, the presence of atherosclerotic type lesions within the vasculature or the graft material would be used as an indicator of increased inflammation. CRP levels were to be analyzed but proved to be prohibitively expensive and were not done.

## Materials and Methods

### Animal Source and Care

Female New Zealand White rabbits (*Oryctolagus cuniculus*) were obtained from Western Oregon Rabbit Company (Philomath, OR, USA) and were allowed to acclimate for at least 14 days before initiating any procedures. Rabbits were fed either normal rabbit chow (Laboratory Rabbit Diet HF, #5326, Lab Diet, Richmond, ID, USA) or chow with 1% cholesterol added, and water *ad libitum* throughout the duration of the study. Average room temperature was 63°F (17-18°C), with a 12hr day/night cycle and 10-12 air changes/hr. All animals appeared clinically normal throughout the 14-day quarantine period and no other pathogen testing was done. Venous blood samples were collected weekly prior to surgery and monthly after surgery for serum cholesterol levels.

### Preoperative Preparation

Rabbits were sedated with an intramuscular dose of ketamine (50mg/kg), the abdominal region shaved, and the rabbit placed in a dorsal recumbent position on a heating pad (heating pad was off during the hypothermic phase of the surgery). Anesthesia was induced and maintained with 1.5-2% Isoflurane/Oxygen mixture administered via a ventilator/anesthesia delivery system (North American Drager, Telford, PA, USA or Isotec 4, Surgivet/Anesco Veterinary Surgical Products, Waukesha, WI, USA), and the level of isoflurane was adjusted as needed to keep the animal sufficiently anesthetized, as evaluated by ear pinch or any evidence of discomfort. The chest cavity was not opened allowing for passive, spontaneous ventilation by the animal<sup>75,76</sup>. The core temperature was monitored with a rectal temperature probe and

electrocardiographic leads were attached so the heart rate could be monitored. Icepacks were placed around and between the hind-legs and along the lower flanks. An intravenous cannula (22 gauge) was introduced into the marginal ear vein and cold (4°C) supplemented Lactated Ringer's Solution was given initiating the hypothermic phase of the surgery. The supplemented Lactated Ringer's solution contained per liter: 20ml sodium bicarbonate (84mg/ml and 50mEq/50ml, American Pharmaceutical Partners, Inc. Los Angeles, CA, USA), 50ml of 20% mannitol solution and 0.5ml dexamethasone sodium phosphate (4mg/ml, American Regent Laboratories, Shirley, NY, USA).

### **Surgical Protocol**

After sterile draping, a midline laparotomy was performed. The skin was retracted with traction sutures and the intestines were displaced to the right side and wrapped in laparotomy sponges moistened with cold sterile saline. Isolation of the abdominal aorta from the surrounding tissues from below the left renal artery to the iliac bifurcation was performed meticulously to avoid accidental injury to the inferior vena cava and its branches. Care was taken to identify all aortic branches along the entire circumference. If feasible, anastomotic sites were planned to avoid cutting of the large dorsal aortic branches. Once all dissection was completed, one ml of heparin was administered i.v. (1000 USP units/ml, American Pharmaceutical Partners, Inc., Los Angeles, CA, USA) and if necessary, further cooling of the animal was achieved by using sterile saline slush applied directly into the abdominal cavity and to the laparotomy sponge covering the intestines.

When the rectal temperature of the animal reached 34.5°C, the ice packs and the saline slush were removed as the temperature continued to drop without additional cooling. The cold supplemented Lactated Ringer's solution was exchanged for warm (37°C). Also, warm packs were placed next to the rabbit under the sterile draping and the heating pad under the rabbit was switched on to start the re-warming phase of the procedure initiating the re-warming period of the surgery.

Dorsal aortic branches within the previously prepared aortic segment were clipped and cut. The aorta was occluded proximally and distally with micro-surgical vascular clamps (MORIA 200/A, Angled, 30mm. Fine Science Tools, Inc. Foster City, CA, USA) placed below the left renal artery and above the inferior mesenteric artery. And keeping in mind the elastic recoil of the vessel, the aorta was cut approximately 1 cm from each clamp to avoid space issues.

All animals had a Corograft™ (~3-4mm ID x ~4cm minimum) previously re-hydrated in heparinized saline, implanted into the infrarenal abdominal aorta. An end-to-end anastomosis (distal then proximal) was performed with a continuous single 8/0 Prolene suture (Polypropylene, Ethicon, Inc., Somerville, NJ, USA). Before tying the suture for the proximal anastomosis, the distal vascular clamp was removed to flush air from the graft by filling the graft with blood to avoid an air embolism. After tying the suture, the proximal vascular clamp was removed and additional 8/0 Prolene suture used (as needed) to control anastomotic or graft bleeding.

The intestines were returned to the abdominal cavity and repeatedly lavaged with warm sterile saline to achieve appropriate re-warming of the animal. When the rectal temperature of the rabbit reached 36.5°C to 37.5°C, the saline was removed and the

laparotomy closed in two layers with 3/0 Vicryl (Polygalactin 910, Ethicon, Inc., Somerville, NJ, USA). The supplemented Lactated Ringer's solution was discontinued, with a total amount of 100-150ml having been administered for both the cold and warm solutions. When the animal was re-warmed to physiological temperature (101-104°F/38-40°C) and movement was seen in the hind-limbs, the animal was returned to its' cage.

Rabbits received 0.2ml flunixin meglumine (50mg/ml, Equileve®, Phoenix Scientific, Inc., St. Joseph, MO, USA) i.m. as an analgesic immediately after surgery, and 0.2ml i.m. flunixin meglumine BID for 4 days post-operatively. All rabbits were monitored for neurologic or ischemic complications of the hind limbs throughout the study. No antibiotic prophylaxis, platelet aggregation inhibitors nor anticoagulants were used postoperatively.

### **Sacrifice**

The animals were sedated and brought to a full surgical plane of anesthesia. The abdominal incision was re-opened and the graft dissected from surrounding tissues. Once isolated, the rabbits were fully heparinized and then sacrificed. The graft was then excised en-bloc and placed into Histo-Choice Tissue Fixative MB (Amresco Inc., Solon, Ohio, USA) for a minimum of 24hrs before further processing.

### **Macroscopic Examination**

Excess non-adherent tissue/fat was trimmed from the exterior of the graft and the graft was photographed with markers placed indicating the suture lines and direction of flow. Each graft was evaluated macroscopically for aneurysmatic changes (indicated by

an area of vessel wall ballooning outwards and being of a greater diameter than the originally implanted graft), atherosclerotic lesions, thrombus, or any other obvious abnormalities.

### **Histology**

Samples (2-3mm) cut from the center of the graft were dehydrated and embedded in PolyFin wax (Polysciences, Inc., Warrington, Pennsylvania, USA), sectioned at 5 $\mu$ m, and collected on slides coated with poly-L-lysine (Sigma Chemical Co., St. Louis, MO, USA) or charged slides (Superfrost<sup>®</sup> plus, VWR Scientific, West Chester, PA, USA). Representative sections were stained with hematoxylin and eosin (H&E) for general tissue/cellular morphology, Masson's Trichrome for collagen and Movat's Pentachrome stain for collagen and elastin.

### **Immunohistology**

Slides for immunohistology were prepared as above. Representative sections were stained for  $\alpha$ -smooth muscle cell actin (a smooth muscle cell/myofibroblast marker), CD3 (pan-T cell antibody) and RAM 11 (rabbit macrophage-specific antibody). Sections stained for  $\alpha$ -SMC actin were deparaffinized, treated with 3% H<sub>2</sub>O<sub>2</sub> for 5min to remove endogenous peroxidases, rinsed with dH<sub>2</sub>O and blocked with 0.05% Tween-20 (Sigma Chemical Co., St. Louis, Missouri, USA) in phosphate buffered saline (PBS-T) for 30min. The slides were incubated for 30min with the appropriate primary antibody diluted in PBS-T, then rinsed with PBS-T. Sections stained for  $\alpha$ -actin were incubated with Protein A-horseradish peroxidase (Sigma Chemical Co., St. Louis, Missouri, USA),

1:500 dilution in PBS-T for 30min. Sections stained for rabbit macrophages (RAM 11) and T cells (CD3) were treated with the components of the LSAB-2 biotin-streptavidin amplification kit (DAKO, Carpinteria, California, USA) according to the supplied instructions with the incorporation of an avidin/biotin blocking procedure. All incubations were carried out in a moist chamber at room temperature. Sections were rinsed with PBS-T and developed by the addition of 100µl of DAB substrate (Sigma Fast DAB, Sigma Chemical Co., St. Louis, Missouri, USA) per slide. The development was stopped with water and the slides counterstained with H&E or hematoxylin alone. The slides were dehydrated, cleared and coverslipped.

Antibody to:	Clone	Dilution	Development	Source
α-Smooth Muscle Cell Actin	1A4	1:400	Protein A-HRP	Sigma
Rabbit Macrophage	RAM 11	1:500	LSAB-2	Dako
T Cell/CD3	Rbt poly	1:50	LSAB-2	Dako

### Macrophage Counts

Macrophages are involved in the inflammatory response toward the graft and in the development and progression of atherosclerosis, and the numbers present were used as an indirect indicator of disease severity and inflammation. Slides stained with the RAM11 antibody were used in this portion of the study. Five random 100X fields were photographed at the junction between graft tissue and abluminal tissue where the majority of the macrophages were located. The number of macrophages and giant cells were counted per image and averaged to obtain the count.



## Zymography

Matrix metalloproteinases (MMPs) are produced by macrophages and other cell types as part of an inflammatory response and could be involved in graft degeneration, therefore pre- and post-operative serum samples were qualitatively evaluated for circulating MMP levels. The conditions present during zymography allow for the detection of both the pro-forms and activated MMPs, due to the dissociation of the active MMPs from inhibitors or the spontaneous activation of zymogens<sup>65,77</sup>.

Serum samples were electrophoresed on 10% polyacrylamide gels containing 1mg/ml Gelatin or Elastin. The samples were diluted 1:10 (v:v) with saline and then 1:1 with 2X Non-denaturing Sample Buffer (no  $\beta$ -Mercaptoethanol), 20 $\mu$ l loaded onto the gel and run at 200 V until completion. The gels were washed 2X 30 min with 2.5% Triton X-100/dH<sub>2</sub>O with agitation, washed 30 min with RT Activation Buffer with agitation, and then incubated O/N in Activation Buffer at 37°C with agitation (Activation buffer 25mM Tris, 10mM CaCl<sub>2</sub>, 1 $\mu$ M ZnCl<sub>2</sub>, 50mM NaCl, pH 7.5). Gels were stained with coomassie brilliant blue and areas of gelatinolytic or elastolytic activity were seen as clear bands against a blue background. The gels were then visually inspected for differences.

MMP activity was confirmed by incubating the gels in the presence of 1mmol/L 1,10-phenantroline (MMP inhibitor) in the activation buffer in both the 30 minute wash and overnight incubation<sup>32</sup>.

## **ELISA for Humoral Response**

Dry graft material was lyophilized to a constant weight, suspended in 1% acetic acid at a concentration of 1mg/ml (w/v) and homogenized. The material was diluted to ~250ug/ml with 0.02M Carbonate buffer (pH 9.6) and 100ul (~25ug/well) of collagen was added to each well of a 96-well plate (Falcon PRO-BIND™, Becton Dickinson and Company, Franklin Lakes, NJ, USA). The plates were evaporated to dryness overnight at room temperature in a hood. Before use, the plates were washed 4X with PBS-T and blocked for 45 min RT (or O/N at 4°C) with 100ul PBS-T/1% BSA per well. The wells were then rinsed 4X with PBS-T and serial 2-fold dilutions of serum were plated in PBS/1% BSA (50ul/well in duplicate). The plates were incubated at RT for 1hr and washed 4X with PBS-T. Anti-Rabbit IgG-HRP (Monoclonal Anti-Rabbit IgG  $\gamma$ -chain specific, Clone RG-96, Peroxidase Conjugate A-1949, Sigma-Aldrich Co, St Louis, MO, USA) was diluted 1:40,000 in PBS-T/1% BSA and 50ul/well was added. The plate was incubated 2hrs at RT and washed 4X with PBS-T. OPD substrate (HRP substrate, Dako Corporation, Carpinteria, CA, USA) was prepared according to the manufacturers instructions (dissolved in room temperature dH<sub>2</sub>O and 30% H<sub>2</sub>O<sub>2</sub> added) and 50ul of the substrate solution was added to each well. The color was allowed to develop 30min at room temperature and the reaction stopped by the addition of 50ul of 0.5M H<sub>2</sub>SO<sub>4</sub> to each well. The absorbance was read at 490nm in a microplate reader (Opsys MR, Dynex Technologies, Chantilly, VA, USA).

Normal rabbit serum was included as the negative control and the values obtained used to adjust for serum absorbance. In all cases the OD value from the normal rabbit

serum was subtracted from the mean valued obtained for the corresponding dilutions of the experimental samples. The titer listed is derived from the last well giving a positive OD after adjustment. Blank values were obtained from wells incubated with PBS-T/1% BSA instead of serum and subtracted from all OD values by the microplate reader software.

## Results

### Post-Operative Survival and Graft Patency

**Normal Diet Rabbits:** Thirteen female New Zealand White rabbits were operated and a small-diameter bovine conduit (internal diameter of 3-4mm) was implanted into the infrarenal abdominal aorta. All grafts were patent immediately after implantation as demonstrated by a visible and palpable pulse, and at sacrifice at 2 (n=3), 4 (n=4), and 6 months (n=3).

Hind-limb paraparesis developed in one rabbit within the first postoperative day and the animal died the third postoperative day. One rabbit became ischemic and was euthanized six days post-operatively. Post-mortem examination did not show graft occlusion. One animal developed bilateral dry ulcerations of the footpad. One rabbit died suddenly at 5 months and post-mortem examination revealed intestinal ischemia and graft thrombosis.

**Cholesterol Diet Rabbits:** Sixteen rabbits were operated and had a small-diameter bovine conduit (internal diameter of 3-4mm) was implanted into the infrarenal abdominal aorta. All grafts were patent immediately after implantation as demonstrated by a visible and palpable pulse. Two rabbits died perioperatively due to complications with anesthesia, one was euthanized due to a spinal injury, and two were euthanized due to paralysis on day 2 and day 4. Five rabbits died on day 1 (n=2), day 2 (n=2), and day 3 (n=1) of unknown causes. Five additional rabbits died of a massive hemorrhage on day 6, 14, 15, 20, and 46. One rabbit survived to 73 days and was sacrificed.

### **Normal diet samples macroscopic**

**Normal Diet 2 months:** Vascular grafts (Corograft™, L and D-Hydro™ treated bovine artery) implanted into the abdominal aorta of the three rabbits (G5824, G5827, and G5828) were slightly dilated on explant. One explanted graft (G5824) had an outpocketing near the distal suture line, the second graft (G5827) had the same and a few thin portions of the graft wall, and the third graft (G5828) did not have any visible thin spots, but the proximal suture line was constricted (**Figure 1-1: 2Mo Macroscopic**).

**Normal Diet 4 months:** One graft (G5586) appeared normal, with a diameter slightly larger than the abdominal aorta, the other three grafts (G5830, G5831, G5832) had large dilated areas, but did not appear to be aneurysmatic (**Figure 1-2: 4Mo Macroscopic**).

**Normal Diet 6 months:** The three explanted grafts (G5581, G5587, and G5588) were normal in appearance, with no visible areas of dilation (**Figure 1-3: 6Mo Macroscopic**).

### **Un-Implanted Graft Histology**

Re-hydrated, un-implanted Corograft™ material was fixed, paraffin embedded, sectioned, and stained with H&E (**Figure 2: Corograft™ Histology**). The histology shows the structures present in a healthy small artery. The graft intima extends from the internal elastic lamina to the luminal surface, and after processing the graft material is devoid of endothelial cells and only the basement membrane remains. The media is defined by the internal elastic lamina and the more diffuse external elastic lamina and contains collagenous fibers, elastic fibers and remnants of smooth muscle cells arranged in a

Figure 1-1: Macroscopic evaluation of samples explanted from 2 month normal diet rabbits. Excess tissue was trimmed from the graft exterior and the graft photographed. The graft was then opened longitudinally along the ventral aspect, pinned open and photographed. Any aneurysmatic changes, atherosclerotic lesions, thrombus, or areas of dilation were noted. Grafts are shown in both an external and internal view. All grafts were slightly dilated upon explant. Several areas of G5824 and G5827 were more dilated and appeared as outpocketings (\*). Diagonal arrows indicate the constriction of the proximal suture line in G5828. ↑ Arrows indicate the suture lines. → Arrow indicates the direction of blood flow.

Figure 1-1: 2 month Macroscopic

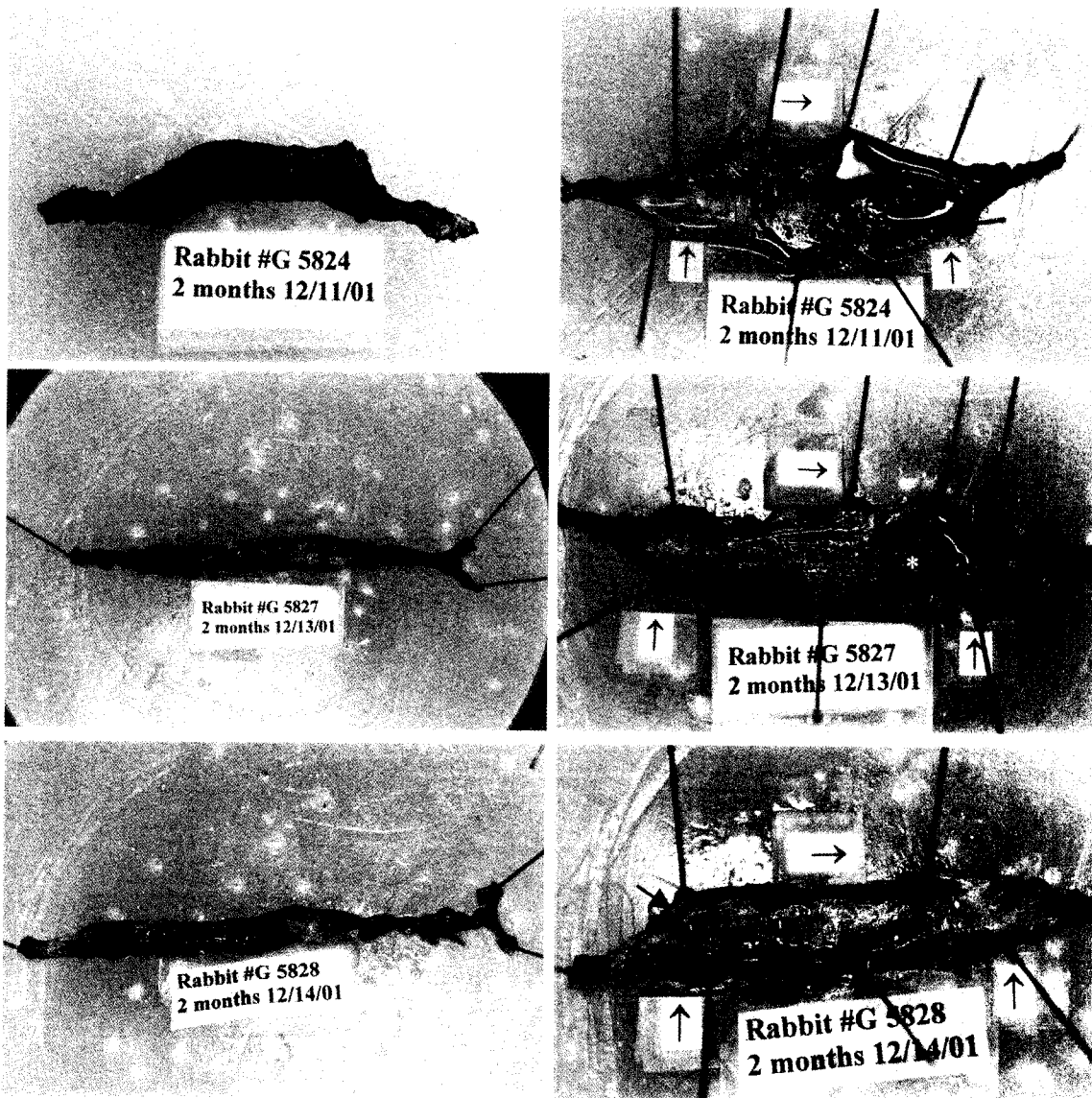


Figure 1-2: Macroscopic evaluation of samples explanted from 4 month normal diet rabbits. Excess tissue was trimmed from the graft exterior and the graft photographed. The graft was then opened longitudinally along the ventral aspect of the graft, panned open and photographed. Any aneurysmatic changes, atherosclerotic lesions, thrombus, or areas of dilation were noted. Grafts are shown in both an external and internal view. All grafts were dilated on explant and G5830, G5831 and G5832 had further areas of areas of dilation that appeared as outpocketings (\*). ↑ Arrows indicate the suture lines. → Arrow indicates the direction of blood flow.



Figure 1-2: 4 month macroscopic

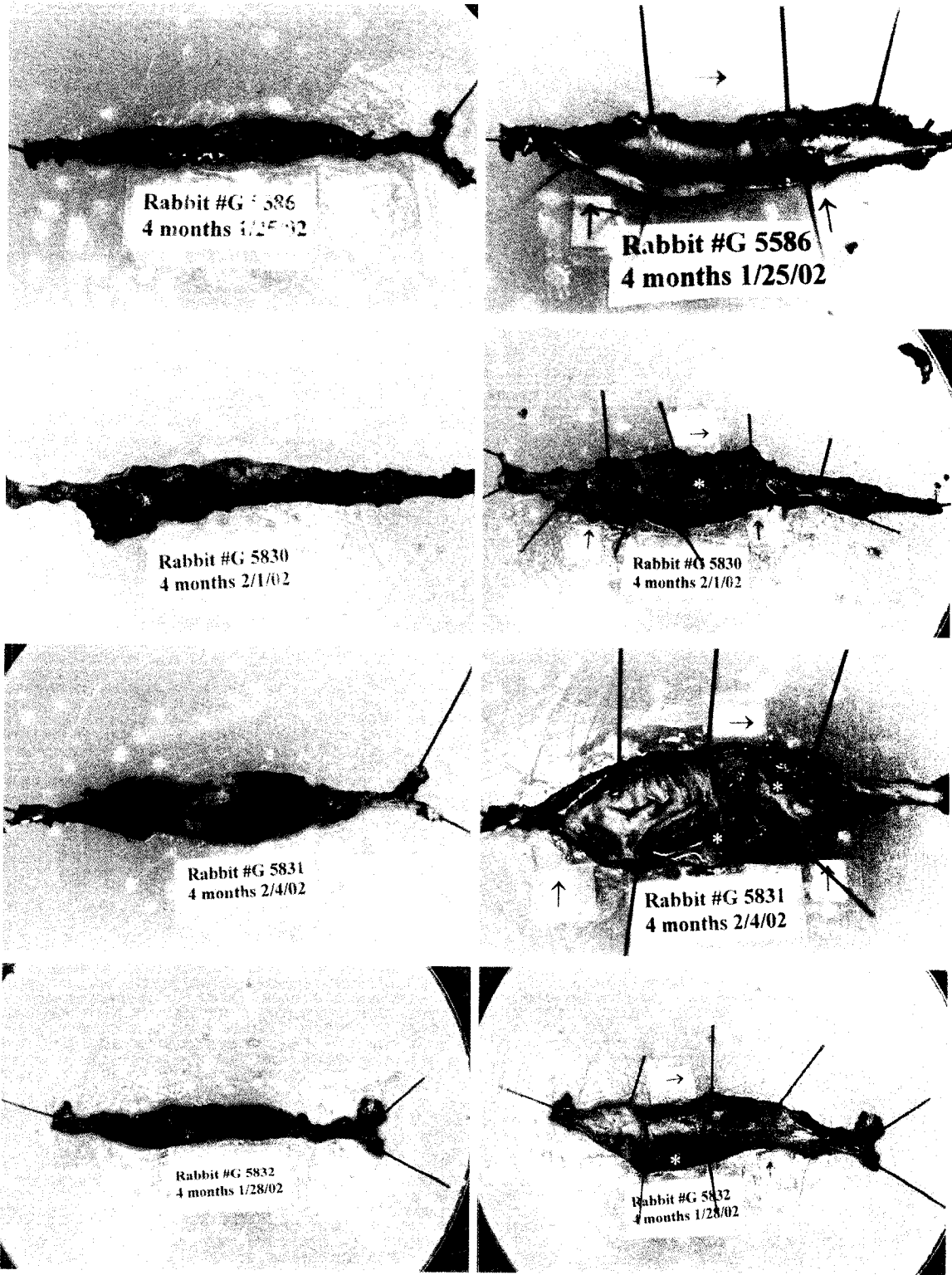
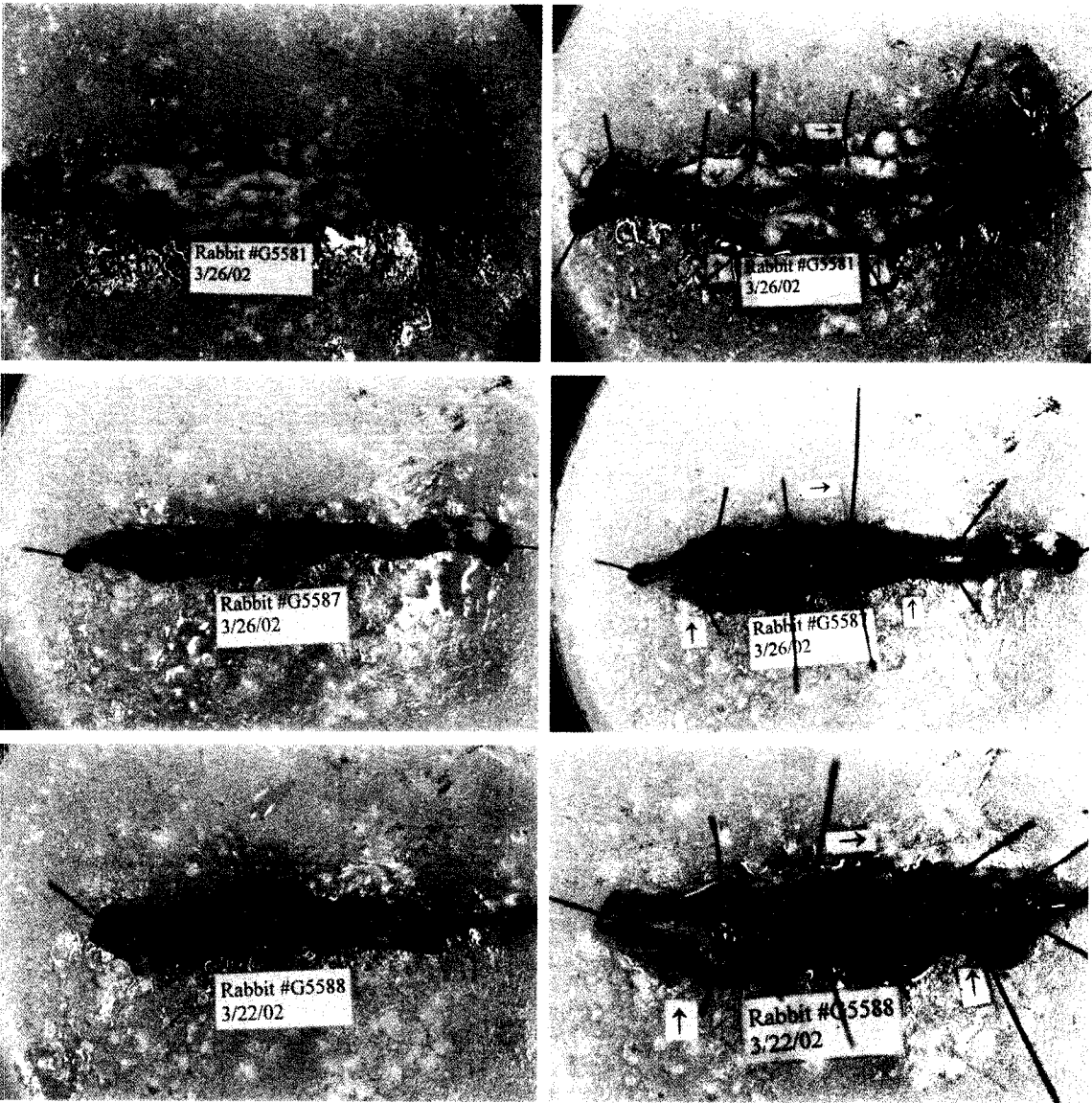


Figure 1-3: Macroscopic evaluation of samples explanted from 6 month normal diet rabbits. Excess tissue was trimmed from the graft exterior and the graft photographed. The graft was then opened longitudinally along the ventral aspect of the graft, pinned open and photographed. Any aneurysmatic changes, atherosclerotic lesions, thrombus, or areas of dilation were noted. Grafts are shown in both an external and internal view. None of the explanted grafts were dilated upon examination. ↑ Arrows indicate the suture lines. → Arrow indicates the direction of blood flow.

Figure 1-3: 6 month macroscopic



circumferential manner. The adventitia is located abluminal to the external elastic lamina where the collagenous fibers appear more longitudinal, have a looser arrangement and are interspersed with elastin fibers that appear more globular in cross section. The nuclei seen within the graft tissue are remnants from the original cells, as this graft is not extracted with detergents or enzymes to remove these cellular components. All further descriptions of implanted graft material will be described with respect to these structures, and where possible the original graft material will be differentiated from host-derived cellular ingrowth and tissue deposition.

### **Histology of Explanted Samples from Normal diet Rabbits**

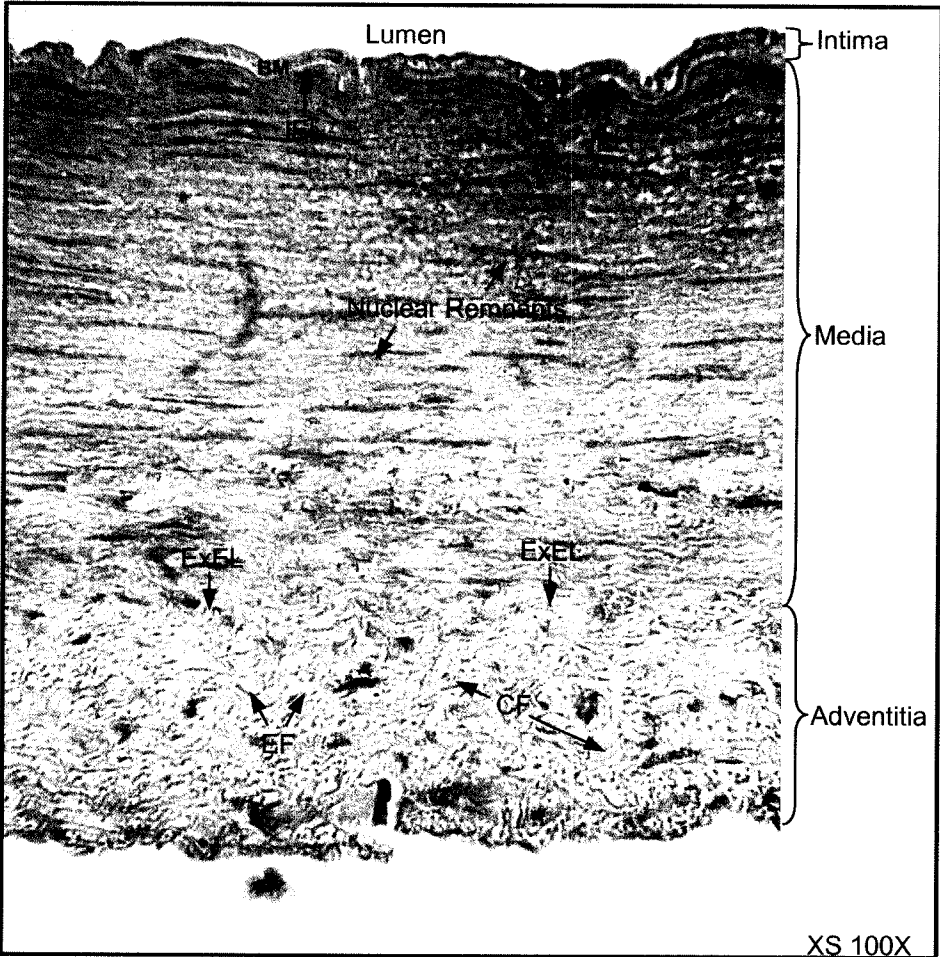
#### **Normal Diet 2 Months (Figure 3: 2Mo Histology)**

The graft matrix was well preserved in G5824 and less organized in G5727 and G5828, and was re-colonized by host cells in all samples. An abluminal layer of tissue was present to the exterior of the grafts composed of loose collagenous tissue, blood vessels, adipose tissue, some giant cells and various other cells. The graft from G5824 had a layer of tissue of variable thickness present on the luminal surface of the graft that contained some red and white blood cells (**Fig. 3-1A**). In G5824 and G5828, a thin layer of cells staining for  $\alpha$ -smooth muscle cells actin were seen located on and just below the luminal surface of the graft, and were present for about a third of the circumference (**Fig. 3-2A&C**). Additional weak actin staining was seen within the graft tissue, but appeared to be remnants of the original actin present prior to processing, as staining was not well-defined, non-specific in nature, not limited to specific cells, and present in the areas comprising the original media. In G5827, the actin staining was confined to several small

Figure 2: H&E of reconstituted unimplanted Corograft™ material. The three major layers of a small artery are clearly visible: the intima, media, and adventitia. The graft intima is composed of the basement membrane sitting on top of the internal elastic lamina. The media is defined by the internal and external elastic laminae. The adventitia is located abluminal to the external elastic lamina. Collagen stains pink, Elastin does not stain and appears as translucent refractive structures.

IEL, Internal Elastic Lamina; ExEL, External Elastic Lamina; CF, Collagen Fibers; EF, Elastic Fibers; BM, Basement Membrane.

Figure 2: Unimplanted Corograft Histology



blood vessels in the adventitia and the occasional actin remnant within the graft (**Fig. 3-2B**). In G5824 and G5827, macrophages and giant cells were located at the interface between the graft tissue and the abluminal layer, and in G5828 formed a complete ring around the graft tissue and were also bound to about a third of the luminal surface on the more ventral aspect of the graft (**Fig. 3-1 A, B and C**). Trichrome staining showed relatively well preserved/organized collagen within the graft in G5824 with some more lightly stained area which appeared to be expanded due to cellular ingrowth, while in G5827 and G5828 the graft collagen was expanded and interspersed with less mature collagen, and little of the original collagen remained (**Fig. 3-3 A, B and C**). Movats of G5824 showed that elastin was present within the graft tissue and the internal elastic lamina was present. In G5827 and G5828, the internal elastic lamina was no longer present, elastin fibrils were present in the medial (circumferential) layer, but the majority of the adventitial (longitudinal) layer and associated elastin was present in G5828 but missing in G5827. CD3+ cells were present within the abluminal layer scattered throughout the tissue.

#### **Normal Diet 4 Months (Figure 4: 4Mo Histology)**

The graft matrix was well preserved in all samples, and appeared as two distinct layers, a more cellular medial layer lumenally and a less cellular adventitial layer more abluminal. For samples G5586 and G5830, the graft was recolonized with cells throughout the thickness with the majority of the cells present within the medial layer, while in G5831 and G5832 the cellularity was evenly distributed throughout the graft tissue (**Fig. 4-1A to D**). A relatively thin layer of tissue was present to the exterior of the

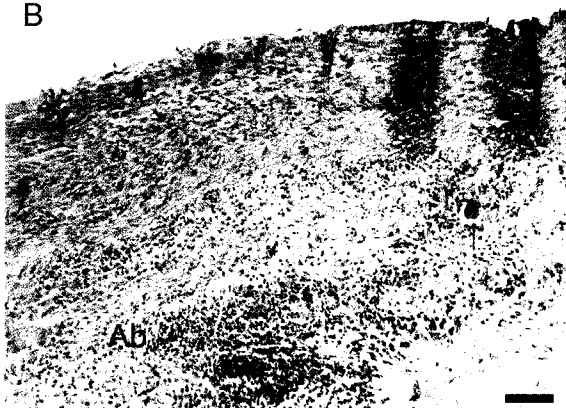
Figure 3-1: 2 month normal diet samples were embedded and 5 $\mu$ m sections were stained with H&E for general tissue morphology and cellularity. All grafts were re-colonized by host-derived cells. All grafts had a host-derived abluminal layer containing loose collagenous tissue, blood vessels, adipose tissue, some giant cells and various other cells (Ab). G5824 had a luminal layer containing some red and white blood cells ( $\downarrow$ ). G5824, G5827 and G5828 had macrophages and giant cells ( $\uparrow$ ) located at the interface between the graft and the abluminal tissue. Scale bar  $\sim$ 100 $\mu$ m.



Figure 3-1: H&E stain of 2 month samples



G5824 2 month Normal Diet



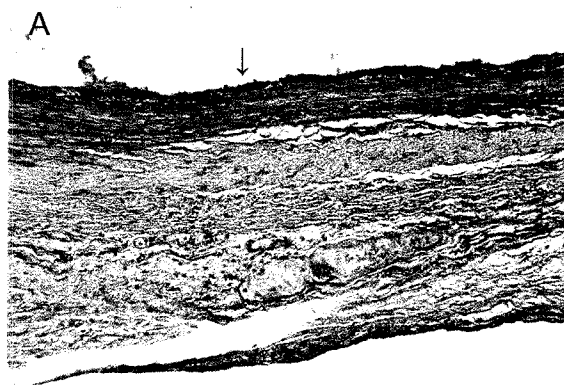
G5827 2 month Normal Diet



G5828 2 month Normal Diet

Figure 3-2: 2 month normal diet samples were embedded and 5 $\mu$ m sections were stained for  $\alpha$ -smooth muscle cell actin, a marker of smooth muscle cells and myofibroblasts. The presence of actin-staining cells would indicate the presence of host-derived myofibroblasts (involved in healing) or smooth muscle cells (cells normally present in blood vessels). G5824 and G5828 had a thin layer of cells staining for  $\alpha$ -smooth muscle cell actin on and just below the luminal surface of the graft ( $\downarrow$ ). Additional weak actin staining was seen within the graft tissue, but appeared to be remnants of the original actin present prior to processing (\*). In G5827, the actin staining was confined to several small blood vessels in the adventitia and the occasional actin remnant within the graft. Scale bar  $\sim$ 100 $\mu$ m.

Figure 3-2: Actin stain of 2 month samples



G5824 2 month Normal Diet



G5827 2 month Normal Diet



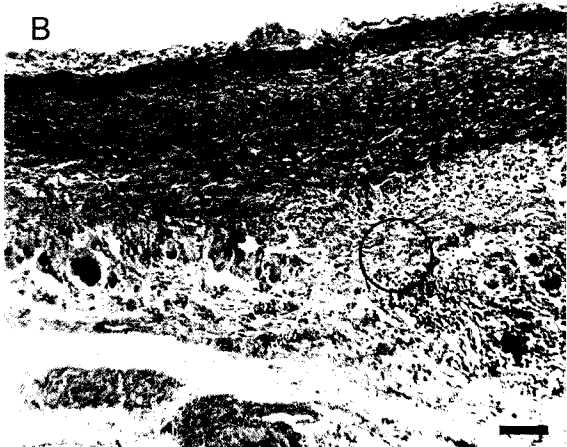
G5828 2 month Normal Diet

Figure 3-3: 2 month normal diet samples were embedded and 5 $\mu$ m sections were stained by Massons Trichrome. This stain is for collagen integrity and organization. The darker blue collagen is considered more mature, while lighter staining collagen is considered indicative of less mature collagen. Trichrome staining showed relatively well preserved/organized collagen within the grafts and more lightly stained areas of remodeled collagen (open circles).

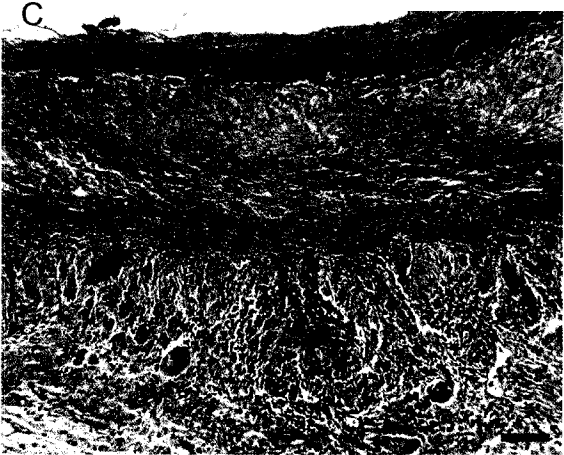
Figure 3-3: Trichrome stain of 2 month samples



G5824 2 month Normal Diet



G5827 2 month Normal Diet



G5828 2 month Normal Diet

graft composed of loose collagenous tissue containing blood vessels, adipose tissue, some giant cells and various other cells. There appeared to be a greater concentration of inflammatory-type cells present at the junction between the graft tissue and the abluminal layer in G5586, and in G5830, G5831 and G5832 inflammatory cells were present as small collections (**Fig. 4-1A to D**). A very thin layer of bland looking material was present on the luminal surface of the graft from G5586. In G5832 a thin layer of clot was seen on 2 portions of lumen overlaying a layer of fibrin material containing PMNs (**Fig. 4-1D**). A thin layer of actin staining-cells was located at the luminal surface for about  $\sim 3/4$  of the circumference in G5586, G5830, and G5832 (**Fig. 4-2A to C**). Some actin staining cells were present within the graft tissue extending for  $\sim 1/2$  of the circumference in G5586 and G5830. In G5832 approximately  $1/5$ th of the graft contained actin staining cells. In G5831, a few actin staining cells were present within the graft tissue, and some staining was seen ablumenally (**Fig. 4-2C**). Macrophages and giant cells were located at the interface between the graft tissue and the abluminal layer and formed a complete ring around the graft in G5586 (**Fig. 4-1A**). In G5830 macrophages and giant cells were located at the interface between the graft tissue and the abluminal layer, but fewer in number than previous samples and did not stain very darkly. However more giant cells were seen within the graft tissue located in the medial (circumferential) layer or on the luminal surface. In G5831 scattered macrophages were present in the abluminal layer and some macrophages were bound to the luminal surface of the graft, few giant cells were present and were located at the edge of the graft. In G5832 macrophages and a few giant cells were located at the interface between the graft tissue and abluminal layer and macrophages were seen within the surface fibrin layer.

Trichrome staining of G5586 and G5830 showed the majority of the collagen present was lightly stained and appeared to be expanded due to cellular ingrowth (**Fig. 4-3A&B**). In G5831, Trichrome staining showed the majority of the collagen present was well preserved and mature fibrils were present more ablumenally. The remainder was lightly stained and appeared to be expanded due to cellular ingrowth (**Fig. 4-3C**). In G5832, Trichrome staining showed a band of more mature collagen at the luminal surface while the more abluminal layer was composed primarily of lightly stained collagenous material (**Fig. 4-3D**). Movats staining of G5586 showed that thicker elastin fibrils were present within the medial (circumferential) graft tissue and elastin was abundant within the longitudinal tissue. Several portions of the internal elastic lamina were still visible. Movats staining of 5830 and 5831 (5832 H&E) showed that little elastin was present and what remained appeared to be remnants of the original graft elastin. No internal elastic lamina visible was visible in these samples. All samples had CD3 + cell present within the abluminal layer scattered throughout the tissue.

#### **Normal Diet 6 Months (Figure 5: 6Mo Histology)**

The graft matrix of all samples was relatively well preserved, appearing as two distinct layers medial (circumferential) and adventitial (longitudinal) for most of the implant, with cellularity that was evenly distributed between the layers. Graft G5587 had two large collections of fibrinous tissue adherent to the luminal surface that occupied about 1/3 of the surface and protruded into the lumen of graft. A relatively thin abluminal layer was present to the exterior of the graft composed of loose collagenous tissue containing blood vessels, adipose tissue, few to no giant cells and various other cells.

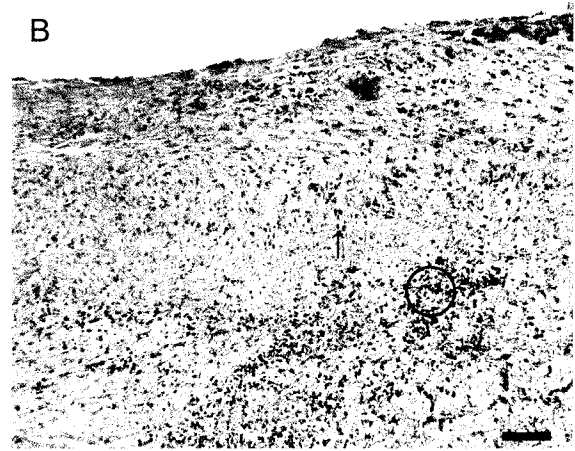
Figure 4-1: 4 month normal diet samples were embedded and 5 $\mu$ m sections were stained with H&E for general tissue morphology and cellularity. All grafts were re-colonized by host-derived cells and had an abluminal layer of tissue containing blood vessels and adipose tissue. Inflammatory cells were seen within the abluminal tissue and representative areas are enclosed within the circles. G5832 had a thin layer of luminal clot containing PMNs ( $\downarrow$ ). Macrophages and giant cells were located at the interface between the graft tissue and the abluminal tissue in all grafts ( $\uparrow$ ). Scale bar  $\sim$ 100 $\mu$ m



Figure 4-1: H&E of 4 month normal diet



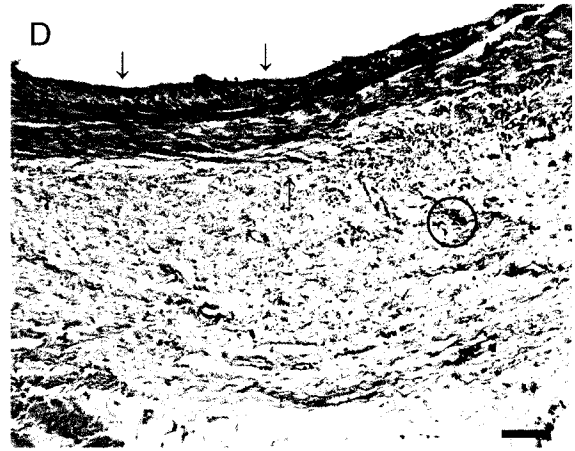
G5586 4 month Normal Diet



G5830 4 month Normal Diet



G5831 4 month Normal Diet



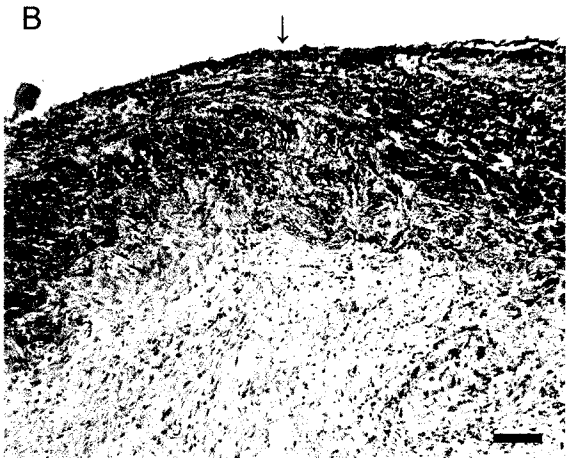
G5832 4 month Normal Diet

Figure 4-2: 4 month normal diet samples were embedded and 5 $\mu$ m sections were stained for  $\alpha$ -smooth muscle cell actin, a marker of smooth muscle cells and myofibroblasts. The presence of actin-staining cells would indicate the presence of host-derived myofibroblasts (involved in healing) or smooth muscle cells (cells normally present in blood vessels). A thin layer of actin staining-cells was located at the luminal surface in G5586, G5830, and G5832 (↓) and varying amount of actin staining cells were seen within the graft tissue of all sample

Figure 4-2: Actin stain of 4 month normal diet



G5586 4 month Normal Diet



G5830 4 month Normal Diet



G5831 4 month Normal Diet



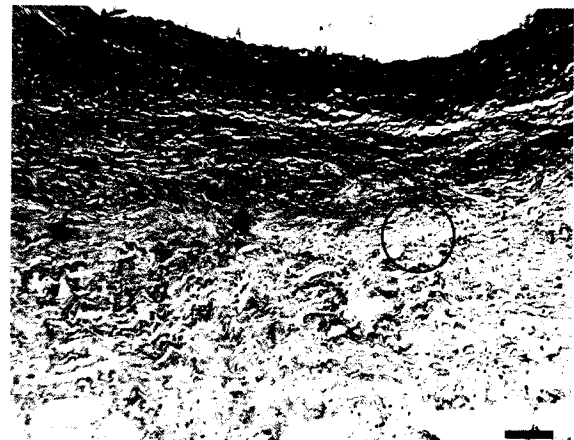
G5832 4 month Normal Diet

Figure 4-3: Trichrome stain of 4 month normal diet samples. Five  $\mu\text{m}$  sections were stained by the Trichrome method of Masson. This stain is for collagen integrity and organization. The darker blue collagen is considered more mature, while lighter staining collagen is considered indicative of less mature collagen. Trichrome staining of G5586 and G5830 showed the collagen appeared to be expanded due to cellular ingrowth (open circle). In G5831, Trichrome staining showed the majority of the collagen present was well preserved and the remainder was appeared expanded due to cellular ingrowth (open circle). In G5832, Trichrome staining showed a band of more mature collagen at the luminal surface while the more abluminal layer was composed primarily of lightly stained collagenous material (open circle). Scale bar  $\sim 100\mu\text{m}$ .

Figure 4-3: Trichrome stain of 4 month normal diet



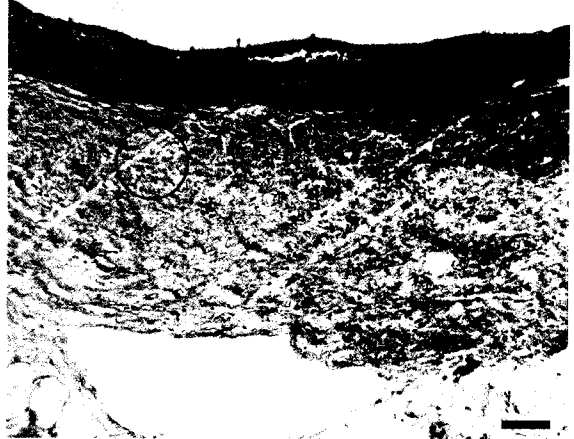
G5586 4 month Normal Diet



G5830 4 month Normal Diet



G5831 4 month Normal Diet



G5832 4 month Normal Diet

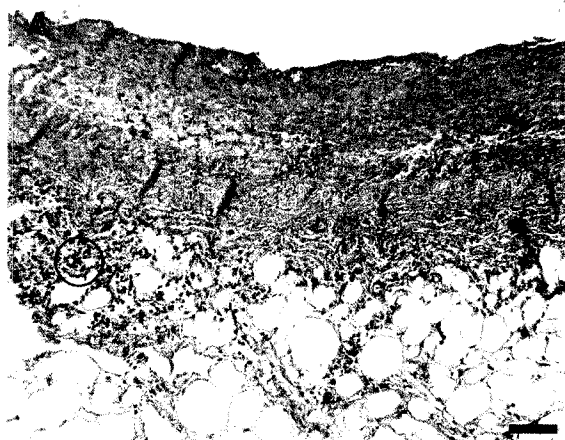
There were few inflammatory-type cells present at the junction between the graft tissue and the abluminal layer (**Fig. 5-1A to C**). No apparent actin staining was seen within the grafts from G5581 and G5588, while an occasional cell was stained for actin in G5587 (**Fig. 5-1A to C**). Few blood vessels were present and stained for actin in the abluminal layer. Scattered macrophages were present in the abluminal layer but few giant cells were present. A few macrophages were bound to the luminal surface of the grafts, and were also present near the surface of the fibrinous tissue in G5587. Trichrome staining of G5581 showed the majority of the collagen present was well preserved and mature fibrils were present in the abluminal layer (**Fig. 5-3A**). The remainder was lightly stained and appears to be expanded due to cellular ingrowth. Trichrome staining of G5587 showed the majority of the collagen present was lightly stained and appears to be expanded due to cellular ingrowth (**Fig. 5-3B**). Trichrome staining of G5588 showed a minority of the collagen present was as mature fibrils that appeared to be remnants of the original graft (**Fig. 5-3C**). The remainder was lightly stained and appeared to be expanded due to cellular ingrowth. Movats of G5581 and G5587 showed that a few elastin fibrils were present, but appeared to be remnants of original graft elastin in the adventitial (longitudinal) layer. Fragments of the internal elastic lamina were visible in G5581 and 5587, but absent in G5588. CD3 + cells were present scattered throughout the abluminal layer.

### **Cholesterol-diet samples macroscopic**

**Cholesterol Diet 2 months:** The graft from the single cholesterol diet rabbit (G6185) appeared dilated, with a large outpocketing just below the proximal suture line where

Figure 5-1: H&E stain of 6 month normal diet samples. Five  $\mu\text{m}$  sections were stained with H&E for general tissue morphology and cellularity. The graft matrix of all samples was well preserved and appeared as two distinct layers that were re-colonized by host-derived cells. All grafts had a relatively thin abluminal layer exterior to the graft material composed of loose collagenous tissue containing blood vessels, adipose tissue, scattered macrophages and a few inflammatory-type cells (circles).

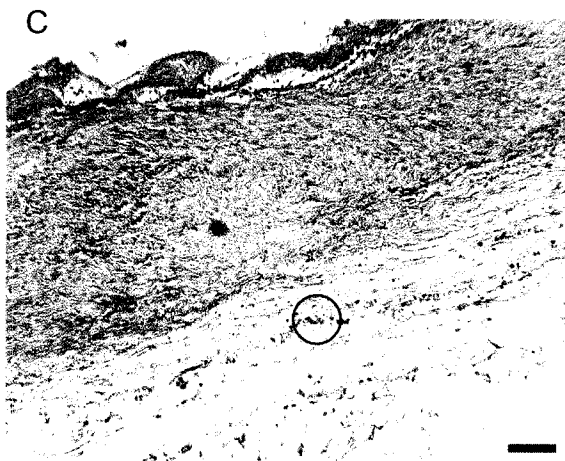
Figure 5-1: H&E stain of 6 month normal diet



G5581 6 month Normal Diet



G5587 6 month Normal Diet

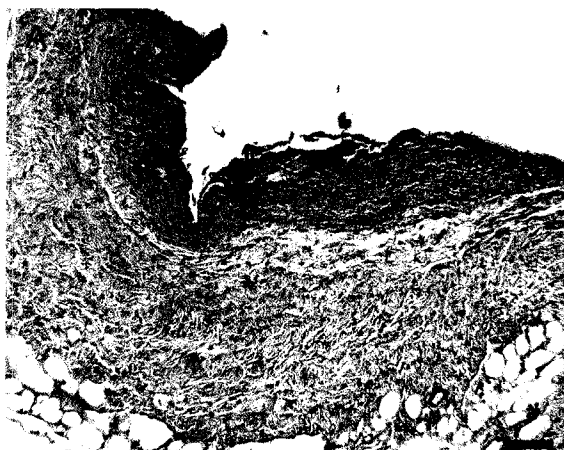


G5588 6 month Normal Diet

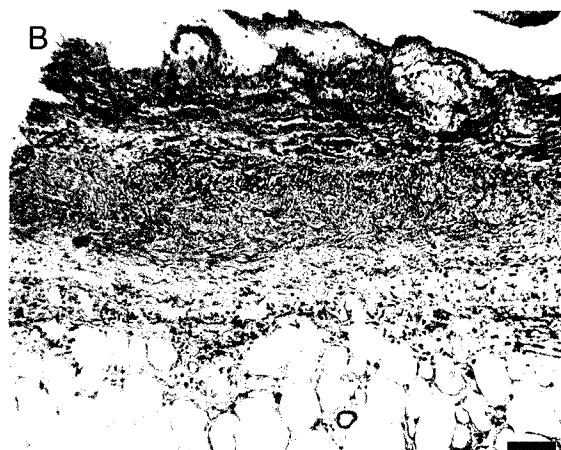


Figure 5-2: Actin stain of 6 month normal diet samples. Five  $\mu\text{m}$  sections were stained for  $\alpha$ -smooth muscle cell actin, a marker of smooth muscle cells and myofibroblasts. The presence of actin-staining cells would indicate the presence of host-derived myofibroblasts (involved in healing) or smooth muscle cells (cells normally present in blood vessels). No apparent actin staining within the grafts from G5581 and G5588, while an occasional cells was stained for actin in G5587 (\*).

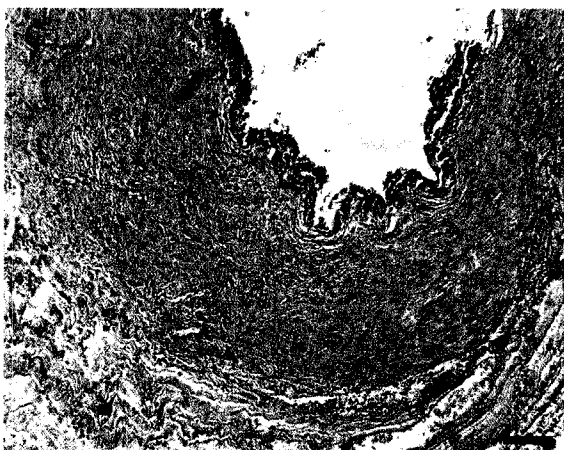
Figure 5-2: Actin stain of 6 month normal diet



G5581 6 month Normal Diet



G5587 6 month Normal Diet



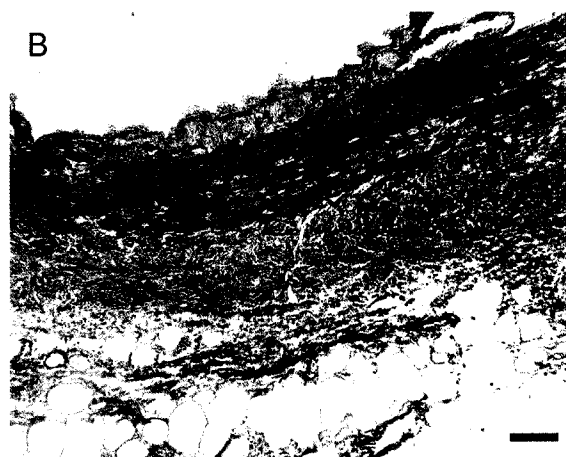
G5588 6 month Normal Diet

Figure 5-3: Trichrome stain of 6 month normal diet samples. Five  $\mu\text{m}$  sections were stained by the Trichrome method of Masson. This stain is for collagen integrity and organization. The darker blue collagen is considered more mature, while lighter staining collagen is considered indicative of less mature collagen. Trichrome staining of G5581 and G5587 shows a portion of the collagen was well preserved and the remainder appears expanded due to cellular ingrowth (open circle). Trichrome staining of G5588 showed a minority of the collagen present was as mature fibrils that appeared to be remnants of the original graft (\*). The remainder was lightly stained and appeared to be expanded due to cellular ingrowth (open circle).

Figure 5-3: Trichrome stain of 6 month normal diet



G5581 6 month Normal Diet



G5587 6 month Normal Diet



G5588 6 month Normal Diet

wall of the graft was thinner than the remainder (**Figure 6A and B**): **Cholesterol diet Macroscopic**).

### **Cholesterol diet Macroscopic Aneurysm samples (Figure 6C to F)**

Five cholesterol-diet rabbits died postoperatively on days 6, 14, 15, 20, and 46. Post-mortem examination revealed the presence of a massive hemorrhage either into the abdominal cavity or retroperitoneally due to an apparent graft rupture.

### **Cholesterol-diet Histology**

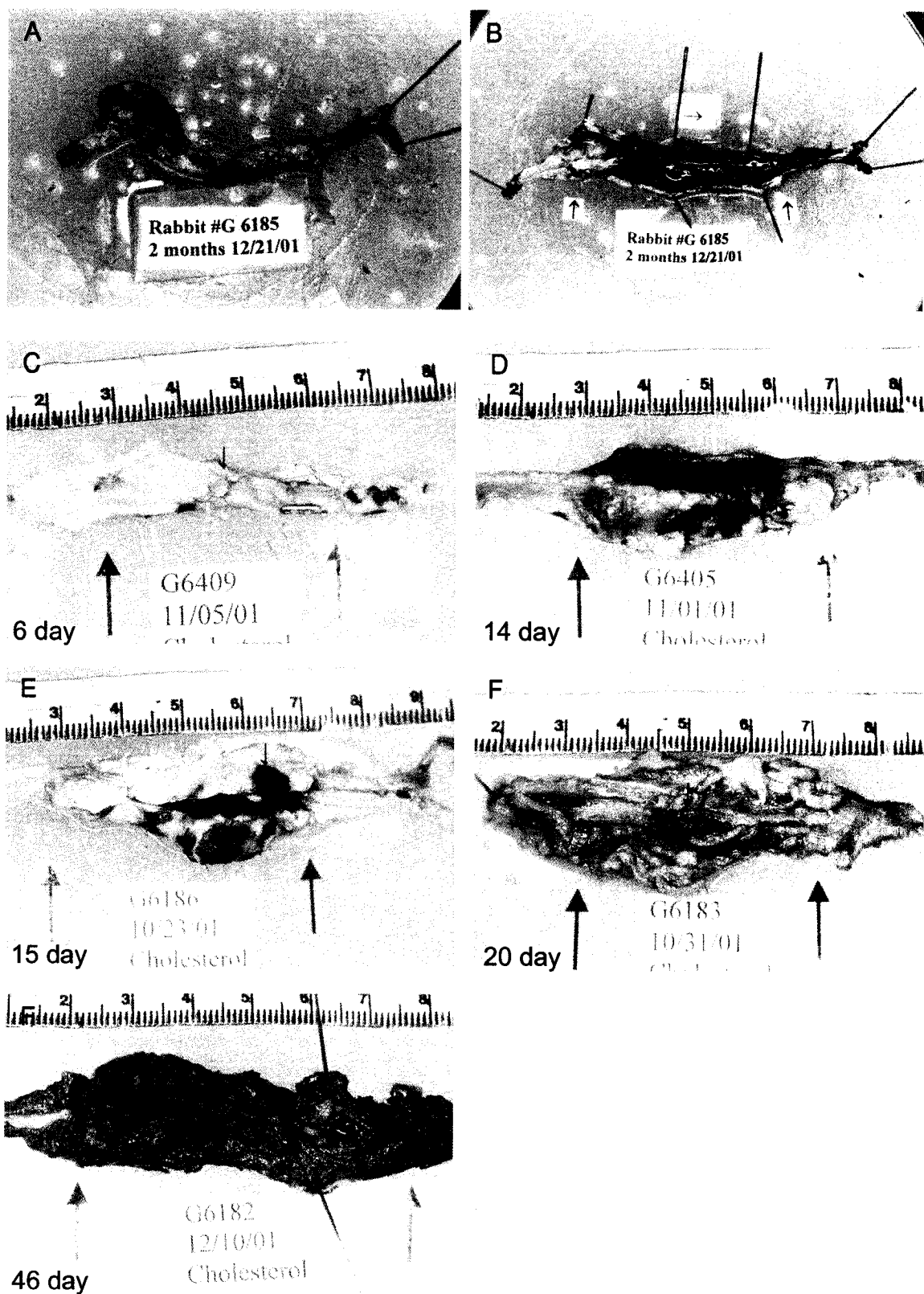
#### **2 Months (Figure 7-1: 2Mo Histology)**

Graft matrix was unorganized, and less cellular than the normal counterparts. The abluminal layer contained very loose collagenous tissue, blood vessels, some adipose tissue, as well as many giant cells and a several large patches of inflammatory cells. The medial layer appeared expanded, while the adventitial layer was a thick layer of very loose tissue containing many cells with large cytoplasmic areas containing translucent granular material that appear to be foam cells (**Fig. 7-1A**). A thin layer of actin staining-cells were located at or on the luminal surface staining for about a third of the circumference (**Fig. 7-1B**). Actin staining was also seen in two small blood vessels in the adventitia and the occasional actin remnant within the graft. Giant cells, macrophages and foam cells were located within the expanded adventitial tissue. Macrophages also formed an almost complete layer at the luminal surface of the graft (**Fig. 7-1A**).

Trichrome indicated that the majority of the graft collagen was degraded and what remained was mainly less mature collagen with a filamentous appearance (**Fig. 7-1C**).

Figure 6: Macroscopic evaluation of cholesterol diet samples. Panels A&B are photographs of the graft harvested from the cholesterol diet rabbit at 2 months and shows the outpocketing of the graft near the proximal suture line (\*). Panels C to F are aneurysm samples at 6, 14, 15, 20 and 46 days respectively. The area of rupture for these samples is indicated by the ↓ arrows. ↑ Arrows indicate the suture lines and the flow of blood is from left to right.

Figure 6: Cholesterol Diet and Aneurysm Samples Macroscopic



The majority of the internal elastic lamina was present with fine filamentous elastin fibrils present in the expanded medial (circumferential) layer with no apparent organization. Single scattered CD3+ cells and several small groupings were present in the abluminal layer.

### **Rabbits (Figure 7-2: Cholesterol Diet Aneurysm Histology)**

Extensive collagen and elastin fragmentation was seen in all samples (**Figure 7-2A, C, E and I**). In all cases, the normal vessel architecture was disrupted due to the infiltration of the graft matrix by numerous macrophage/foam cells (**Figure 7-2B, D, F and J**). No evidence of actin staining was seen in any of the samples except in the occasional abluminal blood vessel. The internal elastic lamina was still intact in the 6 and 14 day samples, but was fragmented in the 15, 20, and 46 day samples. The adventitial elastin was degraded in 14, 15, 20 and 46 day samples. In one case (15 day sample) extravascular blood was seen within the graft matrix. The graft matrix in these samples resembled atheroma that developed in the thoracic artery (**Figure 7-3: Atheroma**).

### **Macrophage Counts**

Slides stained with RAM11, a rabbit-macrophage-specific antibody, were used in this portion of the study. Photographs of 5 high-power fields were taken at the junction of the graft adventitial tissue and the abluminal layer where macrophages/giant cells were common. If possible, the field contained a portion of the graft adventitial tissue. The macrophage counts from the five random 100X fields were averaged for each sample, and the mean number of macrophages per group generated from these values.



Figure 7-1: Histology of 2 month cholesterol diet sample. Panel A is the H&E stain of the graft. The graft matrix was less cellular than the normal counterparts at 2 months and the graft material was expanded. Giant cells, macrophages and foam cells were located within the expanded adventitial tissue (M). Macrophages also formed an almost complete layer at the luminal surface of the graft (\*). Panel B is the actin stain of the graft and shows a thin layer of actin staining-cells located at or on the luminal surface (↓). Panel C is the Trichrome showing that the majority of the graft collagen was degraded and had a filamentous appearance (open circle). Scale Bar ~100µm

Figure 7-1: H&E, Actin and Trichrome of 2 month Cholesterol Diet Graft

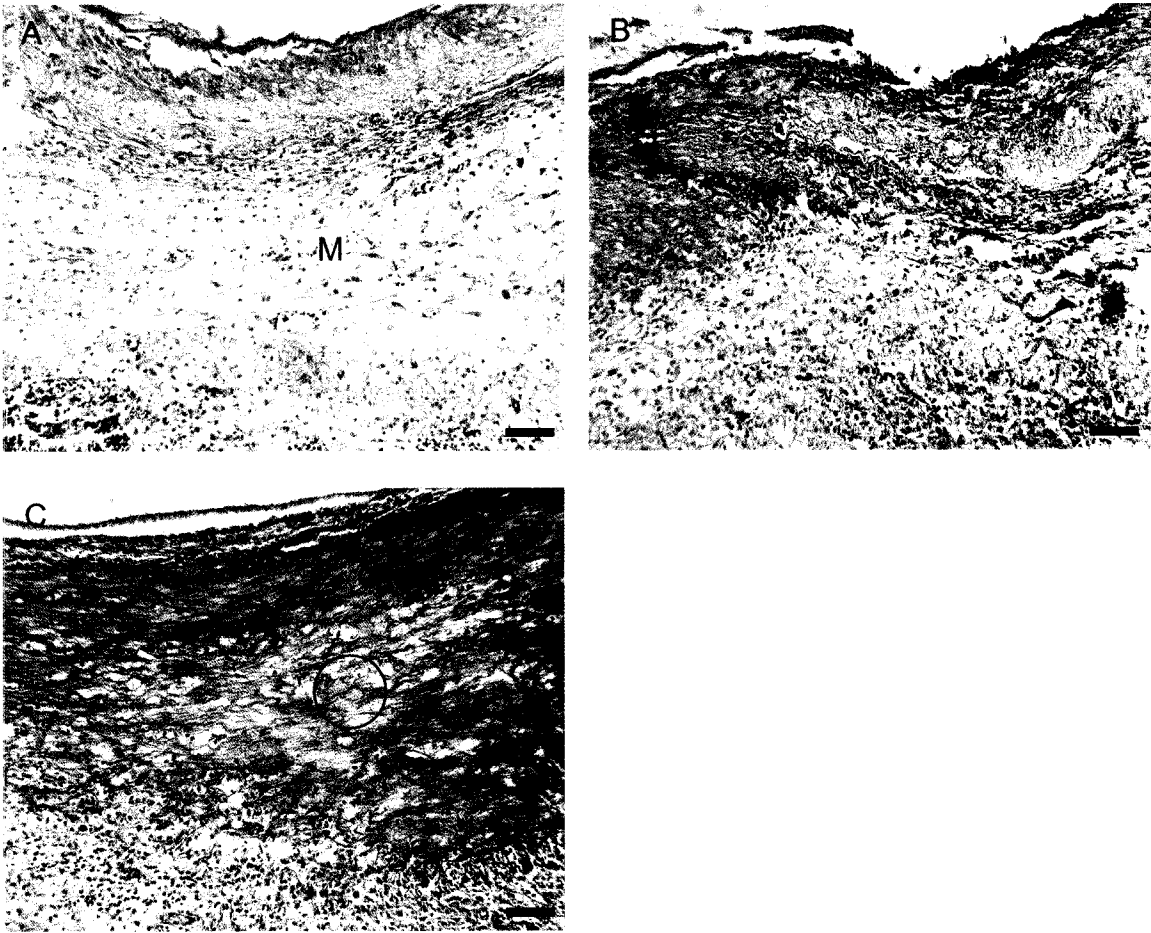
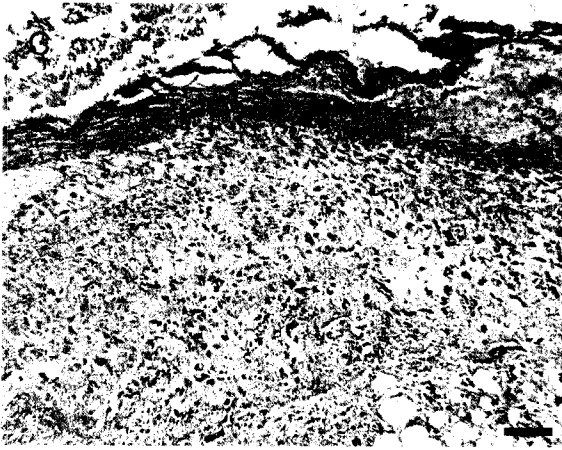


Figure 7-2: Cholesterol Diet Aneurysm Histology. Panels A, C, E, G and I are H&E stains of the samples. In all samples the collagenous graft material has been degraded and a cellular influx is seen in all samples. These cells are presumably macrophage derived foam cell based on the cellular morphology and foamy-looking cytoplasm. Panel B, D, F and J are RAM11 macrophage stains, confirming the identity of these cells as macrophages (open circles).

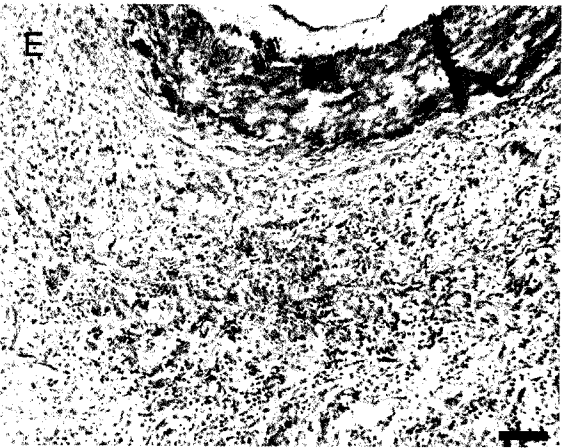
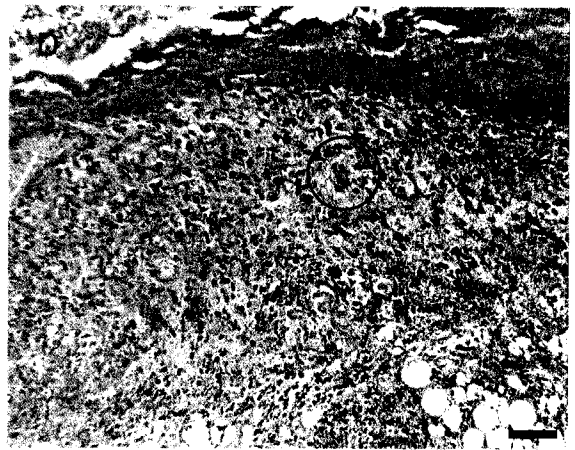
Figure 7-2: Aneurysm Histology



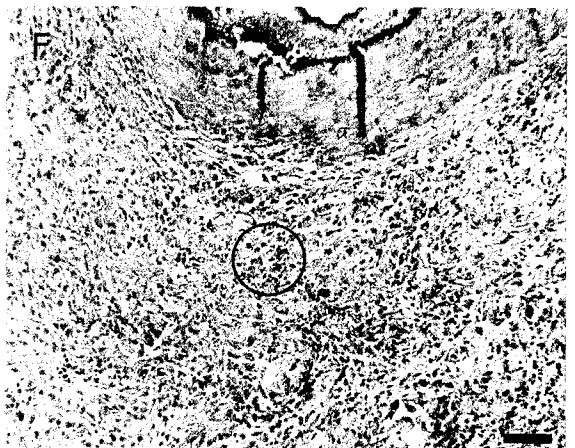
H6409 6 days

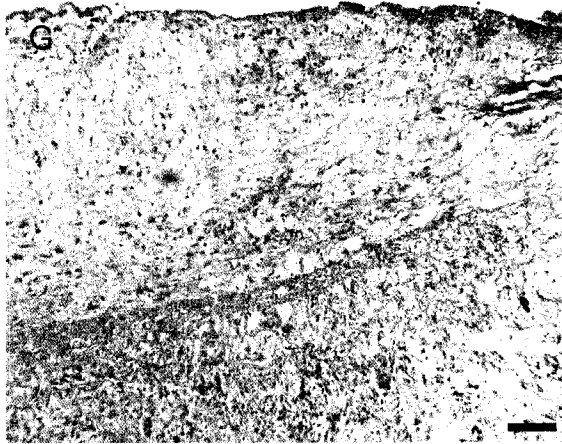


H6405 14 days

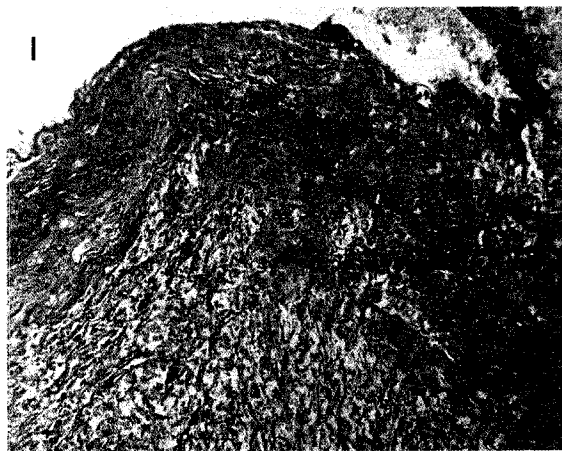


H6186 15 days





H6183 20 days



H6182 46 days

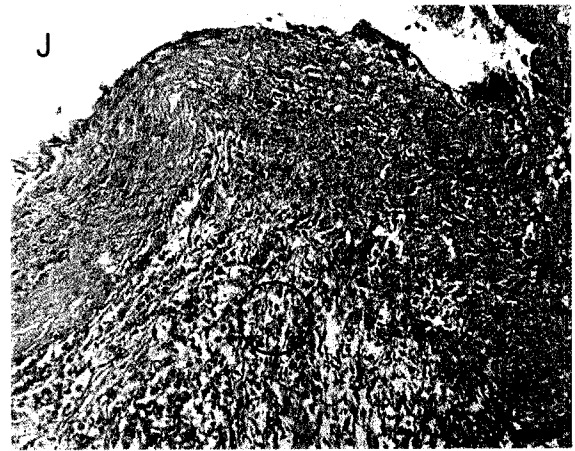
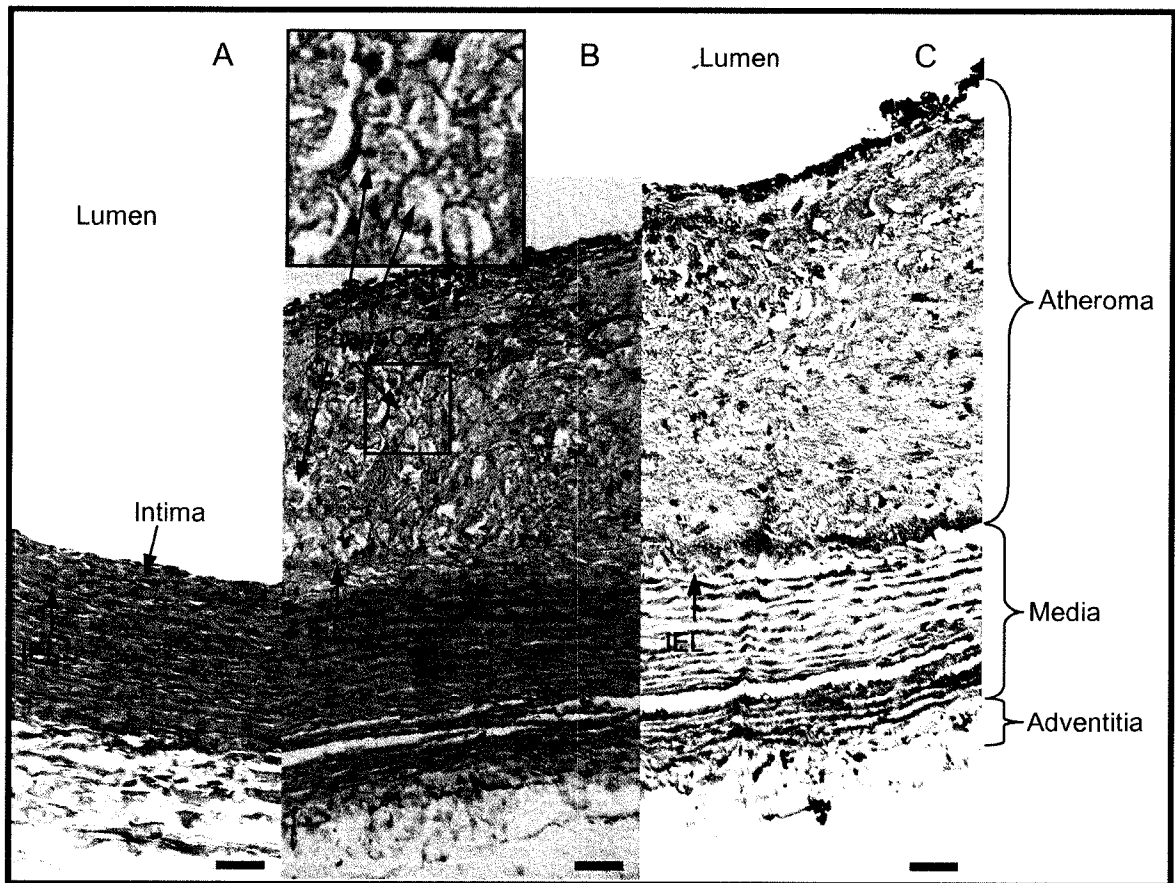


Figure 7-3: Histology of the thoracic aorta from normal and atherosclerotic rabbits. In panel A the histology of a normal rabbit thoracic artery is visible showing the Intima (\*Endothelial cells), Media and Adventitia. Panels B and C show a well developed Atheroma in a rabbit thoracic aorta stained with H&E for morphology and RAM11 for macrophages, respectively. The layers of the artery are visible, though little evidence of the aortic intima remains. The atheroma has developed above the internal elastic lamina (IEL) and protrudes into the lumen. The atheroma is dominated by foam cells and extracellular matrix, giving it a loose, disorganized appearance. The inset shows the foam cells (granular, vacuolated cytoplasm) and extracellular matrix in more detail. Scale bar ~100µm

Figure 7-3: Normal and Atherosclerotic Aorta



No statistically significant differences were seen between 2, 4 and 6 month samples from rabbits fed a normal diet. Cholesterol diet samples from aneurysm samples showed numerous macrophages but could not be counted due to overlap. The macrophage count from the cholesterol diet rabbit sacrificed at 2 months was similar to the normal diet samples and was not significantly different.

### **Zymography**

No major observable differences in band intensity were seen between surgery and sacrifice samples (**Figure 8: Zymograms**). The MMP profile did not change between groups, or between normal diet and cholesterol diet. Development in the presence of 1,10-phenanthroline MMP inhibitor indicated that the majority of the gelatinolytic activity was due to MMPs, with very little due to proteases (data not shown).

### **Humoral ELISA (Host Humoral Immune Response toward Graft)**

In all cases the humoral response to the graft increased between surgery and sacrifice (**Table 4: ELISA Titers**). The overall trend over the 6 month period was a reduction in the humoral response toward the graft material (**Figure 9: Log ELISA**). No statistical significance could be determined between groups as the number of samples in each group were too few.



Table 3: Macrophage counts were done on slides stained for RAM11 from normal and cholesterol diet samples. Five high-power fields were photographed at the junction of the graft material and the abluminal host tissue where the majority of the macrophages were located. The macrophages were manually counted, and the number averaged to obtain the given values. No significant differences were seen between groups. Values are Mean  $\pm$  SEM

Table 3: Macrophage Counts - Diet

Rabbit #	Diet	Avg # of Macrophages *	Mean # of Macrophages <sup>#</sup>
G5824 2 month	Normal	42.6	26.8±7.9
G5827 2 month	Normal	19.2	
G5828 2 month	Normal	18.6	
G5586 4 month	Normal	41.2	27.05±5.1
G5830 4 month	Normal	22	
G5831 4 month	Normal	27.4	
G5832 4 month	Normal	17.6	
G5581 6 month	Normal	41.6	37.8±8.1
G5587 6 month	Normal	33.6	
G5588 6 month	Normal	38.4	
G6185 2 month	Cholesterol	34.8	34.8
G6409 6 day†	Cholesterol	TNTC	ND
G6405 14 day†	Cholesterol	TNTC	ND
G6186 15 day†	Cholesterol	TNTC	ND
G6183 20 day†	Cholesterol	TNTC	ND
G6182 46 day†	Cholesterol	TNTC	ND

\* Average of 5 high-power fields

<sup>#</sup> Mean ± SEM

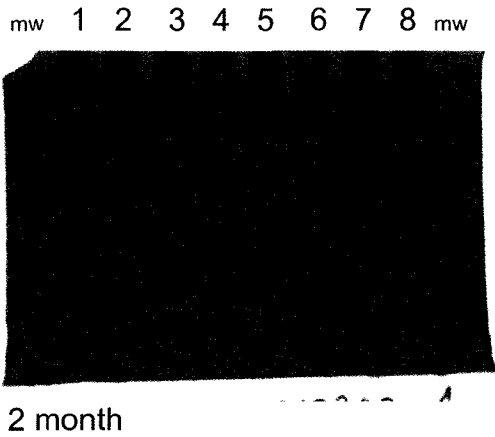
TNTC – Too numerous to count

ND – Not done

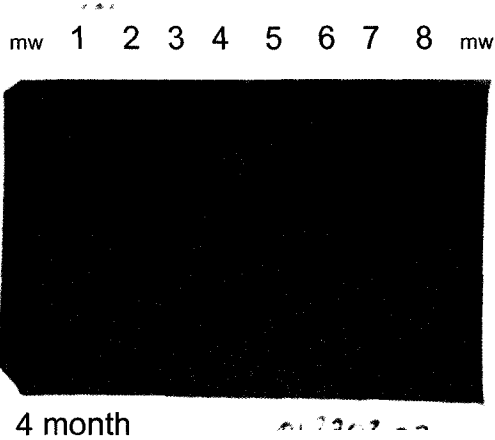
† Aneurysm Samples

Figure 8: To analyze differences in MMP presence or expression between surgery and sacrifice samples, equivalent amounts of serum were electrophoresed on 10% acrylamide gels containing 1% gelatin. The gels were run to completion, washed to remove SDS, and incubated in activation buffer (with and without MMP inhibitor) for the appropriate time. Gels were stained with coomassie brilliant blue, and active bands appear as clear bands on a blue background. No observable differences were seen within or between groups, or between diet types for all rabbits. \*Cholesterol diet

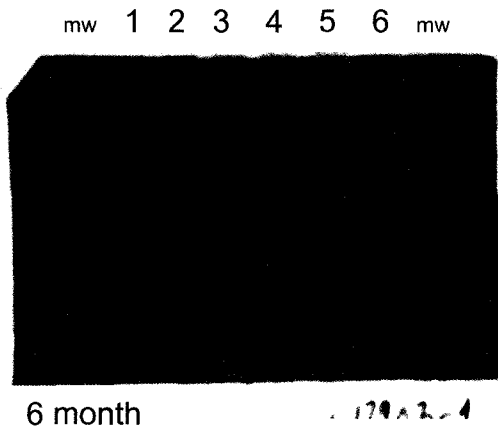
Figure 8: Zymograms of 2, 4 and 6 month Samples - Diet



- 2 month Samples  
Lanes:  
1- G5824 Surgery  
2- G5824 Sacrifice  
3- G5827 Surgery  
4- G5827 Sacrifice  
5- G5828 Surgery  
6- G5828 Sacrifice  
7- G6185 Surgery\*  
8- G6185 Sacrifice\*



- 4 month Samples  
Lanes:  
1- G5586 Surgery  
2- G5586 Sacrifice  
3- G5830 Surgery  
4- G5830 Sacrifice  
5- G5831 Surgery  
6- G5831 Sacrifice  
7- G5832 Surgery  
8- G5832 Sacrifice



- 6 month Samples  
Lanes:  
1- G5581 Surgery  
2- G5581 Sacrifice  
3- G5587 Surgery  
4- G5587 Sacrifice  
5- G5588 Surgery  
6- G5588 Sacrifice

Table 4: Serum samples were collected and stored at  $-60^{\circ}\text{C}$  until all had been collected then the humoral response toward the graft material was quantified by the humoral ELISA. Each sample was analyzed in duplicate, with each plate containing an internal blank. All readings were averaged, adjusted for normal rabbit serum OD, and the reciprocal given.

Table 4: ELISA titers of 2, 4 and 6 Month Samples - Diet

Rabbit #	Titer @ Surgery	Titer @ Sacrifice
G5824 Normal Diet 2Mo	20	20480
G5827 Normal Diet 2Mo	20	10240
G5828 Normal Diet 2Mo	40	20480
G5586 Normal Diet 4Mo	20	640
G5830 Normal Diet 4Mo	20	1280
G5832 Normal Diet 4Mo	20	1280
G5831 Normal Diet 4Mo	20	20480
G5588 Normal Diet 6Mo	20	320
G5581 Normal Diet 6Mo	20	640
G5587 Normal Diet 6Mo	20	1280
G6185 Cholesterol Diet 2Mo	20	20480

Figure 9: The log of the ELISA titers were plotted to graphically show the differences between the humoral response to the graft material at surgery and then at sacrifice. In all cases there was an increased humoral response to the graft between surgery and sacrifice. Over the 6 month period the overall trend shows a decreased humoral response toward the graft material. No statistical significance could be determined as there were too few samples in each group. Normal diet 2 month samples: G5824, G5827 and G5828. Normal diet 4 month samples: G5586, G5830, G5831 and G5832. Normal diet 6 month samples: G5581, G5587 and G5588. Cholesterol diet 2 month sample: G6185.

Figure 9: Humoral ELISA of 2, 4 and 6 Month Samples - Diet

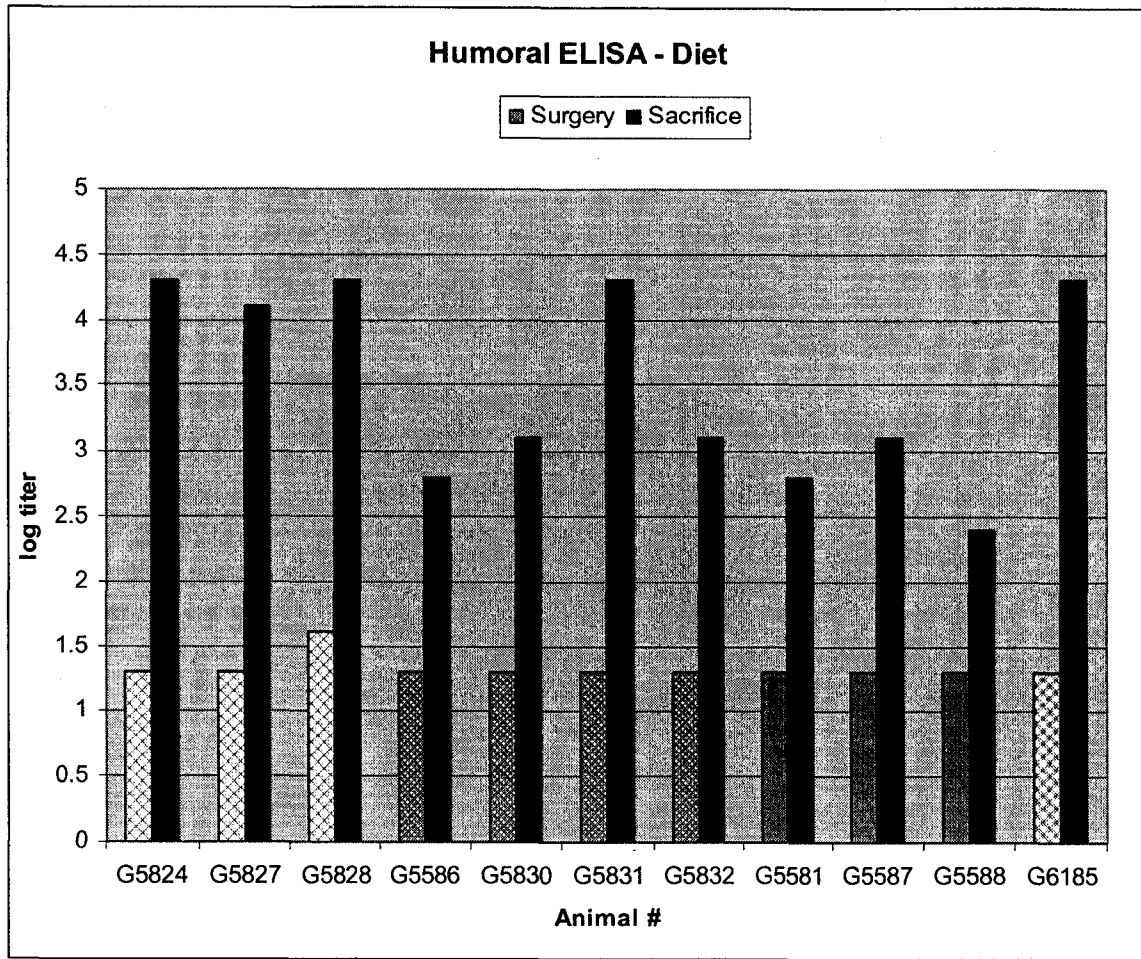




Table 5: The histology, immunohistology, macrophage counts, and ELISA information were summarized to provide an overview of the results for the 2, 4 and 6 Month Samples.

Table 5: Compiled results for 2, 4 and 6 month samples - Diet

Animal #	Graft Cellularity	Actin	Collagen Remodel	Macrophage Presence	Tissue Destruction	Humoral response
G5824 2mo	+	++	+	+	-	++++
G5827 2mo	+++	+	++	+	-	++++
G5828 2mo	+++	+	++	++++	-	++++
G6185 2mo*	-/+	+	++++	++	++++	++++
G5586 4mo	++	++++	+++	+	-	+++
G5830 4mo	+	++++	+++	+	-	+++
G5831 4mo	+	+	+	+	-	+++
G5832 4mo	+	++	+	-	-	++++
G5581 6mo	++	+	+++	+	-	++
G5587 6mo	++	+	+++	+	-	+++
G5588 6mo	+	-	+++	-/+	-	++

\* Cholesterol Diet

Graft Cellularity -(0%) → ++++ (100%) re-colonization of graft material by host cells.

Actin -(0%) → ++++ (100%) recolonization of graft media by actin-positive cells.

Collagen Remodel -(0%) → ++++ (90-100%) newly produced collagen vs. mature.

Macrophage Presence -(few macrophages) → ++++ (40-50) avg. # macrophages.

Tissue Destruction -(0%) → ++++ (100%) destruction of original graft material.

Humoral Response -(0%) → ++++ (100%) of maximum response, rated relative to the highest response seen for all grafts.

## Discussion

### Effects of Atherosclerosis

With the need for alternative bypass conduits increasing each year, the effects of hypercholesterolemia on non-autologous grafts needs to be studied, and grafts need to be tested in a less-than-favorable environment to more accurately determine durability and outcome. Many studies have implanted autologous, heterologous, xenogenic or synthetic vascular grafts into the circulation of normal animals, while other studies have evaluated the effect of an atherogenic diet on the development atherosclerosis. Few studies have directly evaluated the effect of atherosclerosis on vascular grafts, and then the effect of experimental atherosclerosis on autologous vein grafts<sup>16,52,53</sup> or synthetic grafts<sup>59,78</sup> in rabbits was examined.

Review of published literature shows little has been published on the effect of experimental hypercholesterolemia on xenograft durability. This chapter addresses this issue directly, and was designed to assess the role of inflammation on the graft material by increasing inflammation via diet-induced atherosclerosis. Two groups of rabbits were fed a normal diet or an atherogenic diet supplemented with cholesterol, allowing for the evaluation of the long-term outcome of this graft in a disease model, which had not previously been done. Weekly bleeds were done on both the normal and cholesterol diet rabbits to monitor serum cholesterol levels and inclusion of cholesterol into the diet resulted in a considerable elevation in pre-operative serum cholesterol compared to rabbits fed a normal diet.

### **Normal diet rabbits**

Rabbits fed the normal diet recovered well from surgery and on explant at 2, 4 and 6 months the grafts were found to be incorporated into the host. The grafts were covered with host-derived tissue with little evidence fibrosis. Further microscopic analysis of the samples showed the graft material was re-colonized by host-derived cells. However, macrophages were a common finding in the tissue surrounding the grafts and giant cells and scattered T-cells were also present. This indicated that the graft material did appear to elicit a chronic inflammatory type response, but the response was not severe enough to result in graft failure. This could be considered an advantage as the inflammatory response appears to promote the formation of new vessels that may support the graft tissue. The healing of the grafts appeared to be ongoing out to 6 months and longer studies would be interesting as they would show whether the graft becomes fully incorporated into the host and develops a functional intima and media. Functional studies could also be done to show whether the vessels becomes responsive to stimuli normally present in the vasculature (vasodilatation and vasoconstriction).

### **Cholesterol diet rabbits**

By comparison the majority of cholesterol-diet rabbits did not survive longer than a few days post-operatively. The reasons for this are unclear, but may be a due to the combined stress of the surgery in conjunction with the systemic stress of atherosclerosis resulting in the death of the animals. This could be explored by the addition of sham surgeries as an experimental group, in which the entire surgical procedure including cross-clamping the aorta for 30 minutes without implanting the graft, would be

performed. This would allow us to evaluate the effect of the surgery on post-operative survival in hypercholesterolemic rabbits, and see whether the surgery is contributing to the increased mortality.

### **The effects of hypercholesterolemia on the graft**

Five of the rabbits that survived the immediate post-operative period died of a burst aneurysm of the graft material between 6 and 46 days. Microscopic examination of these post-mortem aneurysm samples, as well as graft material from the single surviving cholesterol-diet rabbit at 2 months, showed the presence of numerous foam cells, little collagen and elastin, and extensive destruction of tissue architecture. The appearance of the expanded graft tissue as well as atheromatous plaque tissue harvested from the thoracic aorta was very similar, and both contained numerous macrophage-derived foam cells. The ubiquitous presence of foam cells and the lack of other cell types in the area of the aneurysm, in conjunction with the graft tissue destruction in these areas, appears to implicate these cells in the development and progression of the aneurysm leading to rupture.

The histology data suggest that hypercholesterolemia is associated with an increased presence of foam cells and degradation of the graft material. This could lead to graft degeneration as well as aneurysm formation and rupture, which could be due to the increased production and activity of lytic enzymes by the macrophages in atherosclerotic rabbits. Previously published studies have shown that hypercholesterolemia increases the presence of macrophages within the aortic tissue of rabbits<sup>53,79,80</sup> and withdrawal of dietary cholesterol reduces the presence of macrophages within atherosclerotic lesions<sup>81</sup>.

Atherosclerosis has been associated with the development of aneurysms due to an increase in the inflammatory response and the production of lytic enzymes that degrade extracellular matrix components<sup>33,78</sup> that are secreted by macrophages<sup>82</sup>.

The zymography data did not show an increase in circulating serum MMPs, but the serum levels may not accurately reflect the levels of MMPs within the graft material. Even though the presence of MMPs in serum is supposedly proportional to the amount in tissue (at least in published studies of aneurysm formation), the serum samples collected in this study may not truly reflect the MMP amount and activity within the graft tissue. Additionally, the degeneration within the grafts is localized to a small portion of the vasculature and the differences may not be detectable with the methodology employed. Also, the MMP activity seen reflects the total amount of MMP present within the serum<sup>65,77</sup> and does not differentiate between what was originally active or inactive<sup>83</sup>. Western blotting of graft extracts or immunohistology of graft sections for the presence and relative amounts specific lytic enzymes known to degrade matrix components (such as MMP2 and 9) could be used to explore the differences between the normal and atherosclerotic grafts.

### **Graft durability in an atherosclerotic rabbit model**

The grafts harvested from the one surviving rabbit fed an atherogenic diet and the samples obtained from the cholesterol-diet rabbits that died from ruptured grafts provide an interesting glimpse into the effect of atherosclerosis on graft durability and these observations may directly apply to the failure of grafts in human patients and merits further investigation. One of the original goals for the study was to study the effect

atherosclerosis on the long-term durability of graft material, but due to the elevated mortality this was difficult to assess using this model. However, atherosclerosis appears to have a negative effect on long-term durability due to the increased inflammatory response. However major modifications of this model would be required before further studies could be done to address the role of atherosclerosis on graft durability.

Several studies could be done to further explore this phenomenon. Initially a study would be done to correlate the level of cholesterol to the level of inflammation seen in the rabbit, so a particular stage in the formation of atherosclerosis (early, intermediate or late stage) could be targeted and then the graft could be implanted. A study could be done in which the graft would be implanted into the abdominal aorta and upon recovery the hypercholesterolemic diet would be started. This should demonstrate the effect of atherosclerosis on the graft for an extended period of time. Another study would involve inducing hypercholesterolemia in the rabbit but adjusting the diet to keep the serum cholesterol in the clinically significant range for humans and then implanting the graft. This would be a more relevant model to explore the effect of atherosclerosis on the graft under similar conditions to humans.

## **Conclusions**

Rabbits fed a normal diet survive the surgery well and the grafts remain patent for up to 6 months. The explanted grafts are recolonized by host cells and the arrangement of these cells corresponds with the normal distribution of cells within a normal artery. However, in this rabbit model the grafts elicit a chronic-type inflammatory response

which would allow this model to be used for further study in which the inflammatory response could be addressed by the incorporation of anti-inflammatory drugs.

Rabbits fed a cholesterol-supplemented diet had a very high incidence of post-operative mortality attributed to systemic and operative stress. Aneurysm formation was seen in several rabbits. Hypercholesterolemia increases the presence of macrophages within the grafts which are known to produce MMPs that degrade matrix components, while fragments of matrix could serve as an additional stimulus, leading to an increased response toward the graft tissue. Based upon the histological data there seemed to be an accelerated development of atherosclerotic lesions with the graft tissue, leading to rupture and death in a select subset of these animals. While this model is flawed as a way to assess the effect of atherosclerosis on the graft material over an extended period of time, the methodology could be re-designed to allow for longer term observations.



## Appendix

Table 6: Surgery and sacrifice data for all the rabbits in this study are compiled in this table. The weights at surgery and sacrifice are listed, and the cholesterol diet rabbits had a lower operative weight compared to the normal diet rabbits, which was increased at sacrifice . The average graft length for the normal diet group was 4.4cm and 4.5cm for the cholesterol diet groups. The cross-clamp times did not differ significantly between the groups (22min normal vs. 19min cholesterol).

**Table 6: Surgery and Graft Data - Diet**

Rabbit #	Surgery Date	Weight @ Surgery	Graft Length	X-Clamp (min)	Graft #	Date Opened	Sacrifice Date	Weight @ Sacrifice
<i>Normal Diet</i>								
G5588	09/17/01	4.4kg	4.5cm	20	AP25.225	09/17/01	03/22/02	5.68kg
G5583	09/18/01	4.3	4.3	21	AP25.225	09/17/01	09/21/01	N/A
G5581	09/19/01	4.5	4.6	21	AP25.225	09/17/01	03/26/02	5.56
G5584	09/20/01	4	4.5	23	AP25.225	09/17/01	03/09/02	N/A
G5587	09/20/01	4.3	4.5	17	AP25.225	09/17/01	03/26/02	4.88
G5586	09/21/01	3.8	3.6	22	AR25.21	09/21/01	01/25/02	4.66
G5830	09/25/01	4.8	4.5	22	AR25.21	09/21/01	02/01/02	5.7
G5832	09/25/01	4.3	4.5	20	AR25.21	09/21/01	01/28/02	5.1
G5831	09/27/01	4.7	4.7	24	AR25.21	09/21/01	02/04/02	4.09
G5828	09/27/01	4	4.7	20	AR25.21	09/21/01	12/14/01	4.65
G5825	09/28/01	4.2	4.4	29	AR25.211	09/28/01	10/04/01	N/A
G5824	09/28/01	4.7	4.3	18	AR25.211	09/28/01	12/11/01	4.7
G5827	10/03/01	4.3	4.6	19	AR25.211	09/28/01	12/13/01	5.4
G5826	N/A	3.8	N/A	N/A	N/A	N/A	N/A	N/A
<b>Mean ± Std Dev</b>		<b>4.29±0.3</b>	<b>4.44±0.3</b>	<b>22±3</b>				<b>5.04±0.5</b>
<i>Cholesterol Diet</i>								
G6186	10/08/01	4	4.1	22	AR25.211	09/28/01	10/23/01*	N/A
G6185	10/09/01	2.7	4.5	15	AR25.211	09/28/01	12/21/01	2.95kg
G6182	10/10/01	3.8	4.7	21	AR25.211	09/28/01	12/10/01*	N/A
G6183	10/11/01	3.3	4.5	20	AR25.222	10/11/01	10/31/01*	N/A
G6184	10/11/01	3.4	4.5	21	AR25.222	10/11/01	10/14/01*	N/A
G6188	10/12/01	3	4.8	15	AR25.222	10/11/01	N/A	N/A
G6404	10/15/01	3.1	4.5	18	?AR25.222	10/11/01	N/A	N/A
G6407	10/15/01	3.1	4.5	18	?AR25.222	10/11/01	N/A	N/A
G6403	10/18/01	3	4.6	21	AR25.216	10/18/01	N/A	N/A
G6405	10/18/01	3	4.1	12	AR25.216	10/18/01	11/01/01*	N/A
G6402	10/19/01	2.9	4.5	14	?AR25.216	10/18/01	10/23/01*	N/A
G6406	10/19/01	2.9	4.3	24	?AR25.216	10/18/01	10/21/01*	N/A
G6408	10/30/01	3	4.6	27	?AR25.216	10/18/01	N/A	N/A
G6409	10/30/01	3.2	4	20	?AR25.216	10/18/01	11/05/01*	N/A
G6187	11/01/01	3.5	4.9	17	AP25.215	11/01/01	11/03/01*	N/A
G6189	11/01/01	3.3	4.7	21	AP25.215	11/01/01	11/03/01*	N/A
<b>Mean ± Std Dev</b>		<b>3.15±0.3</b>	<b>4.51±0.3</b>	<b>18.9±3.9</b>				<b>2.95</b>
*Found dead on the listed date								

Table 7: The sacrifice dates are listed for all rabbits, as is the duration of the graft implantation. The causes of death are listed and rabbits were sacrificed on time, euthanized due to complications or found dead.

**Table 7: Sacrifice - Diet**

<b>Rabbit #</b>	<b>Cause of Death</b>	<b>Duration</b>
<b>Normal Diet Rabbits</b>		
G5588	Sacrificed	6 months/186 days
G5581	Sacrificed	6 months/188 days
G5587	Sacrificed	6 months/187 days
G5586	Sacrificed	4 months/126 days
G5830	Sacrificed	4 months/129 days
G5832	Sacrificed	4 months/125 days
G5831	Sacrificed	4 months/130 days
G5828	Sacrificed	2 months/78 days
G5824	Sacrificed	2 months/74 days
G5827	Sacrificed	2 months/71 days
G5583	Paralysis - Euthanized	3 days
G5825	Ischemia - Euthanized	6 days
G5584	Died - Intestinal Ischemia	5+ months/170 days
G5826	Spinal Injury - Euthanized	N/A
<b>Cholesterol Diet Rabbits</b>		
G6185	Sacrificed	73 days
G6182 <sup>+</sup>	Hemorrhage	46 days
G6183 <sup>+</sup>	Hemorrhage	20 days
G6186 <sup>+</sup>	Hemorrhage	15 days
G6405 <sup>+</sup>	Hemorrhage	14 days
G6409 <sup>+</sup>	Hemorrhage	6 days
G6184	Surgical Hemorrhage	3 days
G6408	Surgical Complications	1 day
G6404	Spinal Injury - Euthanized	N/A
G6403	Peri-operative - Anesthesia	N/A
G6188	Peri-operative - Anesthesia	N/A
G6402	Paralysis - Euthanized	4 days
G6406	Paralysis - Euthanized	2 days
G6189	Paralysis - Euthanized	2 days
G6187	Died	2 days
G6407	Died	1 day

## Literature Cited

1. Cotran RS, Kumar V, Robbins SL. Inflammation and Repair. In: *Robbins Pathologic Basis of Disease, 5th Edition*. 5th ed. Philadelphia, PA: W.B. Saunders Company; 1994:51-92.
2. Wagner E, Guidoin R, Marois M, Mantovani D, Roy R, Ricci M, Marois Y, King MW, Gill F, Awad JA. Histopathologic findings in synthetic and biologic explanted grafts used in peripheral arterial reconstruction. *Asaio J*. 1994;40:M279-83.
3. Burkel WE. The challenge of small diameter vascular grafts. *Med Prog Technol*. 1988;14:165-75.
4. Marx N, Mackman N, Schonbeck U, Yilmaz N, Hombach VV, Libby P, Plutzky J. PPARalpha Activators Inhibit Tissue Factor Expression and Activity in Human Monocytes. *Circulation*. 2001;103:213-219.
5. Zwolak RM, Adams MC, Clowes AW. Kinetics of vein graft hyperplasia: association with tangential stress. *J Vasc Surg*. 1987;5:126-36.
6. Wilson NV, Salisbury JR, Kakkar VV. The effect of low molecular weight heparin on intimal hyperplasia in vein grafts. *Eur J Vasc Surg*. 1994;8:60-4.
7. Newby AC, Zaltsman AB. Molecular mechanisms in intimal hyperplasia. *J Pathol*. 2000;190:300-9.
8. Shah PK. Inflammation, neointimal hyperplasia, and restenosis: as the leukocytes roll, the arteries thicken. *Circulation*. 2003;107:2175-7.
9. Saenz NC, Hendren RB, Schoof DD, Folkman J. Reduction of smooth muscle hyperplasia in vein grafts in athymic rats. *Lab Invest*. 1991;65:15-22.

10. Connolly E, Bouchier-Hayes DJ, Kaye E, Leahy A, Fitzgerald D, Belton O. Cyclooxygenase isozyme expression and intimal hyperplasia in a rat model of balloon angioplasty. *J Pharmacol Exp Ther.* 2002;300:393-8.
11. Cox JL, Chiasson DA, Gotlieb AI. Stranger in a strange land: the pathogenesis of saphenous vein graft stenosis with emphasis on structural and functional differences between veins and arteries. *Prog Cardiovasc Dis.* 1991;34:45-68.
12. Stary HC, Blankenhorn DH, Chandler AB, Glagov S, Insull W, Jr., Richardson M, Rosenfeld ME, Schaffer SA, Schwartz CJ, Wagner WD, et al. A definition of the intima of human arteries and of its atherosclerosis-prone regions. A report from the Committee on Vascular Lesions of the Council on Arteriosclerosis, American Heart Association. *Circulation.* 1992;85:391-405.
13. Loscalzo J. Vascular matrix and vein graft failure. Is the message in the medium? *Circulation.* 2000;101:221-3.
14. Davies MG, Hagen PO. Pathobiology of intimal hyperplasia. *Br J Surg.* 1994;81:1254-69.
15. Davies MG, Dalen H, Kim JH, Barber L, Svendsen E, Hagen PO. Control of accelerated vein graft atheroma with the nitric oxide precursor: L-arginine. *J Surg Res.* 1995;59:35-42.
16. Klyachkin ML, Davies MG, Svendsen E, Kim JH, Massey MF, Barber L, McCann RL, Hagen PO. Hypercholesterolemia and experimental vein grafts: accelerated development of intimal hyperplasia and an increase in abnormal vasomotor function. *J Surg Res.* 1993;54:451-68.
17. Lusis AJ. Atherosclerosis. *Nature.* 2000;407:233-41.

18. Ross R. The pathogenesis of atherosclerosis--an update. *N Engl J Med*. 1986;314:488-500.
19. Boyle EM, Jr., Lille ST, Allaire E, Clowes AW, Verrier ED. Endothelial cell injury in cardiovascular surgery: atherosclerosis. *Ann Thorac Surg*. 1997;63:885-94.
20. AHA. American Heart Association. 2002 Heart and Stroke Statistical Update. In. Dallas, TX: American Heart Association; 2001.
21. Stry HC, Chandler AB, Glagov S, Guyton JR, Insull W, Jr., Rosenfeld ME, Schaffer SA, Schwartz CJ, Wagner WD, Wissler RW. A definition of initial, fatty streak, and intermediate lesions of atherosclerosis. A report from the Committee on Vascular Lesions of the Council on Arteriosclerosis, American Heart Association. *Circulation*. 1994;89:2462-78.
22. Stry HC, Chandler AB, Dinsmore RE, Fuster V, Glagov S, Insull W, Jr., Rosenfeld ME, Schwartz CJ, Wagner WD, Wissler RW. A definition of advanced types of atherosclerotic lesions and a histological classification of atherosclerosis. A report from the Committee on Vascular Lesions of the Council on Arteriosclerosis, American Heart Association. *Circulation*. 1995;92:1355-74.
23. Hoch JR, Stark VK, van Rooijen N, Kim JL, Nutt MP, Warner TF. Macrophage depletion alters vein graft intimal hyperplasia. *Surgery*. 1999;126:428-37.
24. Bojakowski K, Religa P, Bojakowska M, Hedin U, Gaciong Z, Thyberg J. Arteriosclerosis in rat aortic allografts: early changes in endothelial integrity and smooth muscle phenotype. *Transplantation*. 2000;70:65-72.

25. Faries PL, Marin ML, Veith FJ, Ramirez JA, Suggs WD, Parsons RE, Sanchez LA, Lyon RT. Immunolocalization and temporal distribution of cytokine expression during the development of vein graft intimal hyperplasia in an experimental model. *J Vasc Surg.* 1996;24:463-71.
26. Watanabe T, Haraoka S, Shimokama T. Inflammatory and immunological nature of atherosclerosis. *Int J Cardiol.* 1996;54 Suppl:S51-60.
27. Blum A, Miller HI. The role of inflammation in atherosclerosis. *Isr J Med Sci.* 1996;32:1059-65.
28. Libby P, Ridker PM, Maseri A. Inflammation and atherosclerosis. *Circulation.* 2002;105:1135-43.
29. Ross R. The pathogenesis of atherosclerosis: a perspective for the 1990s. *Nature.* 1993;362:801-9.
30. Rosenfeld ME. Cellular mechanisms in the development of atherosclerosis. *Diabetes Res Clin Pract.* 1996;30 Suppl:1-11.
31. Crea F, Biasucci LM, Buffon A, Liuzzo G, Monaco C, Caligiuri G, Kol A, Sperti G, Cianflone D, Maseri A. Role of inflammation in the pathogenesis of unstable coronary artery disease. *Am J Cardiol.* 1997;80:10E-16E.
32. Freestone T, Turner RJ, Coady A, Higman DJ, Greenhalgh RM, Powell JT. Inflammation and matrix metalloproteinases in the enlarging abdominal aortic aneurysm. *Arterioscler Thromb Vasc Biol.* 1995;15:1145-51.
33. Freestone T, Turner RJ, Higman DJ, Lever MJ, Powell JT. Influence of hypercholesterolemia and adventitial inflammation on the development of aortic aneurysm in rabbits. *Arterioscler Thromb Vasc Biol.* 1997;17:10-7.



34. Wassef M, Baxter BT, Chisholm RL, Dalman RL, Fillinger MF, Heinecke J, Humphrey JD, Kuivaniemi H, Parks WC, Pearce WH, Platsoucas CD, Sukhova GK, Thompson RW, Tilson MD, Zarins CK. Pathogenesis of abdominal aortic aneurysms: a multidisciplinary research program supported by the National Heart, Lung, and Blood Institute. *J Vasc Surg*. 2001;34:730-8.
35. Goodall S, Crowther M, Hemingway DM, Bell PR, Thompson MM. Ubiquitous elevation of matrix metalloproteinase-2 expression in the vasculature of patients with abdominal aneurysms. *Circulation*. 2001;104:304-9.
36. Hovsepian DM, Ziporin SJ, Sakurai MK, Lee JK, Curci JA, Thompson RW. Elevated plasma levels of matrix metalloproteinase-9 in patients with abdominal aortic aneurysms: a circulating marker of degenerative aneurysm disease. *J Vasc Interv Radiol*. 2000;11:1345-52.
37. Petersen E, Gineitis A, Wagberg F, Angquist KA. Activity of matrix metalloproteinase-2 and -9 in abdominal aortic aneurysms. Relation to size and rupture. *Eur J Vasc Endovasc Surg*. 2000;20:457-61.
38. Longo GM, Xiong W, Greiner TC, Zhao Y, Fiotti N, Baxter BT. Matrix metalloproteinases 2 and 9 work in concert to produce aortic aneurysms. *J Clin Invest*. 2002;110:625-32.
39. Annabi B, Shedid D, Ghosn P, Kenigsberg RL, Desrosiers RR, Bojanowski MW, Beaulieu E, Nassif E, Moundjian R, Beliveau R. Differential regulation of matrix metalloproteinase activities in abdominal aortic aneurysms. *J Vasc Surg*. 2002;35:539-46.

40. Johnson LL, Dyer R, Hupe DJ. Matrix metalloproteinases. *Curr Opin Chem Biol.* 1998;2:466-71.
41. Schwartz RS, Henry TD. Pathophysiology of coronary artery restenosis. *Rev Cardiovasc Med.* 2002;3:S4-9.
42. Taubes G. Cardiovascular disease. Does inflammation cut to the heart of the matter? *Science.* 2002;296:242-5.
43. Koenig W. Inflammation and coronary heart disease: an overview. *Cardiol Rev.* 2001;9:31-5.
44. Cesari M, Penninx BW, Newman AB, Kritchevsky SB, Nicklas BJ, Sutton-Tyrrell K, Rubin SM, Ding J, Simonsick EM, Harris TB, Pahor M. Inflammatory Markers and Onset of Cardiovascular Events: Results From the Health ABC Study. *Circulation.* 2003;108:2317-2322.
45. Jabs WJ, Theissing E, Nitschke M, Bechtel JF, Duchrow M, Mohamed S, Jahrbeck B, Sievers HH, Steinhoff J, Bartels C. Local generation of C-reactive protein in diseased coronary artery venous bypass grafts and normal vascular tissue. *Circulation.* 2003;108:1428-31.
46. Rifai N, Ridker PM. High-sensitivity C-reactive protein: a novel and promising marker of coronary heart disease. *Clin Chem.* 2001;47:403-11.
47. Lind L. Circulating markers of inflammation and atherosclerosis. *Atherosclerosis.* 2003;169:203-14.
48. Vainas T, Lubbers T, Stassen FR, Herngreen SB, van Dieijen-Visser MP, Bruggeman CA, Kitslaar PJ, Schurink GW. Serum C-reactive protein level is

- associated with abdominal aortic aneurysm size and may be produced by aneurysmal tissue. *Circulation*. 2003;107:1103-5.
49. Domanovits H, Schillinger M, Mullner M, Holzenbein T, Janata K, Bayegan K, Laggner AN. Acute phase reactants in patients with abdominal aortic aneurysm. *Atherosclerosis*. 2002;163:297-302.
  50. Corti R, Fuster V, Badimon JJ. Pathogenetic concepts of acute coronary syndromes. *J Am Coll Cardiol*. 2003;41:7S-14S.
  51. Danenberg HD, Szalai AJ, Swaminathan RV, Peng L, Chen Z, Seifert P, Fay WP, Simon DI, Edelman ER. Increased thrombosis after arterial injury in human C-reactive protein-transgenic mice. *Circulation*. 2003;108:512-5.
  52. Zwolak RM, Kirkman TR, Clowes AW. Atherosclerosis in rabbit vein grafts. *Arteriosclerosis*. 1989;9:374-9.
  53. Davies MG, Huynh TT, Fulton GJ, Barber L, Svendsen E, Hagen PO. Early morphology of accelerated vein graft atheroma in experimental vein grafts. *Ann Vasc Surg*. 1999;13:378-85.
  54. Kamimura R, Suzuki S, Sakamoto H, Miura N, Misumi K, Miyahara K. Development of atherosclerotic lesions in cholesterol-loaded rabbits. *Exp Anim*. 1999;48:1-7.
  55. Kamenz J, Seibold W, Wohlfrom M, Hanke S, Heise N, Lenz C, Hanke H. Incidence of intimal proliferation and apoptosis following balloon angioplasty in an atherosclerotic rabbit model. *Cardiovasc Res*. 2000;45:766-76.

56. Holmes DR, Petrincec D, Wester W, Thompson RW, Reilly JM. Indomethacin prevents elastase-induced abdominal aortic aneurysms in the rat. *J Surg Res.* 1996;63:305-9.
57. Miralles M, Wester W, Sicard GA, Thompson R, Reilly JM. Indomethacin inhibits expansion of experimental aortic aneurysms via inhibition of the cox2 isoform of cyclooxygenase. *J Vasc Surg.* 1999;29:884-92; discussion 892-3.
58. Curci JA, Petrincec D, Liao S, Golub LM, Thompson RW. Pharmacologic suppression of experimental abdominal aortic aneurysms: a comparison of doxycycline and four chemically modified tetracyclines. *J Vasc Surg.* 1998;28:1082-93.
59. Baumann DS, Doblus M, Daugherty A, Sicard G, Schonfeld G. The role of cholesterol accumulation in prosthetic vascular graft anastomotic intimal hyperplasia. *J Vasc Surg.* 1994;19:435-45.
60. Cassel WS, Mason RA, Campbell R, Newton GB, Hui JC, Giron F. An animal model for small-diameter arterial grafts. *J Invest Surg.* 1989;2:181-6.
61. Lee ES, Bauer GE, Caldwell MP, Santilli SM. Association of artery wall hypoxia and cellular proliferation at a vascular anastomosis. *J Surg Res.* 2000;91:32-7.
62. Barolet AW, Nili N, Cheema A, Robinson R, Natarajan MK, O'Blenes S, Li J, Eskandarian MR, Sparkes J, Rabinovitch M, Strauss BH. Arterial elastase activity after balloon angioplasty and effects of elafin, an elastase inhibitor. *Arterioscler Thromb Vasc Biol.* 2001;21:1269-74.

63. Naito M, Nomura H, Esaki T, Iguchi A. Characteristics of macrophage-derived foam cells isolated from atherosclerotic lesions of rabbits. *Atherosclerosis*. 1997;135:241-7.
64. Galis ZS, Sukhova GK, Kranzhofer R, Clark S, Libby P. Macrophage foam cells from experimental atheroma constitutively produce matrix-degrading proteinases. *Proc Natl Acad Sci U S A*. 1995;92:402-6.
65. Zaltsman AB, Newby AC. Increased secretion of gelatinases A and B from the aortas of cholesterol fed rabbits: relationship to lesion severity. *Atherosclerosis*. 1997;130:61-70.
66. Davis V, Persidskaia R, Baca-Regen L, Itoh Y, Nagase H, Persidsky Y, Ghorpade A, Baxter BT. Matrix metalloproteinase-2 production and its binding to the matrix are increased in abdominal aortic aneurysms. *Arterioscler Thromb Vasc Biol*. 1998;18:1625-33.
67. McMillan WD, Pearce WH. Increased plasma levels of metalloproteinase-9 are associated with abdominal aortic aneurysms. *J Vasc Surg*. 1999;29:122-7; discussion 127-9.
68. Kunishima A, Takemura G, Takatsu H, Hayakawa Y, Kanoh M, Qiu X, Fujiwara T, Fujiwara H. Mode and role of cell death during progression of atherosclerotic lesions in hypercholesterolemic rabbits. *Heart Vessels*. 1999;14:295-306.
69. Roselaar SE, Schonfeld G, Daugherty A. Enhanced development of atherosclerosis in cholesterol-fed rabbits by suppression of cell-mediated immunity. *J Clin Invest*. 1995;96:1389-94.

70. Staprans I, Pan XM, Rapp JH, Feingold KR. Oxidized cholesterol in the diet accelerates the development of aortic atherosclerosis in cholesterol-fed rabbits. *Arterioscler Thromb Vasc Biol.* 1998;18:977-83.
71. Wilson RB, Miller RA, Middleton CC, Kinden D. Atherosclerosis in rabbits fed a low cholesterol diet for five years. *Arteriosclerosis.* 1982;2:228-41.
72. Chiesa G, Di Mario C, Colombo N, Vignati L, Marchesi M, Monteggia E, Parolini C, Lorenzon P, Laucello M, Lorusso V, Adamian M, Franceschini G, Newton R, Sirtori CR. Development of a lipid-rich, soft plaque in rabbits, monitored by histology and intravascular ultrasound. *Atherosclerosis.* 2001;156:277-87.
73. Daida H, Yokoi H, Miyano H, Mokuno H, Satoh H, Kottke TE, Hosoda Y, Yamaguchi H. Relation of saphenous vein graft obstruction to serum cholesterol levels. *J Am Coll Cardiol.* 1995;25:193-7.
74. Campeau L. Lipid lowering and coronary bypass graft surgery. *Curr Opin Cardiol.* 2000;15:395-9.
75. Kreitmann B, Riberi A, Zeranska M, Novakovitch G, Metras D. Growth potential of aortic autografts and allografts: effects of cryopreservation and immunosuppression in an experimental model. *Eur J Cardiothorac Surg.* 1997;11:943-52.
76. Kazama S, Miyoshi Y, Nie M, Imai H, Lin ZB, Kurata A, Machii M. Protection of the Spinal Cord with Pentobarbital and Hypothermia. *Ann Thorac Surg.* 2001;71:1591-5.

77. Senior RM, Griffin GL, Fliszar CJ, Shapiro SD, Goldberg GI, Welgus HG. Human 92- and 72-kilodalton type IV collagenases are elastases. *J Biol Chem.* 1991;266:7870-5.
78. Greisler HP, Klosak JJ, Endean ED, McGurrin JF, Garfield JD, Kim DU. Effects of hypercholesterolemia on healing of vascular grafts. *J Invest Surg.* 1991;4:299-312.
79. Boger RH, Bode-Boger SM, Kienke S, Stan AC, Nafe R, Frolich JC. Dietary L-arginine decreases myointimal cell proliferation and vascular monocyte accumulation in cholesterol-fed rabbits. *Atherosclerosis.* 1998;136:67-77.
80. Ito T, Tsukada T, Ueda M, Wanibuchi H, Shiomi M. Immunohistochemical and quantitative analysis of cellular and extracellular components of aortic atherosclerosis in WHHL rabbits. *J Atheroscler Thromb.* 1994;1:45-52.
81. Verhamme P, Quarck R, Hao H, Knaapen M, Dymarkowski S, Bernar H, Van Cleemput J, Janssens S, Vermynen J, Gabbiani G, Kockx M, Holvoet P. Dietary cholesterol withdrawal reduces vascular inflammation and induces coronary plaque stabilization in miniature pigs. *Cardiovasc Res.* 2002;56:135-44.
82. Lijnen HR. Extracellular proteolysis in the development and progression of atherosclerosis. *Biochem Soc Trans.* 2002;30:163-7.
83. Opdenakker G, Van den Steen PE, Van Damme J. Gelatinase B: a tuner and amplifier of immune functions. *Trends Immunol.* 2001;22:571-9.

## Chapter 3

### The effect of a decreased inflammatory response on graft survival

#### Introduction

#### Inflammation

Inflammation has been linked to the development of intimal hyperplasia<sup>1,2</sup>, atherosclerosis<sup>3-8</sup> and aneurysm<sup>9-11</sup> and in all cases there is a response involving resident and inflammatory cells, matrix metalloproteases (MMPs) and the extracellular matrix. During an inflammatory type response there is an influx of cells into the area and macrophages are a major component of this influx later in the response. This is significant because macrophages have been implicated in the degradation of collagen under normal and pathological conditions. They are present during the development and progression of atherosclerosis<sup>12-15</sup> and in aneurysm formation<sup>16</sup> where their activity is due to increased MMP production or activity<sup>9,17</sup>. *In vitro*, binding to collagen increased the differentiation of monocytes to macrophages and increased the release of MMP9<sup>18</sup>. Based on these observations, macrophages appear to be directly involved in the degeneration of the graft material and eventual failure leading to the hypothesis that **inflammation plays a key role in vascular graft failure.**

It was hypothesized that any inflammatory response seen toward the graft material in the previous chapter would be reduced by the administration of anti-inflammatory or anti-macrophage drugs to the rabbits. Two drugs were selected: Indomethacin, a non-specific anti-inflammatory agent and Etidronate, a specific anti-



macrophage agent to test this hypothesis and compared the results to a control group treated with saline. Treatment with these drugs would allow for the determination of whether a reduction in the overall inflammatory response (Indomethacin) would increase graft durability or if macrophages specifically could be targeted to increase durability (Etidronate).

### **Indomethacin**

Indomethacin belongs to the family of non-steroidal anti-inflammatory drugs (NSAIDs) that include aspirin and ibuprofen, and exert their action by specifically inhibiting the activity of cyclooxygenase (COX). In contrast to the action of aspirin, which irreversibly inactivates COX 1 and 2 via an acetylation reaction, Indomethacin causes a slow and reversible enzyme inhibition by the formation of a salt bridge between the carboxylate of indomethacin and the arginine at position 120 of COX 1 and 2, located in the hydrophobic tunnel constituting the active site of the enzyme<sup>19</sup>. COX 3 is inhibited by acetaminophen<sup>20</sup> but no mechanism is suggested.

The cyclooxygenases (COX 1 and 2, alternately spliced isozymes) are involved in the production of prostaglandins from arachidonic acid. COX 1 is mostly present in platelets, is constitutively expressed, and is involved in the production of platelets, prostaglandin E<sub>2</sub> for kidney function, and prostaglandin I<sub>2</sub> for mucus production in the stomach, while COX 2 is the isoform that is induced in cells by an inflammatory stimulus, and is involved in the production of prostaglandin E<sub>2</sub> (PGE<sub>2</sub>) which produces the redness, swelling and vasodilatation in the inflammatory process<sup>21,22</sup>. COX 3, a

variant of COX 1, is present in brain tissue<sup>20,23</sup> and appears to be involved in the fever response.

Indomethacin has been used experimentally to reduce the severity of atherosclerosis in rabbits<sup>24,25</sup> and to prevent elastase-induced aneurysm formation in the rat<sup>26,27</sup>. In both atherosclerosis and aneurysm formation, macrophages are known to elaborate matrix metalloproteinases (MMPs), which are involved in the degradation of extracellular matrix components of the tissue and it is this action that is involved in the pathology and progression of these diseases. Indomethacin exerts an effect via inhibition of COX 2, down-regulating PGE2 expression and in doing so, down-regulating the production of MMP9<sup>27</sup> and attenuating aneurysm formation in an elastase-perfused abdominal aortic rat model<sup>26</sup>. Administration of indomethacin also suppressed the formation of intimal hyperplasia in a balloon injury rat model in a COX 1-dependent manner<sup>28</sup>. Administration of indomethacin should therefore inhibit both aneurysm formation and anastomotic hyperplasia. .

### **Etidronate**

Bisphosphonates are very stable non-hydrolyzable analogs of pyrophosphate characterized by two chemically and enzymatically stable C-P bonds<sup>29,30</sup>. This class of drugs are used therapeutically in diseases of the bone (e.g. Osteoporosis, Paget's disease, Ectopic calcification, Hypercalcemia), specifically inhibiting bone resorption and mineralization<sup>30,31</sup> by inhibiting the growth/breakdown of hydroxyapatite crystals by binding tightly to calcium.

Bisphosphonates can be subdivided into non-amino and amino containing compounds which function by different mechanisms. The mode of action of non-amino containing bisphosphonates (e.g. Clodronate and Etidronate) appears to be primarily due to a 'suicide' mechanism, whereby the drugs are metabolized by macrophage-like cells by incorporation into ATP<sup>32,33</sup>. This produces a non-hydrolyzable ATP analog and accumulation leads to cell death (osteoclasts and macrophages)<sup>29,34</sup>. The remainder of the (amino-) bisphosphonates (e.g. Pamidronate and Alendronate) inhibit isopentenyl diphosphate synthase or farnesyl diphosphate synthase in the mevalonate pathway which ultimately affects the prenylation of small GTP-binding proteins<sup>35,36</sup>, inhibiting the formation of cholesterol, and ultimately activate caspases leading to apoptosis<sup>37</sup>.

The effect of bisphosphonates on macrophage function and survival is well documented in the literature<sup>31,32,38-44</sup>. These drugs are shown to accumulate in the tissues of both normal and atherosclerotic rabbits<sup>31</sup>, reduce plaque formation and severity<sup>42,43</sup>, as well as calcification<sup>43</sup>. An unexpected collateral effect of bisphosphonates are their anti-inflammatory effects<sup>33,35</sup> which could be attributed to the induction of macrophage apoptosis.

**Specific Aim: To evaluate the role of decreased inflammation via drug treatment on the xenogenic graft material.**

### **Rationale**

Previous studies have shown that Indomethacin<sup>24-27</sup> and Etidronate<sup>33,35</sup> exert an anti-inflammatory action in the rabbit. Both drugs also have an effect on macrophage

activity and survival and it was hypothesized that administration of anti-inflammatory drugs would reduce the severity of the inflammatory response towards the Corograft™ conduit and the effect of decreased inflammation on the vascular graft could be assessed.

### **Experimental Design**

In this portion of the study, 3 groups of 5 rabbits were treated with saline, Indomethacin or Etidronate prior to implantation of the graft, and the drug treatments were continued post-operatively. Blood samples were also collected prior to surgery and at sacrifice. The grafts were harvested at 63 days and analyzed by histology and immunohistology. Also, zymograms for MMP activity and a Humoral ELISA were performed on surgery and sacrifice serum samples. As both drugs would affect macrophages, a reduction in the number of macrophages would be used as an indicator of drug treatment efficacy. CRP levels were to be analyzed but proved to be prohibitively expensive and were not done.

## Materials and Methods

### Animal Source and Care

Female New Zealand White rabbits (weighing ~3-4kg) were purchased from Western Oregon Rabbit Company (Philomath, OR, USA) and allowed to acclimate for at least 7 days before initiating any procedures. Rabbits had access to normal rabbit chow and water *ad libitum* through out the duration of the study. Average room temperature was 63°F (17-18°C), with a 12hr day/night cycle and 10-12 air changes/hr. All animals appeared clinically normal throughout the 7 day quarantine period and no other pathogen testing was done. Baseline blood sample was collected prior to the first injection of drug.

### Drug Administration

Each group was pretreated with drug 1-2 hours prior to surgery. This time was chosen because previously published studies with indomethacin had shown that the arachidonic acid cascade is initiated early on in inflammation<sup>45,46</sup>, and in order to keep everything equivalent the same time was used for Etidronate. Dosage: Normal Saline (2ml SC), Indomethacin (4mg/kg SC), Etidronate (2.5mg/kg SC). Each drug was administered once daily as described for the 63 day period of the study with weekly adjustments for weight gain/loss. Normal saline (0.9% Sodium Chloride Irrigation, USP, Baxter Healthcare Corporation, Deerfield, IL, USA), Indomethacin, USP (Sigma Chemical Co., St. Louis, MO, USA) dissolved in 100% EtOH at 20mg/ml (maximum solubility), Etidronate disodium (Didronel<sup>®</sup> I.V. Infusion, 50mg/ml, MGI Pharma, Inc. Minnetonka, MN, USA).

## **Preoperative Preparation**

Rabbits were sedated with an intramuscular dose of ketamine (50mg/kg), the abdominal region shaved, and the rabbit placed in a dorsal recumbent position on a heating pad (heating pad was off during the hypothermic phase of the surgery). Anesthesia was induced and maintained with 1.5-2% Isoflurane/Oxygen mixture administered via a ventilator/anesthesia delivery system (North American Drager, Telford, PA, USA or Isotec 4, Surgivet/Anesco Veterinary Surgical Products, Waukesha, WI, USA), and the level of isoflurane was adjusted as needed to keep the animal sufficiently anesthetized, as evaluated by ear pinch or any evidence of discomfort. The chest cavity was not opened allowing for passive, spontaneous ventilation by the animal<sup>47,48</sup>. The core temperature was monitored with a rectal temperature probe and electrocardiographic leads were attached so the heart rate could be monitored. Icepacks were placed around and between the hind-legs and along the lower flanks. An intravenous cannula (22 gauge) was introduced into the marginal ear vein and cold (4°C) supplemented Lactated Ringer's Solution was given initiating the hypothermic phase of the surgery. The supplemented Lactated Ringer's solution contained per liter: 20ml sodium bicarbonate (84mg/ml and 50mEq/50ml, American Pharmaceutical Partners, Inc. Los Angeles, CA, USA), 50ml of 20% mannitol solution and 0.5ml dexamethasone sodium phosphate (4mg/ml, American Regent Laboratories, Shirley, NY, USA).

## **Surgical Protocol**

After sterile draping, a midline laparotomy was performed. The skin was retracted with traction sutures and the intestines were displaced to the right side and

wrapped in laparotomy sponges moistened with cold sterile saline. Isolation of the abdominal aorta from the surrounding tissues from below the left renal artery to the iliac bifurcation was performed meticulously to avoid accidental injury to the inferior vena cava and its branches. Care was taken to identify all aortic branches along the entire circumference. If feasible, anastomotic sites were planned to avoid cutting of the large dorsal aortic branches. Once all dissection was completed, one ml of heparin was administered i.v. (1000 USP units/ml, American Pharmaceutical Partners, Inc., Los Angeles, CA, USA) and if necessary, further cooling of the animal was achieved by using sterile saline slush applied directly into the abdominal cavity and to the laparotomy sponge covering the intestines.

When the rectal temperature of the animal reached 34.5°C, the ice packs and the saline slush were removed as the temperature continued to drop without additional cooling. The cold supplemented Lactated Ringer's solution was exchanged for warm (37°C). Also, warm packs were placed next to the rabbit under the sterile draping and the heating pad under the rabbit was switched on to start the re-warming phase of the procedure initiating the re-warming period of the surgery.

Dorsal aortic branches within the previously prepared aortic segment were clipped and cut. The aorta was occluded proximally and distally with micro-surgical vascular clamps (MORIA 200/A, Angled, 30mm. Fine Science Tools, Inc. Foster City, CA, USA) placed below the left renal artery and above the inferior mesenteric artery. And keeping in mind the elastic recoil of the vessel, the aorta was cut approximately 1 cm from each clamp to avoid space issues.

All animals had a Corograft™ (~3-4mm ID x ~4cm minimum) previously re-hydrated in heparinized saline, implanted into the infrarenal abdominal aorta. An end-to-end anastomosis (distal then proximal) was performed with a continuous single 8/0 Prolene suture (Polypropylene, Ethicon, Inc., Somerville, NJ, USA). Before tying the suture for the proximal anastomosis, the distal vascular clamp was removed to flush air from the graft by filling the graft with blood to avoid an air embolism. After tying the suture, the proximal vascular clamp was removed and additional 8/0 Prolene suture used (as needed) to control anastomotic or graft bleeding.

The intestines were returned to the abdominal cavity and repeatedly lavaged with warm sterile saline to achieve appropriate re-warming of the animal. When the rectal temperature of the rabbit reached 36.5°C to 37.5°C, the saline was removed and the laparotomy closed in two layers with 3/0 Vicryl (Polygalactin 910, Ethicon, Inc., Somerville, NJ, USA). The supplemented Lactated Ringer's solution was discontinued, with a total amount of 100-150ml having been administered for both the cold and warm solutions. When the animal was re-warmed to physiological temperature (101-104°F/38-40°C) and movement was seen in the hind-limbs, the animal was returned to its' cage.

Rabbits received 0.2ml flunixin meglumine (50mg/ml, Equileve®, Phoenix Scientific, Inc., St. Joseph, MO, USA) i.m. as an analgesic immediately after surgery, and 0.2ml i.m. flunixin meglumine BID for 4 days post-operatively. All rabbits were monitored for neurologic or ischemic complications of the hind limbs throughout the study. No antibiotic prophylaxis, platelet aggregation inhibitors nor anticoagulants were used postoperatively.



For rabbits in the drug treatment groups, the flunixin dosage (50mg/ml, Equileve®, Phoenix Scientific, Inc., St. Joseph, MO, USA) was adjusted to 1.1mg/kg postoperatively and then 1.1mg/kg BID for the following 3 days.

### **Sacrifice**

The animals were sedated, brought to a full surgical plane of anesthesia, and sacrificed before graft isolation. The abdominal incision was re-opened and the graft dissected from surrounding tissues. The graft was then excised en-bloc and placed into Histo-Choice Tissue Fixative MB (Amresco Inc., Solon, Ohio, USA) for a minimum of 24hrs before further processing.

### **Macroscopic Examination**

Excess non-adherent tissue/fat was trimmed from the exterior of the graft and the graft was photographed with markers placed indicating the suture lines and direction of flow. Each graft was evaluated macroscopically for aneurysmatic changes (indicated by an area of vessel wall ballooning outwards and being of a greater diameter than the originally implanted graft), atherosclerotic lesions, thrombus, or any other obvious abnormalities.

### **Histology**

Samples (2-3mm) cut from the center of the graft were dehydrated and embedded in PolyFin wax (Polysciences, Inc., Warrington, Pennsylvania, USA), sectioned at 5µm, and collected on slides coated with poly-L-lysine (Sigma Chemical Co., St. Louis, MO,

USA) or charged slides (Superfrost<sup>®</sup> plus, VWR Scientific, West Chester, PA, USA).

Representative sections were stained with hematoxylin and eosin (H&E) for general tissue/cellular morphology, Masson's Trichrome for collagen and Movat's Pentachrome stain for collagen and elastin

### **Immunohistology**

Slides for immunohistology were prepared as above. Representative sections were stained for  $\alpha$ -smooth muscle cell actin (a smooth muscle cell/myofibroblast marker), CD3 (pan-T cell antibody) and RAM 11 (rabbit macrophage-specific antibody). Sections stained for  $\alpha$ -SMC actin were deparaffinized, treated with 3% H<sub>2</sub>O<sub>2</sub> for 5min to remove endogenous peroxidases, rinsed with dH<sub>2</sub>O and blocked with 0.05% Tween-20 (Sigma Chemical Co., St. Louis, Missouri, USA) in phosphate buffered saline (PBS-T) for 30min. The slides were incubated for 30min with the appropriate primary antibody diluted in PBS-T, then rinsed with PBS-T. Sections stained for  $\alpha$ -actin were incubated with Protein A-horseradish peroxidase (Sigma Chemical Co., St. Louis, Missouri, USA), 1:500 dilution in PBS-T for 30min. Sections stained for rabbit macrophages (RAM 11) and T cells (CD3) were treated with the components of the LSAB-2 biotin-streptavidin amplification kit (DAKO, Carpinteria, California, USA) according to the supplied instructions with the incorporation of an avidin/biotin blocking procedure. All incubations were carried out in a moist chamber at room temperature. Sections were rinsed with PBS-T and developed by the addition of 100 $\mu$ l of DAB substrate (Sigma Fast DAB, Sigma Chemical Co., St. Louis, Missouri, USA) per slide. The development was

stopped with water and the slides counterstained with H&E or hematoxylin alone. The slides were dehydrated, cleared and coverslipped.

Antibody to:	Clone	Dilution	Development	Source
$\alpha$ -Smooth Muscle Cell Actin	1A4	1:400	Protein A-HRP	Sigma
Rabbit Macrophage	RAM 11	1:500	LSAB-2	Dako
T Cell/CD3	Rbt poly	1:50	LSAB-2	Dako

### **Macrophage Counts**

Macrophages are involved in the inflammatory response toward the graft, and the numbers present were used as an indirect indicator of disease severity or efficacy of drug treatment. Slides stained with the RAM11 antibody were used in this portion of the study. Five random 100X fields were photographed at the junction between graft tissue and abluminal tissue where the majority of the chronic-type inflammatory reaction was located. The images were imported into Corel Photo-Paint, gamma adjusted to sharpen the color, and counted manually. The number of single macrophages and giant cells were counted per image and averaged to obtain the count.

### **Zymography**

MMPs are produced as part of an inflammatory response and are involved in graft degeneration, therefore pre- and post-operative serum samples were qualitatively evaluated for circulating MMP levels. The conditions present during zymography allow for the detection of both the pro-forms and activated MMPs, due to the dissociation of the active MMPs from inhibitors or the spontaneous activation of zymogens<sup>49,50</sup>.

Serum samples were electrophoresed on 10% polyacrylamide gels containing 1mg/ml Gelatin or Elastin. The samples were diluted 1:10 (v:v) with saline and then 1:1

with 2X Non-denaturing Sample Buffer (no  $\beta$ -Mercaptoethanol), 20 $\mu$ l loaded onto the gel and run at 200 V until completion. The gels were washed 2X 30 min with 2.5% Triton X-100/dH<sub>2</sub>O with agitation, washed 30 min with RT Activation Buffer with agitation, and then incubated O/N in Activation Buffer at 37°C with agitation (Activation buffer 25mM Tris, 10mM CaCl<sub>2</sub>, 1 $\mu$ M ZnCl<sub>2</sub>, 50mM NaCl, pH 7.5). Gels were stained with coomassie brilliant blue and areas of gelatinolytic or elastolytic activity were seen as clear bands against a blue background. MMP activity was confirmed by incubating the gels in the presence of 1mmol/L 1,10-phenantroline (MMP inhibitor) in the activation buffer in both the 30 minute wash and overnight incubation<sup>9</sup>.

The MMP profile for all groups did not change between the surgery and sacrifice samples within groups, between groups, or between normal diet and cholesterol diet. Also, no major observable differences in band intensity were seen between surgery and sacrifice samples by visual examination.

### **ELISA for Humoral Response**

Dry graft material was lyophilized to a constant weight, suspended in 1% acetic acid at a concentration of 1mg/ml (w/v) and homogenized. The material was diluted to ~250ug/ml with 0.02M Carbonate buffer (pH 9.6) and 100ul (~25ug/well) of collagen was added to each well of a 96-well plate (Falcon PRO-BIND™, Becton Dickinson and Company, Franklin Lakes, NJ, USA). The plates were evaporated to dryness overnight at room temperature in a hood. Before use, the plates were washed 4X with PBS-T and blocked for 45 min RT (or O/N at 4°C) with 100ul PBS-T/1% BSA per well. The wells were then rinsed 4X with PBS-T and serial 2-fold dilutions of serum were plated in

PBS/1% BSA (50ul/well in duplicate). The plates were incubated at RT for 1hr and washed 4X with PBS-T. Anti-Rabbit IgG-HRP (Monoclonal Anti-Rabbit IgG  $\gamma$ -chain specific, Clone RG-96, Peroxidase Conjugate A-1949, Sigma-Aldrich Co, St Louis, MO, USA) was diluted 1:40,000 in PBS-T/1% BSA and 50ul/well was added. The plate was incubated 2hrs at RT and washed 4X with PBS-T. OPD substrate (HRP substrate, Dako Corporation, Carpinteria, CA, USA) was prepared according to the manufacturers instructions (dissolved in room temperature dH<sub>2</sub>O and 30% H<sub>2</sub>O<sub>2</sub> added) and 50ul of the substrate solution was added to each well. The color was allowed to develop 30min at room temperature and the reaction stopped by the addition of 50ul of 0.5M H<sub>2</sub>SO<sub>4</sub> to each well. The absorbance was read at 490nm in a microplate reader (Opsys MR, Dynex Technologies, Chantilly, VA, USA).

Normal rabbit serum was included as the negative control and the values obtained used to adjust for serum absorbance. In all cases the OD value from the normal rabbit serum was subtracted from the mean valued obtained for the corresponding dilutions of the experimental samples. The titer listed is derived from the last well giving a positive OD after adjustment. Blank values were obtained from wells incubated with PBS-T/1% BSA instead of serum and subtracted from all OD values by the microplate reader software.

## **Results**

### **Post-operative survival**

Twenty-eight rabbits were implanted with a graft during this portion of the study. Fifteen rabbits made up the three experimental groups, which were treated with Saline, Indomethacin or Etidronate. The remaining 13 rabbits were excluded due to complications. Four rabbits died during surgery of unknown causes after unclamping the abdominal aorta. Four were found dead in their cages on day 0 post-operatively, 3 of unknown causes and 1 due to operative complications. Two developed paralysis during the post-operative recovery period and were euthanized on day 0. Three additional rabbits survived the surgery but developed complications unrelated to the graft and were later euthanized. In all cases the implanted grafts were patent upon necropsy.

### **Drug Treated Groups Macroscopic**

No obvious differences were noted between groups. All grafts were patent at explant and were surrounded by host tissue with little to no adhesions seen within the abdominal cavity. No obvious degeneration or aneurysmic dilation of graft material was seen (Figures 10, 11 & 12: Saline, Indomethacin & Etidronate Macroscopic).

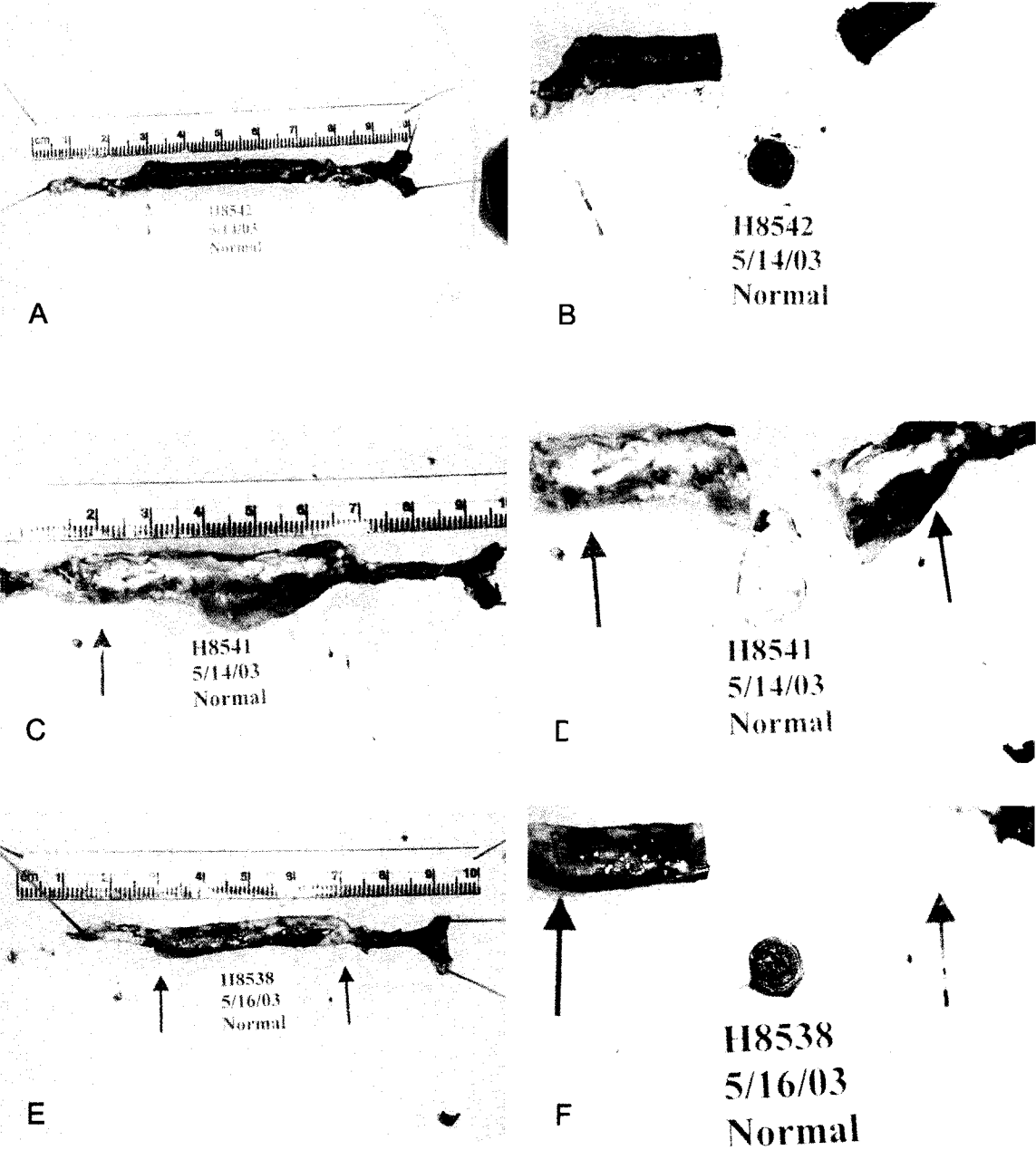
### **Histology**

#### **Saline Controls 2 Months (Figure 13: Saline Control Histology)**

In samples H8542 and H8538, the graft matrix was present in two distinct layers, medial more luminal and adventitial, and some adherent clot was seen in the lumen (post-mortem). The graft tissue was relatively acellular with well-preserved matrix although

Figure 10: Macroscopic images of Saline treated control samples. Grafts are shown in both an external (Panel A, C, E, G, and I) and internal view (Panel B, D, F, H and J). All grafts were patent at explant and were surrounded by host tissue. No dilation was seen in any of the samples. The coagulated blood seen in the lumen of Grafts H8542, H8538 and H8540 is from post-mortem clotting. ↑Arrows indicate the suture lines. In all cases, the flow of blood is from left to right.

Figure 10: Saline sample macroscopic





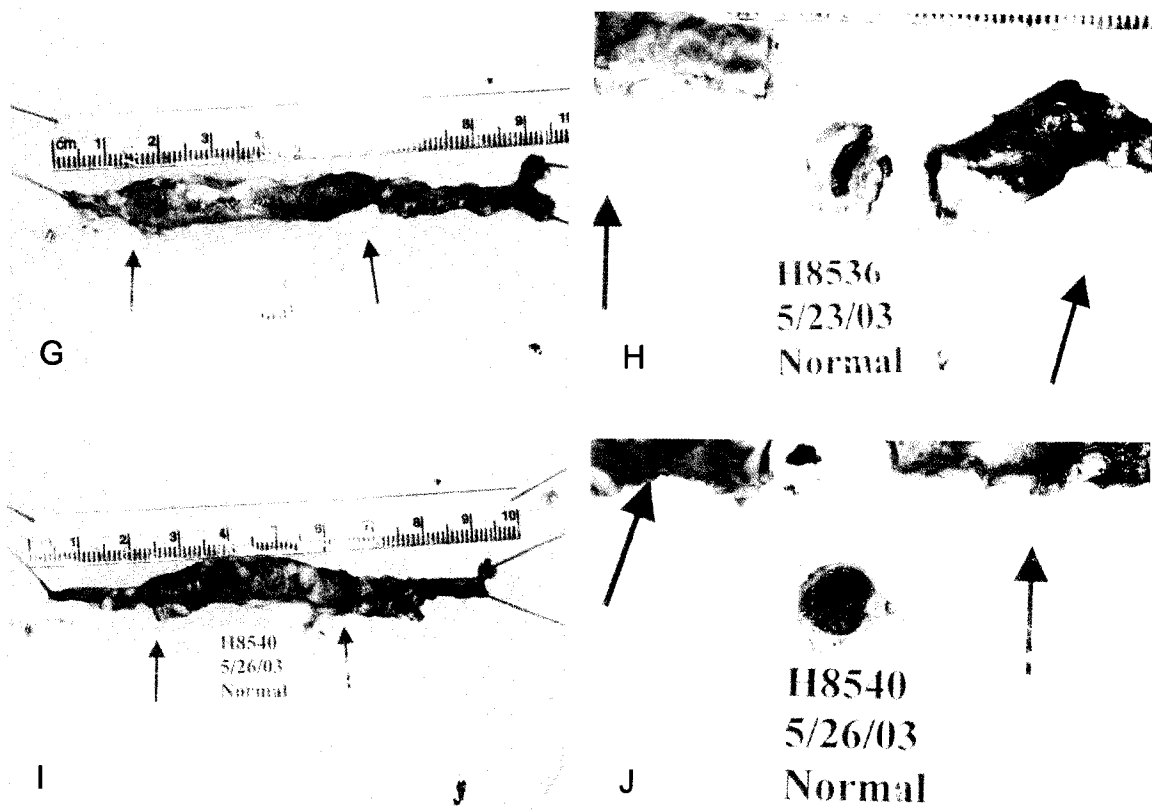
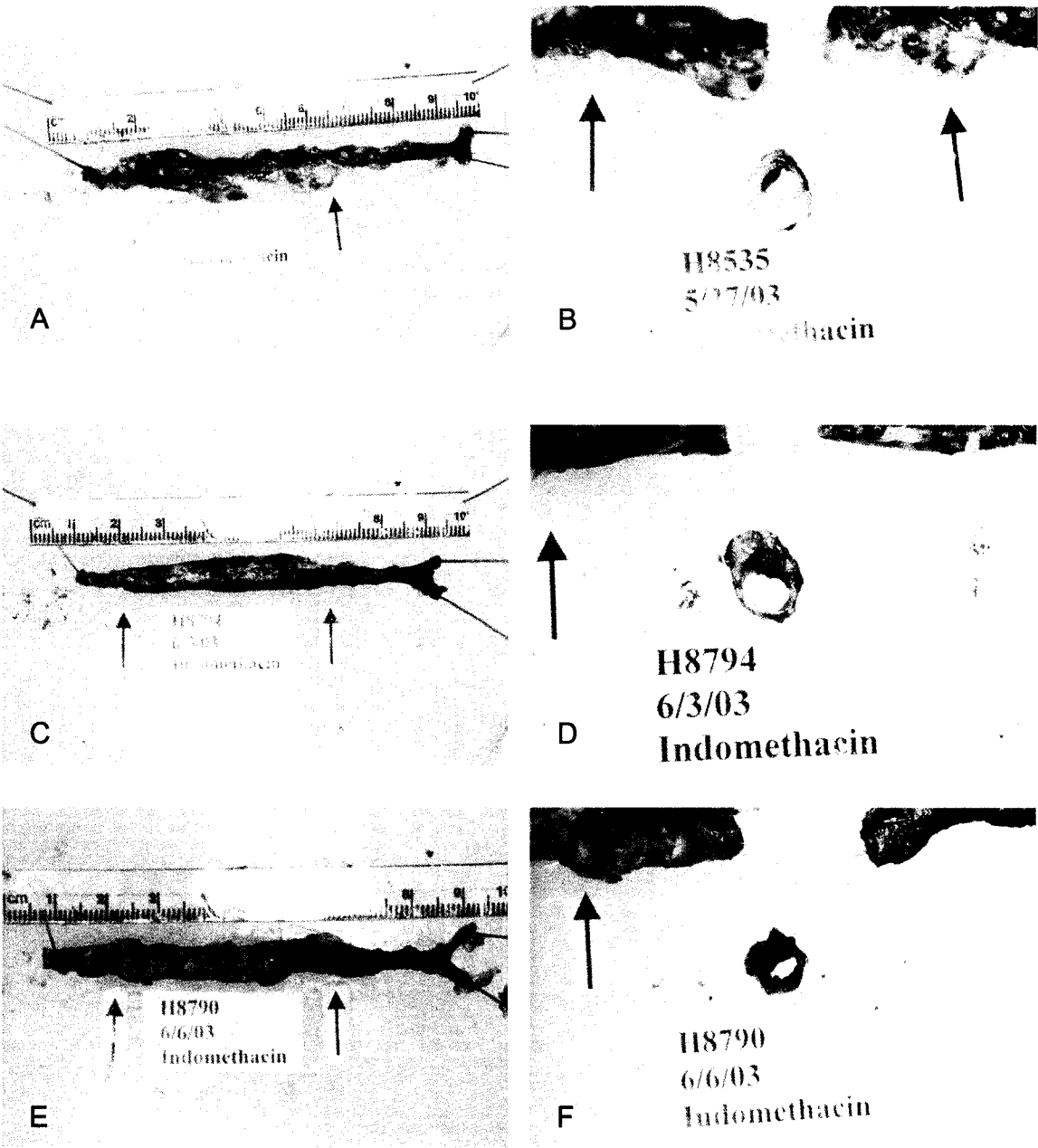


Figure 11: Macroscopic images of Indomethacin treated samples. Grafts are shown in both an external (Panel A, C, E, G, and I) and internal view (Panel B, D, F, H and J). All grafts were patent at explant and were surrounded by host tissue. No dilation was seen in any of the samples. The coagulated blood seen in the lumen of Grafts H8790 and H8707 is from post-mortem clotting. ↑ Arrows indicate the suture lines. In all cases, the flow of blood is from left to right.

Figure 11: Indomethacin treated macroscopic



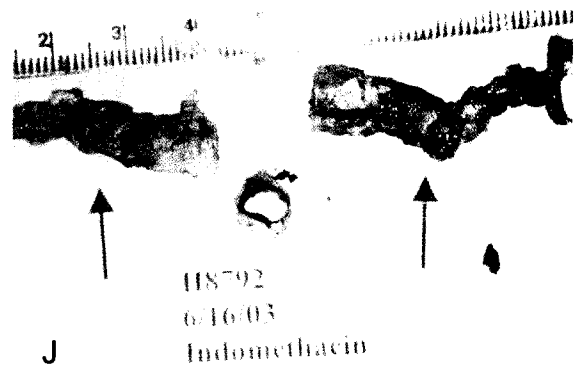
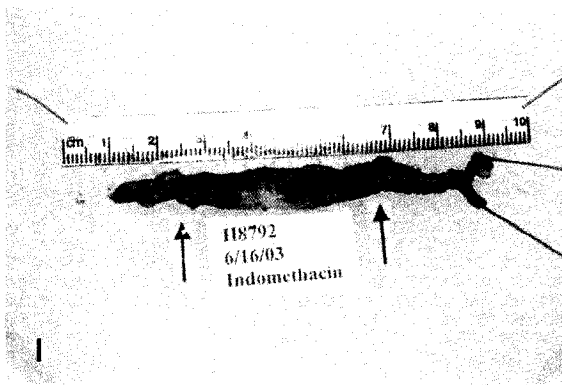
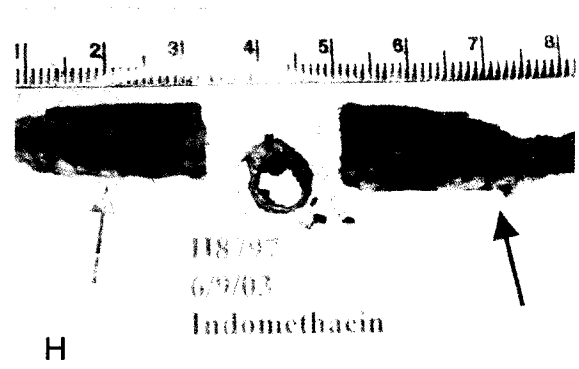
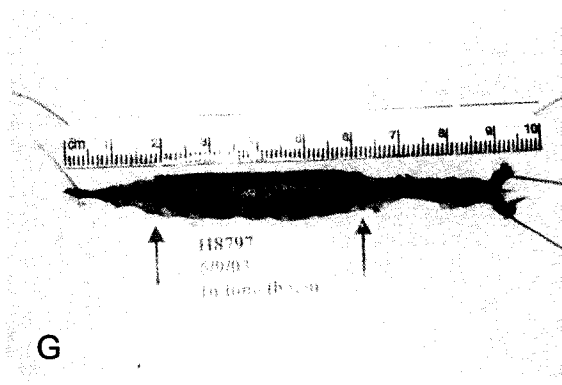
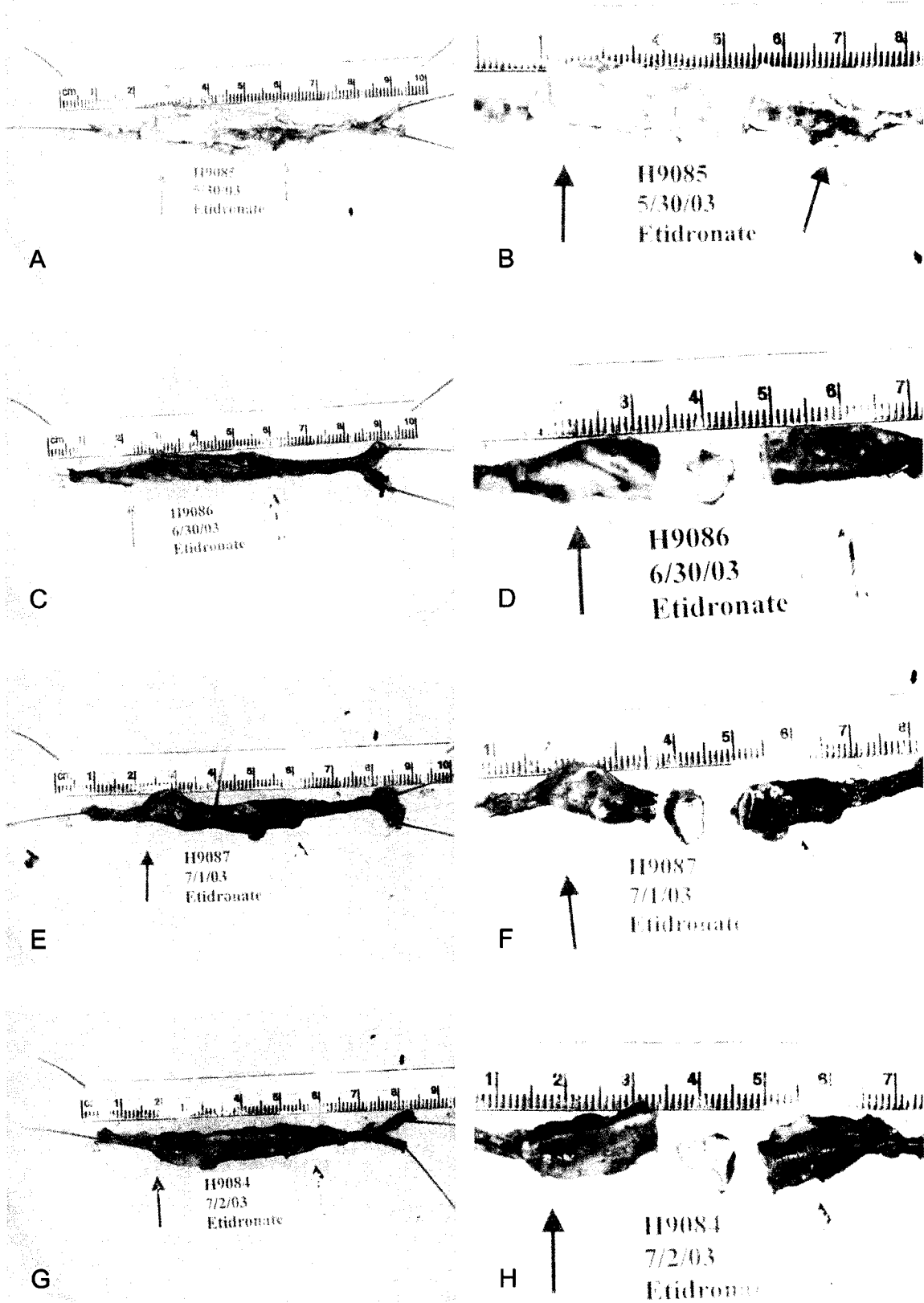
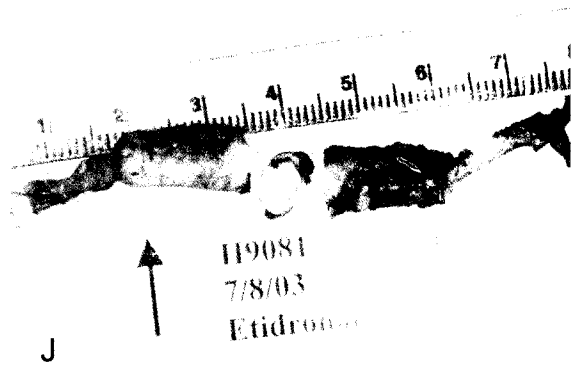
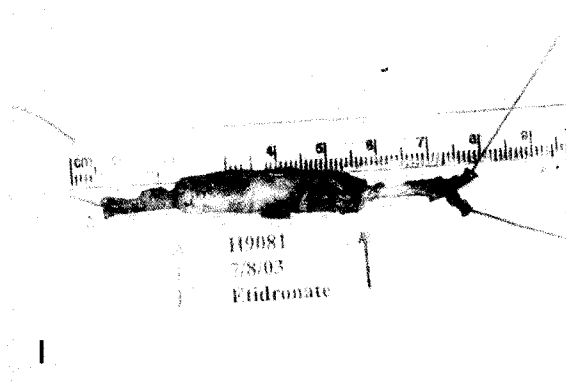


Figure 12: Macroscopic images of Etidronate treated samples. Grafts are shown in both an external (Panel A, C, E, G, and I) and internal view (Panel B, D, F, H and J). All grafts were patent at explant and were surrounded by host tissue. No dilation was seen in any of the samples. The coagulated blood seen in the lumen of Grafts H8790 and H8707 is from post-mortem clotting. ↑Arrows indicate the suture lines. In all cases, the flow of blood is from left to right.

Figure 12: Etidronate treated macroscopic





cells were present within the medial (circumferential) layer (WBCs). In samples H8541, H8536, and H8540 the graft matrix was very cellular, and the layers were not clearly defined due to expansion of the graft material by cells and new matrix material. Grafts H8542 and H8538 had a thin abluminal layer containing mostly loose connective tissue, blood vessels and other cells of unknown type. Grafts H8541, H8536, and H8540 had a relatively thick abluminal layer containing blood vessels, adipose tissue as well as immature collagen fibrils and collections of inflammatory-type cells (**Fig. 13-1A and C**). No actin staining seen within grafts H8542 and H8538, though abluminal blood vessels were staining. In grafts H8541 and H8536 cells staining for  $\alpha$ -SMC actin were present for  $\sim 1/2$  of the circumference in both the medial layer and adventitial (longitudinal) layer (**Fig. 13-2A, C and D**), and in abluminal blood vessels. A few cells staining for actin were present in the more superficial medial layer of graft H8540 although blood vessels were stained. Macrophages and giant cells were located at the junction between the adventitial (longitudinal) layer and the thin abluminal layer of H8542 and H8538. A layer of giant cells separated the medial and adventitial matrix, and formed a ring around the graft tissue of H8541 (**Fig. 13-1D**), and giant cells were also seen within the medial layer. Occasional giant cells were also seen adherent to the luminal surface, and in some cases were located in the more superficial portion of the medial layer and caused a portion of the graft material to protrude into the lumen. In H8536 and H8540 few giant cells were present, mostly located between the medial and the adventitial layers of the graft as well as within the abluminal layer, while single macrophages were present within the adventitial tissue. Trichrome staining of H8542 and H8538 showed the majority of the collagen was mature and well-preserved (**Fig. 13-3B and E**). Trichrome of H8541,



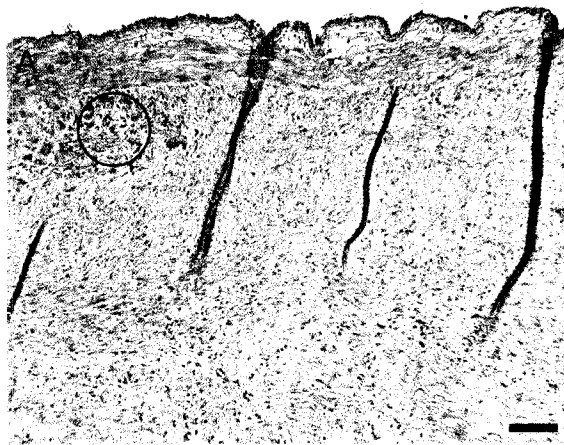
H8536, and H8540 showed that the majority of the collagen present was stained more lightly although remnants of more darkly stained mature collagen fibers were still present in the adventitial layer (**Fig. 13-3A, C and D**), and the abluminal layer contained a loose collection of small, lightly stained collagen fibrils. Movats staining of H8542 and H8538 showed well-preserved elastin in the adventitial (longitudinal) layer, elastic fibrils in the medial (circumferential layer), and a complete internal elastic lamina. In H8541 and H8536, elastin fibers were not readily apparent and no internal elastic lamina remained. In H8540 elastin fibers were present within the medial (circumferential) layer but no internal elastic lamina remained. All samples had cells staining for CD3 scattered throughout the abluminal layer.

#### **Indomethacin Treated 2 Months (Figure 14: Indomethacin Histology)**

Samples from H8535, H8794 and H8792 showed the graft matrix was present in two distinct layers, medial and adventitial with some adherent clot present within the lumen (post-mortem). The graft tissue was relatively acellular with well-preserved matrix although cells were present within the medial layer and appeared to be mostly PMNs (**Fig. 14-1A, C and D**). The graft matrix of H8790 and H8797 was present in two distinct layers with some adherent luminal clot. In these cases, two-thirds of the graft tissue was relatively acellular with well-preserved matrix with PMNs within the medial layer (**Fig. 14-1B and E**), while the remaining third of the graft was re-colonized by host-derived cells. Sample H8790 also had PMNs adherent to the luminal surface. The abluminal layer of samples H8535, H8794, H8790 and H8797 was thin and contained mostly loose connective tissue, blood vessels and some other cells of unknown type,

Figure 13-1: Saline control samples were embedded and 5 $\mu$ m sections were stained with H&E for general tissue morphology and cellularity. The graft tissue in H8538 and H8542 was relatively acellular with well-preserved matrix while in H8536, H8540 and H8541 the graft matrix was very cellular. Collections of inflammatory-type cells were seen in H8536 and H8540 (open circles). Macrophages and giant cells in H8541 formed a ring around the graft tissue and were seen within the medial layer ( $\uparrow$ ). In H8536 and H8540 few giant cells were present. Scale bar  $\sim$ 100 $\mu$ m.

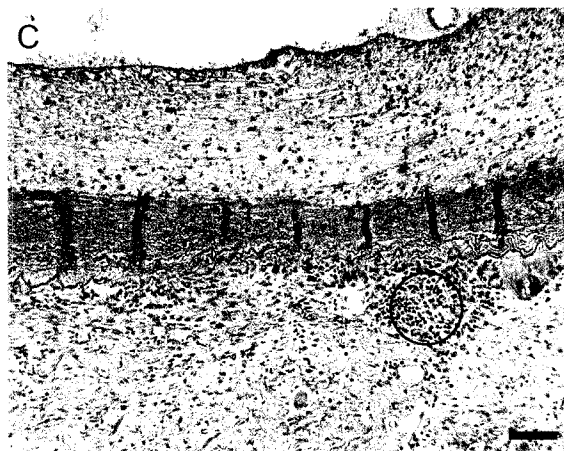
Figure 13-1: H&E stain of Saline control samples



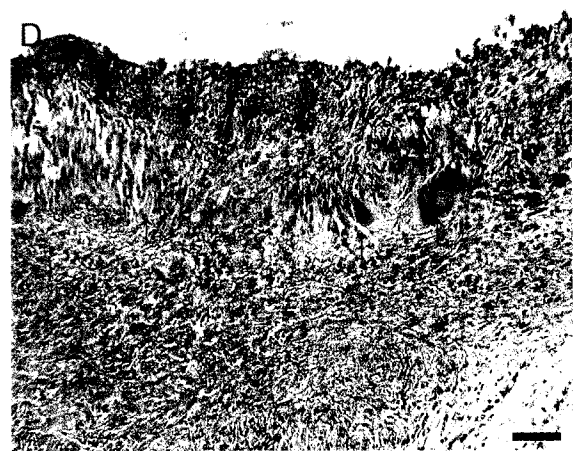
H8536 Saline Control



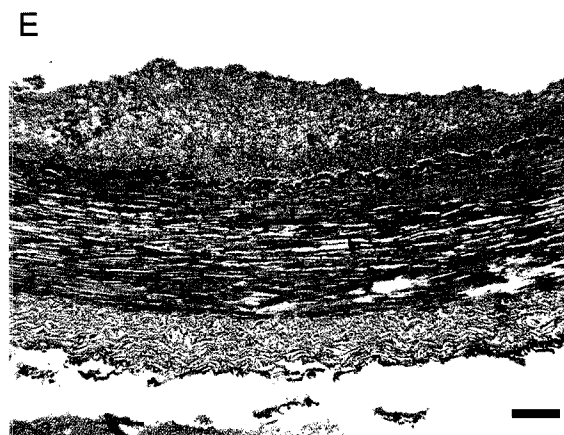
H8538 Saline Control



H8540 Saline Control



H8541 Saline Control



H8542 Saline Control

Figure 13-2: Saline control samples were embedded and 5 $\mu$ m sections were stained for  $\alpha$ -smooth muscle cell actin, a marker of smooth muscle cells and myofibroblasts. The presence of actin-staining cells would indicate the presence of host-derived myofibroblasts (involved in healing) or smooth muscle cells (cells normally present in blood vessels). No actin staining was seen within H8542 and H8538, in H8541 and H8536 cells staining for  $\alpha$ -SMC actin were present in both the medial layer and adventitial layer, and in G8540 a few cells staining for actin were present in the medial layer (open circles). Scale bar  $\sim$ 100 $\mu$ m.

Figure 13-2: Actin stain of Saline control samples



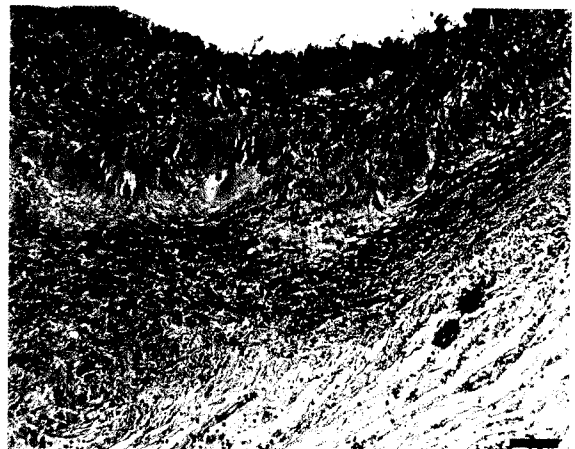
H8536 Saline Control



H8538 Saline Control



H8540 Saline Control



H8541 Saline Control



H8542 Saline Control

Figure 13-3: Saline control samples were embedded and 5 $\mu$ m sections were stained by Massons Trichrome. This stain is for collagen integrity and organization. The darker blue collagen is considered more mature, while lighter staining collagen is considered indicative of less mature collagen. The majority of the collagen was mature and well-preserved in H8538 and H8542 while in H8536, H8540 and H8541 the majority of the collagen present was more lightly stained with remnants of more darkly stained mature collagen fibers in the adventitial layer (open circles). Scale bar ~100 $\mu$ m.

Figure 13-3: Trichrome stain of Saline control samples



H8536 Saline Control



H8538 Saline Control



H8540 Saline Control



H8541 Saline Control



H8542 Saline Control

while graft H8792 had a relatively thicker abluminal layer containing blood vessels, adipose tissue, collagen, few inflammatory-type cells and some macrophages and giant cells. In all grafts (H8535, H8794, H8790, H8797, and H8792), macrophages and giant cells were located at the junction between the adventitial layer of graft tissue and the abluminal layer (**Fig 14-1A to E**). In H8790 macrophages and giant cells were seen adhering to a portion of the lumen directly apposed to the internal elastic lamina. Actin staining was mostly confined to adventitial blood vessels in all samples. In addition to blood vessels, H8794 had a few actin staining cells within the graft at the junction between the medial and adventitial layer, and in H8790 several actin staining cells were seen within the adventitial layer of the graft (**Fig.14-2B and D**). Trichrome showed the majority of the collagen was mature and well-preserved in H8535, H8790, H8797 and H8792 (**Fig 14-3A, B, C and E**). In H8790, H8797 and H8792 the medial layer appeared expanded, and mature collagen and looser connective tissue was seen in the abluminal layer. Trichrome of H8794 showed the majority of the collagen was newer, though mature collagen was present and may be a remnant from the original graft (**Fig. 14-3D**). Movats showed well-preserved elastin in the adventitial layer, fibrils in the medial layer, and a complete internal elastic lamina in H8535, H8797, H8792, while a mostly complete internal elastic lamina was seen in H8794 and H8790. Cells staining for CD3 were scattered throughout the abluminal layer in all samples.

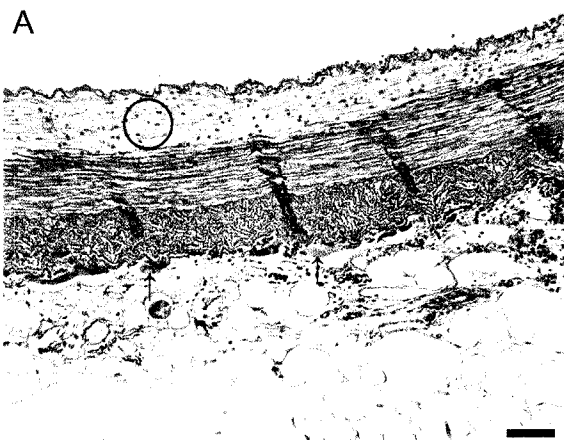
#### **Etidronate Treated 1 Month\* (Figure 15: Etidronate Histology)**

The graft matrix from rabbit H9085 was present in two distinct layers, medial and adventitial. The graft tissue was relatively acellular with well-preserved collagen,

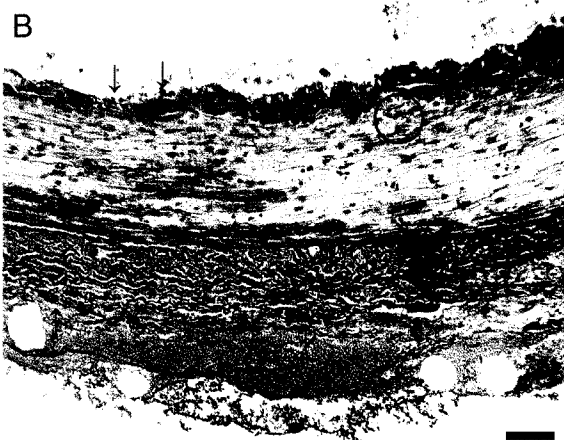


Figure 14-1: Indomethacin samples were embedded and 5 $\mu$ m sections were stained with H&E for general tissue morphology and cellularity. H8535, H8794 and H8792 showed the graft tissue was relatively acellular with well-preserved matrix although cells were present within the medial layer and appeared to be mostly PMNs (open circles). In H8790 and H8797 the majority of the graft tissue was relatively acellular with well-preserved matrix with PMNs within the medial layer. Sample H8790 also had PMNs adherent to the luminal surface ( $\downarrow$ ). In H8535, H8794, H8790, H8797, and H8792 macrophages and giant cells were located at the junction between the adventitial layer of graft tissue and the abluminal layer ( $\uparrow$ ). Scale bar  $\sim$ 100 $\mu$ m.

Figure 14-1: H&E stain of Indomethacin samples



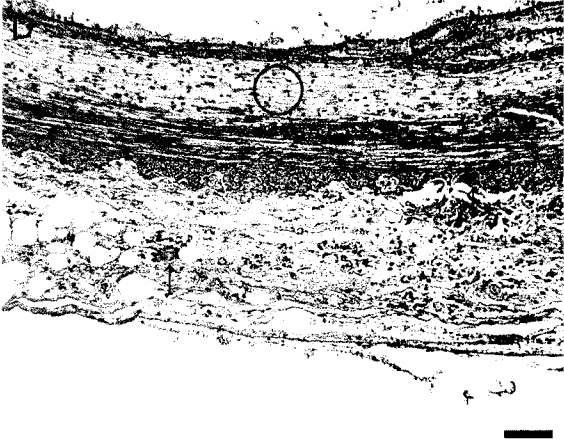
H8535 Indomethacin Sample



H8790 Indomethacin Sample



H8792 Indomethacin Sample



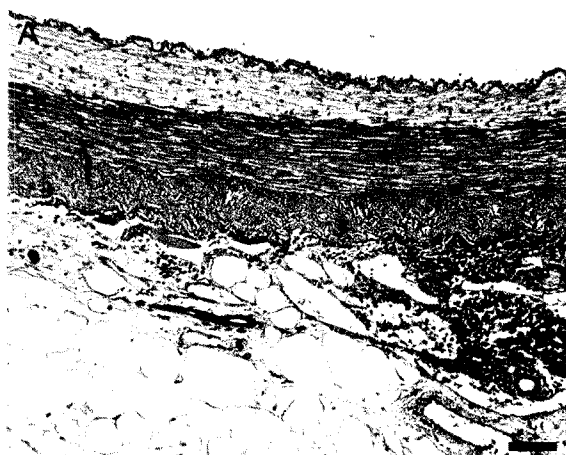
H8794 Indomethacin Sample



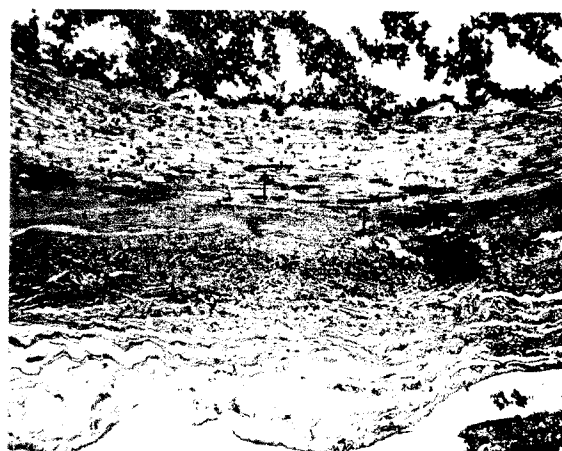
H8797 Indomethacin Sample

Figure 14-2: Indomethacin samples were embedded and 5 $\mu$ m sections were stained for  $\alpha$ -smooth muscle cell actin, a marker of smooth muscle cells and myofibroblasts. The presence of actin-staining cells would indicate the presence of host-derived myofibroblasts (involved in healing) or smooth muscle cells (cells normally present in blood vessels). Actin staining was mostly confined to adventitial blood vessels in all samples. H8794 had a few actin staining cells within the graft at the junction between the medial and adventitial layer, and in H8790 several actin staining cells were seen within the adventitial layer of the graft ( $\uparrow$ ). Scale bar  $\sim$ 100 $\mu$ m.

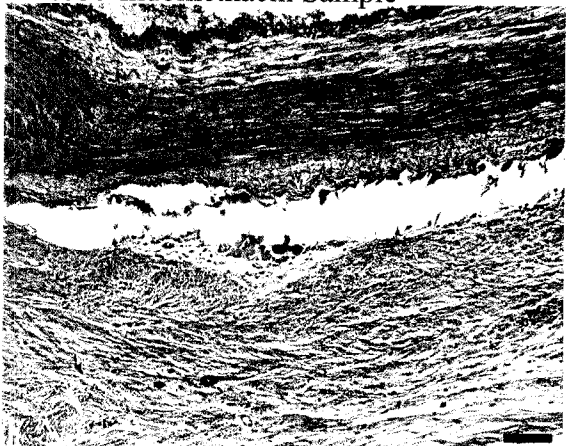
Figure 14-2: Actin stain of Indomethacin samples



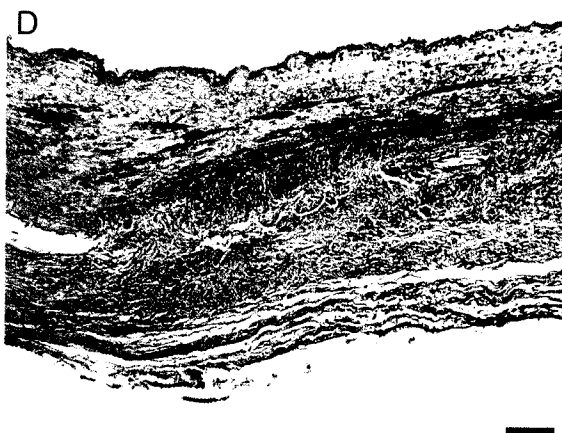
H8535 Indomethacin Sample



H8790 Indomethacin Sample



H8792 Indomethacin Sample



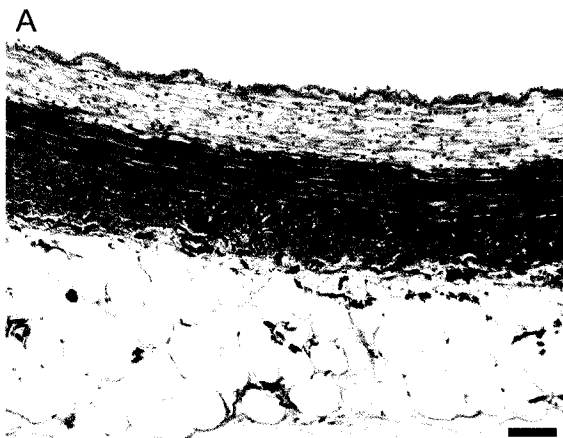
H8794 Indomethacin Sample



H8797 Indomethacin Sample

Figure 14-3: Indomethacin samples were embedded and 5 $\mu$ m sections were stained by Massons Trichrome. This stain is for collagen integrity and organization. The darker blue collagen is considered more mature, while lighter staining collagen is considered indicative of less mature collagen. In H8535, H8790, H8797 and H8792 the majority of the collagen was mature and well-preserved. In H8790, H8797 and H8792 the medial layer appeared expanded (open circles) while in H8794 the majority of the collagen was newer (open circle), though mature collagen was present and may be a remnant from the original graft ( $\uparrow$ ). Scale bar  $\sim$ 100 $\mu$ m.

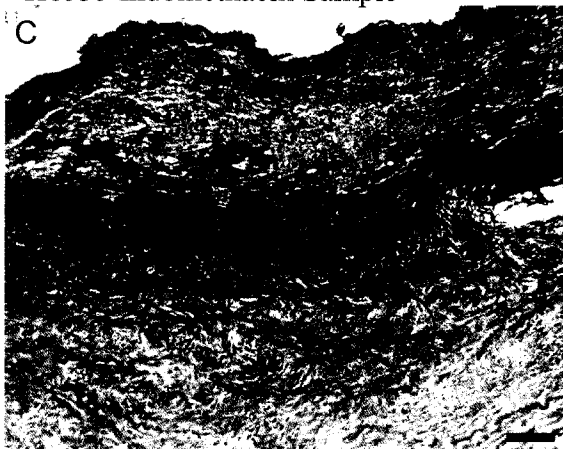
Figure 14-3: Trichrome stain of Indomethacin samples



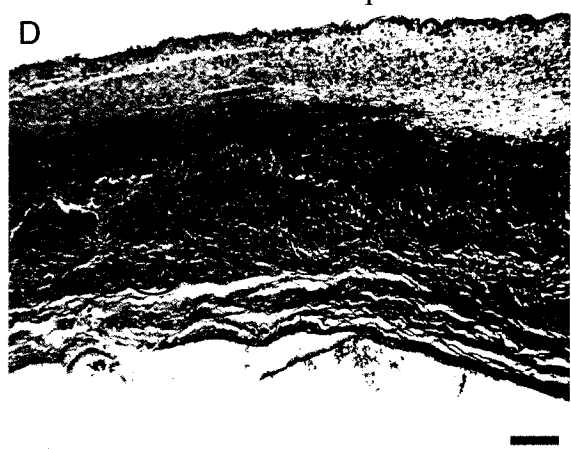
H8535 Indomethacin Sample



H8790 Indomethacin Sample



H8792 Indomethacin Sample



H8794 Indomethacin Sample



H8797 Indomethacin Sample

although cells were present within the medial layer and appeared to be mostly PMNs (**Fig. 15-1C**). A relatively thicker abluminal layer was present containing blood vessels, adipose tissue, collagen, numerous inflammatory-type cells and numerous macrophages and many giant cells that were located at the junction between the adventitial layer of graft tissue and the abluminal layer as well as within this layer (**Fig. 15-1C**). No actin staining cells were seen within the adventitial layer of the graft, and adventitial blood vessels were staining (**Fig. 15-2C**). Trichrome showed that the medial layer appeared expanded, mature collagen and looser connective tissue were seen in the adventitial layer and abluminal layers. Movats showed well-preserved elastin in a majority of the adventitial layer, fibrils in the medial layer, and a complete internal elastic lamina. Occasional cells staining for CD3 were scattered throughout the abluminal layer.

#### **Etidronate Treated 2 Months (Figure 15: Etidronate Histology)**

The graft matrix of H9086, H9087 and H9084 was present in two distinct layers, medial and adventitial. The graft tissue was relatively cellular with well-preserved collagen, and the cells present within the medial layer appear to be mostly PMNs in H9086, mostly PMNs and macrophages with a few fibroblastic-type cells in H9087, while in H9084 were PMNs, macrophages with the majority of this layer repopulated with fibroblastic type cells (**Fig. 15-1B, D and E**). In H9081 the graft matrix was present in two distinct layers, medial and adventitial but was relatively acellular with well-preserved matrix although cells are present within the medial layer and appear to be mostly PMNs (**Fig. 15-1A**). All samples had an abluminal layer of varying thickness containing blood vessels, adipose tissue, collagen, few inflammatory-type cells and macrophages (**Fig. 15-**

**1A, B, D and E).** In H9086 and H9087 few macrophages and giant cells were located at the junction between the adventitial layer of graft tissue and the abluminal layer, and H9087 had more giant cells present within the abluminal layer. Sample H9084 had many giant cells and single macrophages located at the junction of the adventitial and abluminal layer, with more giant cells present within the abluminal layer (**Fig. 15-1B**). H9081 had few macrophages and many giant cells at the junction of the adventitial and abluminal layer as well as deeper in this tissue layer. Macrophage giant cells were also seen adherent to the luminal surface (**Fig. 15-3A**). In addition to actin staining seen in the abluminal tissue of all samples, H9086 had several actin staining cells sparsely distributed within the adventitial layer of the graft (**Fig. 15-2D**). H9087 had numerous actin staining cells distributed within the medial and adventitial layer of the graft and in the abluminal tissue (**Fig. 15-2E**). H9084 had several small collections of actin staining cells that were distributed within the medial and adventitial layers and a larger patch present on the luminal surface of the graft (**Fig. 15-2B**). Although not a complete re-population, actin staining cells were seen within the medial layer at the junction with the adventitial layer of the graft and in the adventitia of H9081 (**Fig. 15-2A**). In all samples, trichrome staining showed the majority of the collagen was mature and well-preserved, the medial layer appeared expanded, and mature collagen and looser connective tissue were seen in the abluminal layer (**Fig. 15-3A to E**). Movats showed well-preserved elastin in a majority of the adventitial (longitudinal) layer, fibrils in the medial (circumferential) layer, with a complete internal elastic lamina in H9086, or an occasional fragment of internal elastic lamina in H9087. In H9084 and H9081, Movats showed well-preserved elastin in a majority of the adventitial layer, few fibrils in the



medial (circumferential) layer, and no internal elastic lamina (H9084) or a fragmented internal elastic lamina (H9081). Occasional cells staining for CD3 were scattered throughout the abluminal layer.

### **Macrophage Counts**

The saline control group had a mean of 44.8 macrophages present, while this number was reduced for the drug-treated groups. The Indomethacin group had a mean of 14.68 macrophages, and the Etidronate group had a mean of 13.5 macrophages (without 9085 25 day) and 20.3 macrophages per 100X field (with 9085). This corresponds to a 67.2% reduction in mean number of macrophages present in the Indomethacin samples, and a 69.95% reduction in mean number of macrophages in the Etidronate group (no 9085). The differences between the saline controls and the drug treatment samples are statistically significant by Dunnett multiple comparison tests (Indomethacin  $P < 0.01$ , Etidronate  $P < 0.05$ )

### **Zymography**

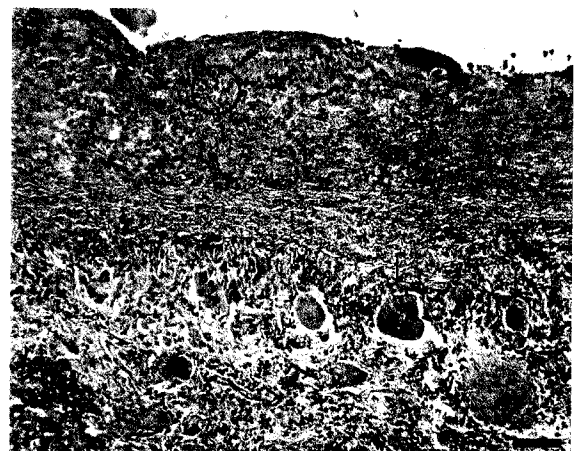
The MMP profiles did not change between the surgery and sacrifice samples and no major observable differences in band intensity were seen between surgery and sacrifice. However, zymograms showed a difference in the MMP profile between control and drug treated samples, seen as an absence of the higher mw MMPs and several minor bands in both the Indomethacin and Etidronate groups. The Etidronate serum samples showed nearly a complete absence of MMP activity, while the activity was very reduced in the Indomethacin samples. Development in the presence of 1,10-phenanthroline (MMP

Figure 15-1: Etidronate samples were embedded and 5 $\mu$ m sections were stained with H&E for general tissue morphology and cellularity. H9085 was relatively acellular with well-preserved collagen, although cells were present within the medial layer and appeared to be mostly PMNs (open circle). Numerous inflammatory-type cells ( $\uparrow$ ), macrophages and giant cells ( $\downarrow$ ) were located at the junction between the adventitial layer of graft tissue and the abluminal layer and within this layer. H9086, H9087 and H9084 was relatively cellular with well-preserved collagen, and the cells present within the medial layer appear to be mostly PMNs in H9086, PMNs and macrophages with a few fibroblastic-type cells in H9087, H9084 were PMNs, macrophages and fibroblastic type cells (open circle). H9081 the graft matrix was relatively acellular with well-preserved matrix although the cells present within the medial layer appear to be PMNs (open circles). H9086 and H9087 few macrophages and giant cells were located at the junction between the graft tissue and the abluminal layer, and H9087 had more giant cells present within the abluminal layer. H9084 had many giant cells and single macrophages located at the junction of the graft and abluminal layer. H9081 had few macrophages and many giant cells giant cells at the junction of the graft and abluminal layer with macrophage giant cells adherent to the luminal surface. Fewer inflammatory-type cells ( $\uparrow$ ) were present in H9081, H9086, H9087 and H9084 compared to H9085. Scale bar  $\sim$ 100 $\mu$ m.

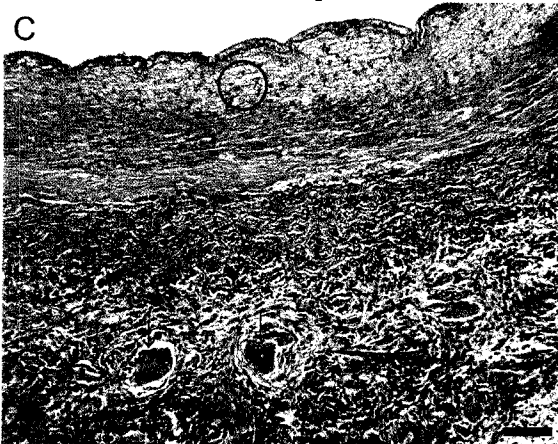
Figure 15-1: H&E stain of Etidronate samples



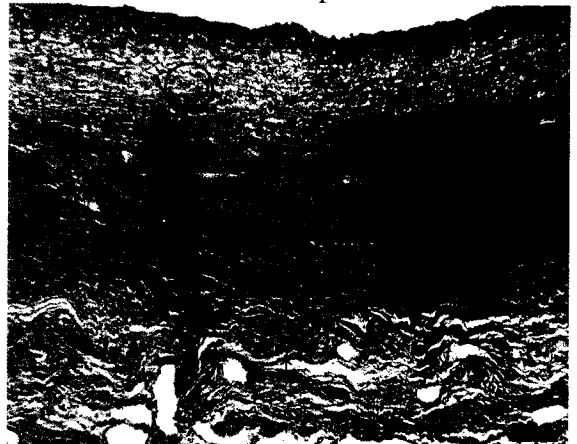
H9081 Etidronate Sample



H9084 Etidronate Sample



H9085 Etidronate Sample - 1 month



H9086 Etidronate Sample



H9087 Etidronate Sample

Figure 15-2: Etidronate samples were embedded and 5 $\mu$ m sections were stained for  $\alpha$ -smooth muscle cell actin, a marker of smooth muscle cells and myofibroblasts. The presence of actin-staining cells would indicate the presence of host-derived myofibroblasts (involved in healing) or smooth muscle cells (cells normally present in blood vessels). In H9085 no actin staining was seen within the graft. H9086 had several actin staining cells sparsely distributed within the adventitial layer of the graft. H9087 had numerous actin staining cells distributed within the medial and adventitial layers of the graft. H9084 had several small collections of actin staining cells within the medial and adventitia layers with a larger patch present on the luminal surface ( $\downarrow$ ). Actin staining cells were seen within the medial layer at the junction with the adventitial layer of the graft of H9081. Scale bar  $\sim$ 100 $\mu$ m.

Figure 15-2: Actin stain of Etidronate samples



H9081 Etidronate Sample



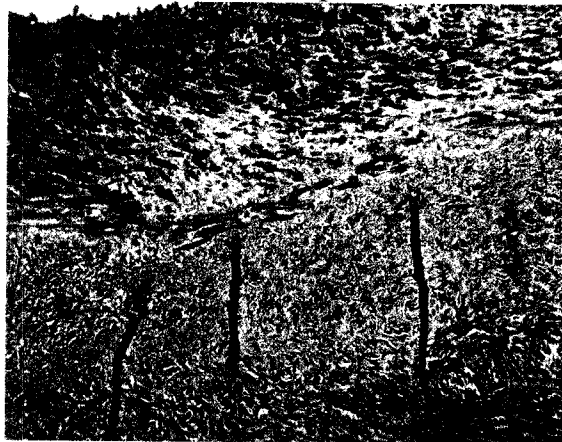
H9084 Etidronate Sample



H9085 Etidronate Sample



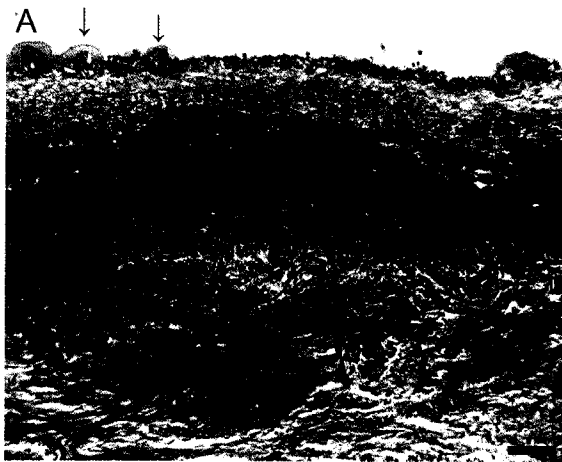
H9086 Etidronate Sample



H9087 Etidronate Sample

Figure 15-3: Etidronate samples were embedded and 5 $\mu$ m sections were stained by Massons Trichrome. This stain is for collagen integrity and organization. The darker blue collagen is considered more mature, while lighter staining collagen is considered indicative of less mature collagen. In all samples, Trichrome staining showed the majority of the collagen was mature and well-preserved with newer collagen present (open circles). Scale bar ~100 $\mu$ m.

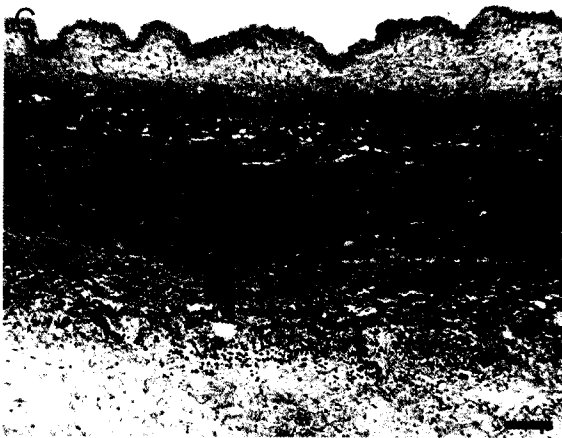
Figure 15-3: Trichrome stain of Etidronate samples



H9081 Etidronate Sample



H9084 Etidronate Sample



H9085 Etidronate Sample



H9086 Etidronate Sample



H9087 Etidronate Sample

inhibitor) indicated that the majority of the gelatinolytic activity was due to MMPs, with very little due to other proteases (data not shown). No elastolytic activity was observed in any of the samples at 4 days.

### **Humoral ELISA**

Statistical analysis of the ELISA titer log values indicated that there were no significant differences between surgery and sacrifice in the saline treated groups (paired two-tail T test). Statistically significant differences (paired two-tailed T test) were seen between the surgery and sacrifice samples for Indomethacin ( $P < 0.0001$ ) and Etidronate ( $P = 0.0054$ ). However no significant differences were seen between the control and drug-treated samples at sacrifice.



Table 8: Macrophage counts from Drug treatment samples.

Slides stained for RAM11 were used to generate the counts. Five high-power fields were photographed at the junction of the graft material and the abluminal host tissue. The macrophages were counted, and the number averaged to obtain the given values. Values are Mean  $\pm$  SEM.

Table 8: Macrophage Counts - Drug Treatment

Rabbit #	Average # of Macrophages	Mean # of Macrophages <sup>#</sup>	% Reduction in # Macrophage
Control			
H8541 2 month	56.2	44.8±6.4	N/A
H8542 2 month	40.2		
H8538 2 month	46.8		
H8536 2 month	22.8		
H8540 2 month	57.8		
Indomethacin			
H8535 2 month	16.8	14.6±2.6	67.2%
H8794 2 month	18.8		
H8790 2 month	10.6		
H8797 2 month	20.6		
H8792 2 month	6.6		
Etidronate			
H9085* 1 month	12.6	22.15±8.6 (20.3±6.9*)	50.5% (54.6%*)
H9086 2 month	47.4		
H9087 2 month	13.8		
H9084 2 month	18.0		
H9081 2 month	9.4		

\*Indicates numbers calculated with the 1 month sample

<sup>#</sup>Mean ± SEM

Figure 16: To analyze differences in MMP presence or expression between surgery and sacrifice samples, equivalent amounts of serum were electrophoresed on 10% acrylamide gels containing 1% gelatin. The gels were run to completion, washed to remove SDS, and incubated in activation buffer (with and without MMP inhibitor) for the appropriate time. Gels were stained with coomassie brilliant blue, and active bands appear as clear bands on a blue background. No observable differences were seen within or between groups, or between diet types for all rabbits.

Figure 16: Zymograms of Normal, Indomethacin and Etidronate samples

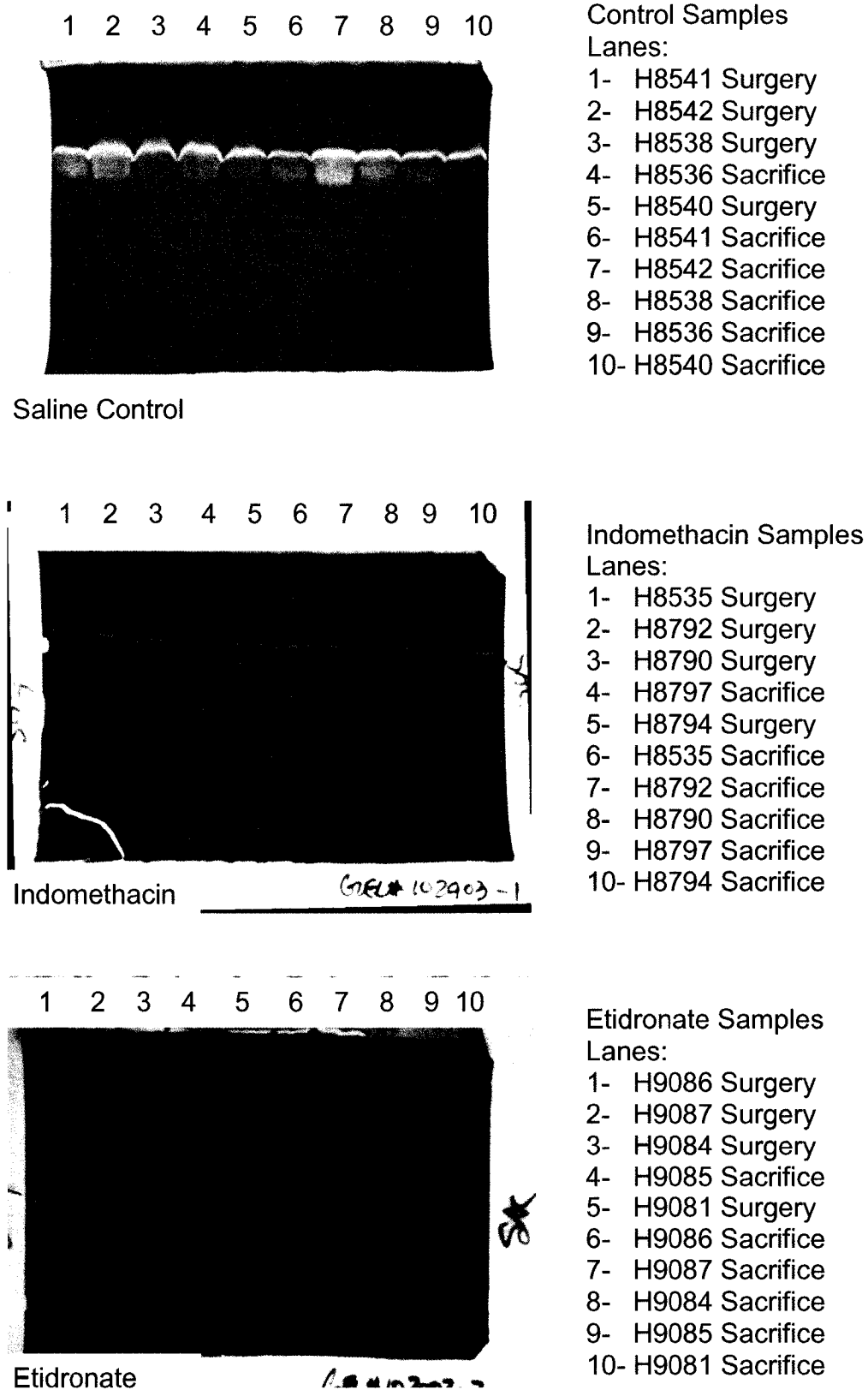


Table 9: Serum samples were collected and stored at  $-60^{\circ}\text{C}$  until all had been collected then the humoral response toward the graft material was quantified by the humoral ELISA. Each sample was analyzed in duplicate, with each plate containing an internal blank. All readings were averaged, adjusted for normal rabbit serum OD, and the reciprocal given.

Table 9: ELISA - Drug Treatment

Rabbit #	Titer @ Surgery	Titer @ Sacrifice
<b>Saline controls</b>		
8541	160	1280
8542	2560	320
8538	640	160
8536	320	2560
8540	80	2560
<b>Indomethacin treated</b>		
8535	20	320
8792	20	320
8790	40	320
8797	40	320
8794	80	320
<b>Etidronate treated</b>		
9086	20	80
9087	20	10240
9084	20	2560
9085*	20	2560
9081	20	2560

Figure 17: The log of the ELISA titers were plotted to graphically show the differences between the humoral response to the graft material at surgery and then at sacrifice. In all cases except 2 (saline H8542 and H8538), there was an increased humoral response to the graft between surgery and sacrifice. Statistically significant differences (paired two-tailed T test) were seen between the surgery and sacrifice samples for Indomethacin ( $P < 0.0001$ ) and Etidronate ( $P = 0.0054$ ). However no significant differences were seen between the control and drug-treated samples at sacrifice.

Figure 17: ELISA of Control, Indomethacin and Etidronate Samples

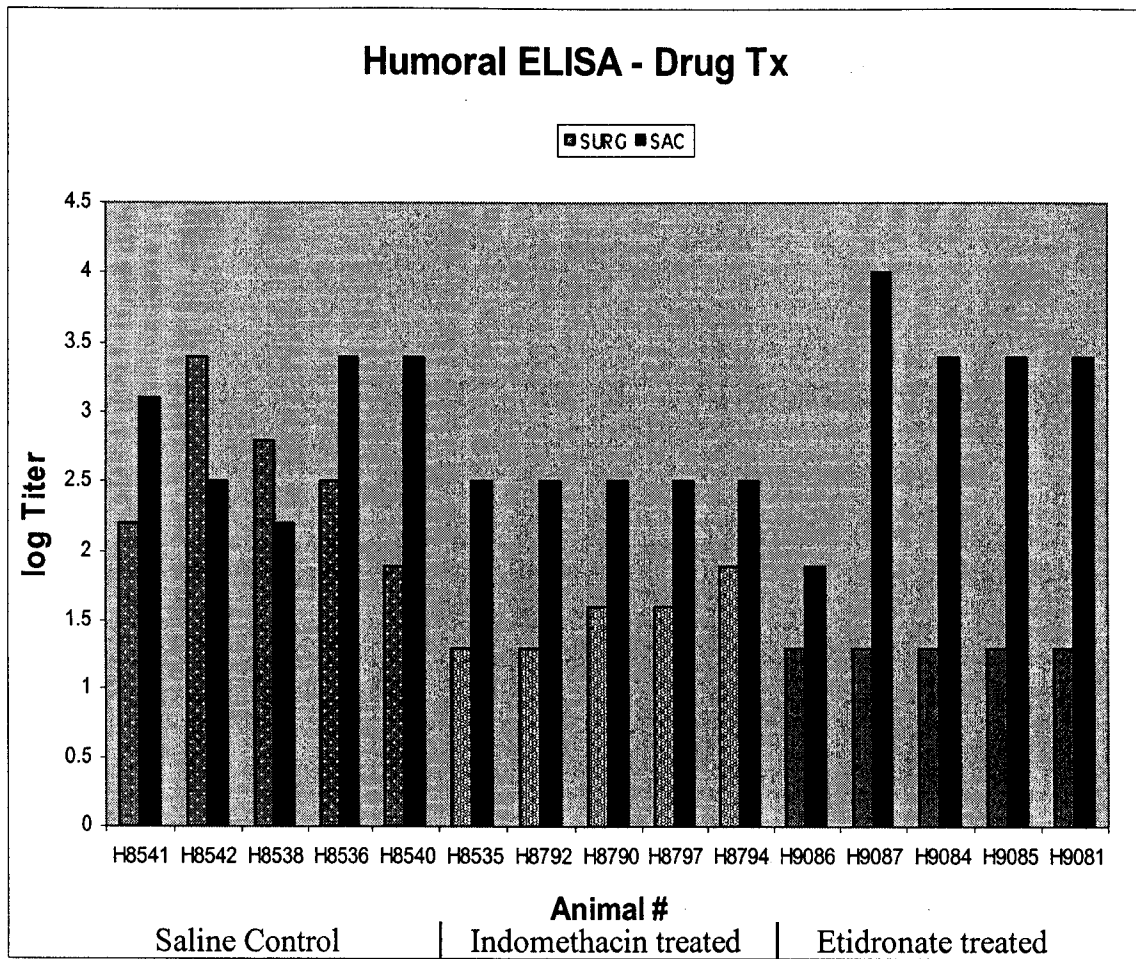




Table 10: Compiled Results of Saline, Indomethacin and Etidronate treated samples. The histology, immunohistology, macrophage counts, and ELISA information are summarized to provide an overview of the results.

Table 10: Compiled Results of Drug Treatment Samples

Animal #	Graft Cellularity	Actin	Collagen Remodel	Macrophage Presence	Tissue Destruction	Humoral Response
Saline control						
H8536	++++	++++	+++	+++	-	+++
H8538	+	-	+	+++	-	+
H8540	+	+	+	++	-	+++
H8541	+++	+++	++++	++	+	+++
H8542	-	-	+	+	-	++
Indomethacin treated						
H8535	-	-	-/+	+	-	++
H8790	-/+	-/+	-/+	+	-	++
H8792	-	-/+	+	+	-	++
H8794	-/+	+	+++	+	-	++
H8797	++	-	++	+	-	++
Etidronate treated						
H9081	+	++	++	++	-	+++
H9084	++	+	+	+	-	+++
H9085	-/+	-	+	+	-	+++
H9086	+	+	+	+	-	+/-
H9087	+++	+++	++	+	-	++++

Graft Cellularity -(0%) → ++++ (100%) re-colonization of graft material by host cells.

Actin -(0%) → ++++ (100%) recolonization of graft media by actin-positive cells.

Collagen Remodel -(0%) → ++++ (100%) newly produced collagen vs. mature.

Macrophage Presence -(few macrophages) → ++++ (40-50) avg. # macrophages.

Tissue Destruction -(0%) → ++++ (100%) destruction of original graft material.

Humoral Response -(0%) → ++++ (100%) of maximum response, rated relative to the highest response seen for all grafts.

## Discussion

### Reduce Inflammation: Effect of Anti-Inflammatory Drugs

Observations from the previous portion of the study suggest that these rabbits developed a chronic inflammatory-type response toward the graft material. A common finding in the previous chapter was the constant presence of macrophages and giant cells in the abluminal tissue, suggesting a chronic-type inflammatory reaction. This led to the use of this model of grafting to evaluate additional treatment strategies to enhance the durability of graft material *in vivo*. As macrophages are important players in inflammation and have been implicated in graft degeneration, the drugs chosen for this portion of the study had previously been shown in published studies to reduce macrophages in rabbit models of atherosclerosis, and it was speculated that they might also improve the durability of the grafts in this study.

Macroscopically, none of the grafts in the 3 groups showed any evidence of aneurysm or dilation which is in direct contrast to samples from chapter 2. In the previous chapter, little dilation was seen at 2 months and was increased at 4 months, while in this portion of the study two months may be insufficient for graft dilation to occur. In nearly every graft in this study, the graft matrix was either well-preserved or had undergone some remodeling, implying that little collagen degeneration had occurred compared to the 2, 4 and 6 month samples in which more collagen remodeling had occurred. This may be due to differences in the physiology of the animals between the two studies or differences in the graft material. Further studies to explore these differences could include longer studies incorporating these drugs to evaluate the drug effects on the development of dilation, as well as correlating changes in graft matrix

degeneration with dilation or aneurysm development by quantifying the collagen and elastin content of the graft.

### **Indomethacin**

Rabbits were treated with indomethacin prior to and after graft implantation and on explant at 2 months the grafts were found to be incorporated into the host. The grafts were covered with host-derived tissue with little evidence fibrosis. Microscopic analysis of the samples showed the graft material was minimally re-colonized by host-derived cells when compared to controls. The rabbits treated with Indomethacin showed a marked decrease in the number of macrophages present with the graft tissue compared to the saline controls with no incidence of graft degeneration.

Published studies suggest that the reduction in the number of macrophages could be due to the effect of Indomethacin on the arachidonic acid cascade activated during inflammation. Indomethacin inhibits the initial phospholipase cleavage of membrane phospholipids to arachidonic acid<sup>51</sup> reducing the response, and also acts further down the cascade by directly activating peroxisome proliferator-activated receptors (PPAR)  $\alpha$  and  $\gamma$  which are down-regulated by  $LTB_4$  and  $PGJ_2$  respectively during inflammation. This activation results in the apoptosis of activated (PPAR $\alpha$ ) and un-activated (PPAR $\alpha$  and  $\gamma$ ) macrophages<sup>52,53</sup>. The use of PPAR agonists would allow for this mechanism to be explored, allowing for the inhibition of macrophages without affecting the remainder of the inflammatory response, and evaluating the effect on graft durability.

## **Etidronate**

The grafts recovered at 2 months treated with Etidronate before and after surgery also were found to be incorporated into the host. The grafts were covered with host-derived tissue with little evidence fibrosis. Microscopic analysis of the samples showed the graft material was re-colonized by host-derived cells to a greater extent than Indomethacin treated samples. The rabbits treated with Etidronate also showed a marked decrease in the number of macrophages present with the graft tissue compared to the saline controls with no incidence of graft degeneration. Published studies suggest this reduction may be due to the induction of apoptosis in these cells by the drug<sup>39,40</sup>. This mechanism could be further explored by the use of statins in grafted animals, which should also reduce macrophages.

## **Zymography**

No reduction in circulating serum MMPs was seen within groups when Indomethacin or Etidronate treated samples from surgery and sacrifice were compared. This may be due to the methodology which may not be sensitive enough to detect the differences. Another possibility could be that since the graft is a small part of the vasculature and the MMPs secreted within the area of the graft are diluted in the blood stream the differences can not be detected. However, in-depth analysis of the graft samples for MMPs with more sensitive techniques such as immunohistology or western blotting could reveal differences not seen with zymography.

## **Humoral response**

No significant differences were seen in the humoral response between controls and drug treated samples at sacrifice. In all cases the response was increased suggesting the graft material elicits a response and this may be due to components of the xenogenic extracellular matrix (such as collagen) stimulating a response. Extracellular matrix components are known to elicit an immune response<sup>54-57</sup> and the macrophages and giant cells may be presenting graft antigens to T and B cells resulting in the immune response toward the graft material.

However what we are seeing is a snap-shot at a single time-point and does not indicate what the response has been previously or will be in the future. A better way to monitor the humoral response would be to collect multiple samples throughout the duration of the study and to follow the trend of the response. This would more accurately show what is happening over time.

## **Conclusions**

No aneurysm development was seen in any of the drug study samples (controls and treated) but 2 months may not be enough time to develop aneurysm under normocholesterolemic conditions. Both Indomethacin and Etidronate reduced the overall macrophage number present when compared to saline controls, but since macrophages, giant cells and T-cells are still present this suggests that there is still an ongoing response. No statistically significant difference was seen in the humoral response in any of the groups and the zymography data was inconclusive.

Taken together these data suggest that anti-inflammatory treatments affect the host response toward the graft material by reducing the presence of macrophages, but other mechanism could also be responsible. Also, this suggests that the use of adjunct anti-inflammatory treatments after bypass grafting could improve the long-term durability and survival of grafts in the clinical setting by reducing cells involved in graft failure. These data could also lead to further modifications of the original graft material during production, leading to a product with superior resistance to inflammatory degradation. However, care must be taken not to suppress the inflammatory response excessively, as this could lead to detrimental effects on the normal healing process.

## Appendix

Figure 18: This figure illustrates the effects of indomethacin on inflammation as well as the possible mechanisms by which inflammation, macrophages and MMPs are regulated.

Generated from references <sup>25,26,28,52,58-65</sup>



Figure 18: Indomethacin Effects on Inflammation

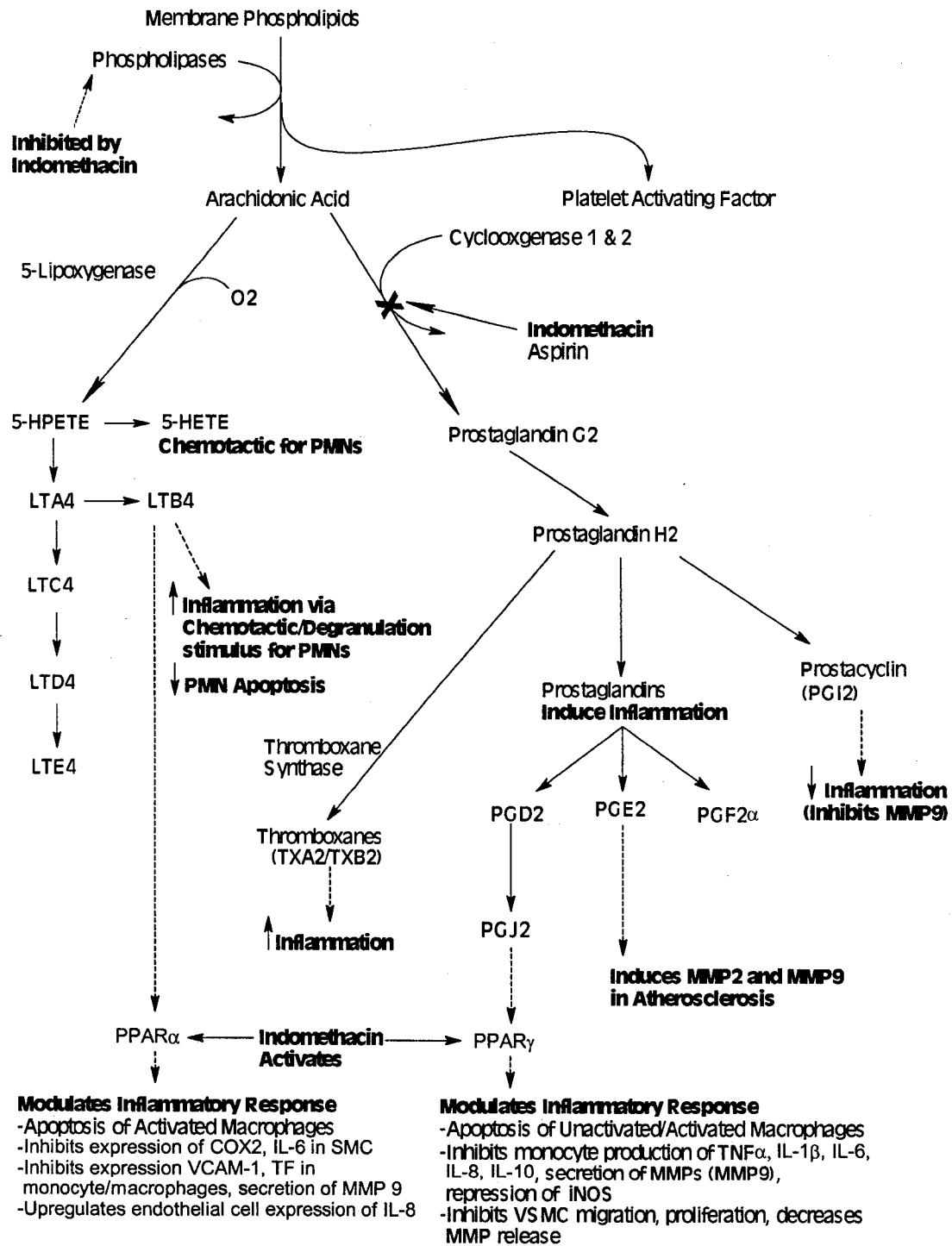


Figure 19: The effects of both bisphosphonate and amino-bisphosphonates on cell survival are illustrated. Amino-bisphosphonates act via inhibition of mevalonate pathway, while bisphosphonates (Etidronate is a member of this group) act on the MST kinases directly, both of which result in the induction of cellular apoptosis. Adapted from references <sup>36,66,67,68</sup>

Figure 19: Bisphosphonate Action

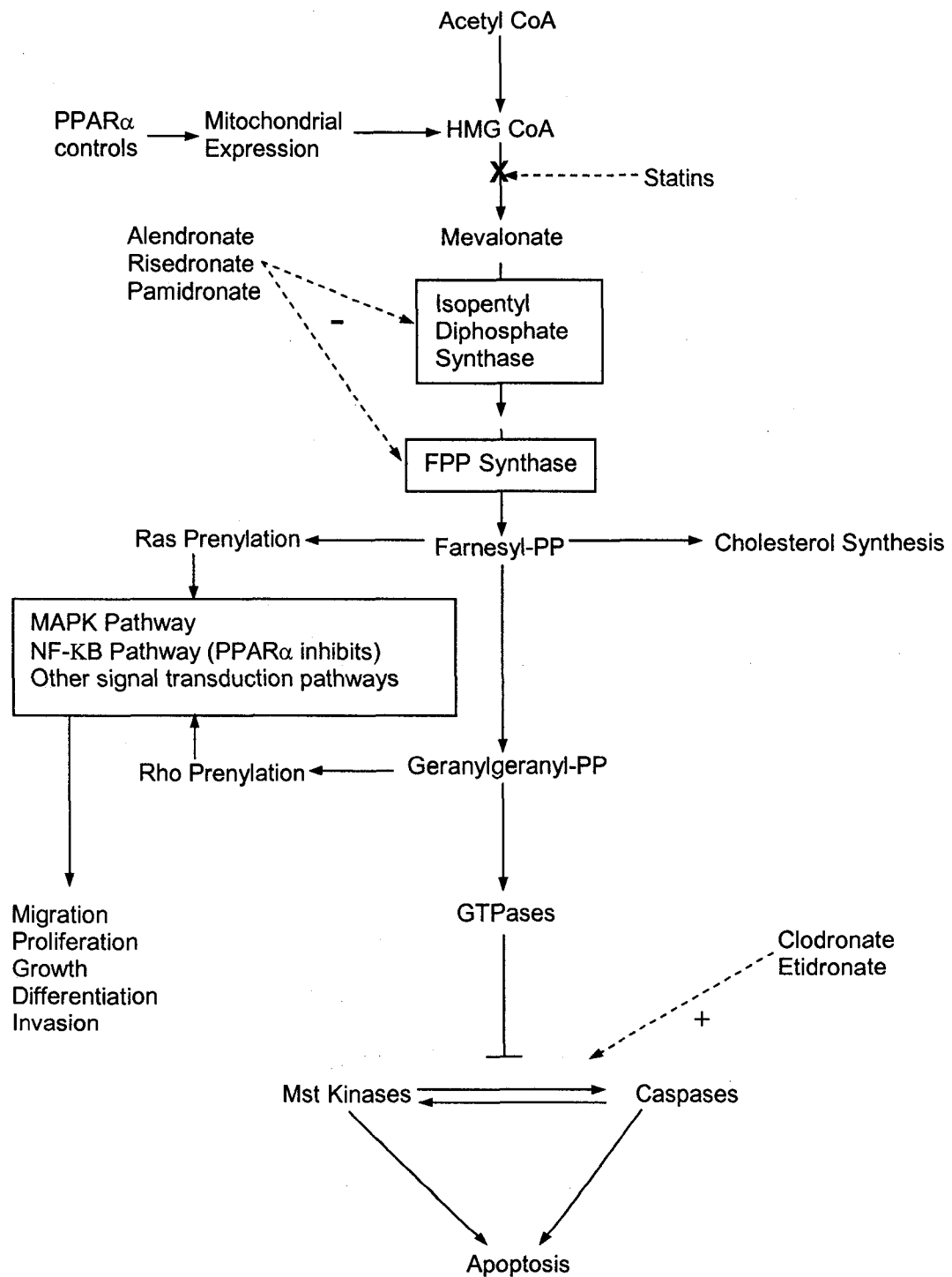


Table 11: Surgery and sacrifice data for all rabbits in this study are compiled in this table. The weights at surgery and sacrifice are listed, the operative weight was not significantly different between groups, while the weight at sacrifice was increased in the saline and indomethacin groups. The average graft length and cross-clamp time did not vary significantly between groups.

**Table 11: Surgery and Graft Data**

Rabbit #	Surgery Date	Weight @ Surgery	Graft Length	X-Clamp (min)	Graft #	Date Opened	Sacrifice Date	Weight @ Sacrifice
<i>Saline Treated</i>								
H8542	03/12/03	3.6kg	4.2cm	27.5	2B0110-03002	03/05/03	05/14/03	4.88kg
H8541	03/12/03	3.4	4	25	2B0110-03015	03/12/03	05/14/03	4.66
H8538	03/14/03	3.75	4	27	2B0110-03013	03/14/03	05/16/03	4.54
H8536	03/21/03	3.86	4	31.5	2B0110-03022	03/20/03	05/23/03	4.88
H8540	03/23/03	3.6	4	25	2B0110-03019	03/21/03	05/26/03	4.5
<b>Mean ± Std Dev</b>		<b>3.64±0.2</b>	<b>4.04±0.2</b>	<b>27.2±2.7</b>				<b>4.69±0.2</b>
<i>Indomethacin Treated</i>								
H8535	03/25/03	3.86kg	4.1	23.2	2B0110-03022	03/05/03	05/27/03	4.89kg
H8794	04/01/03	3.29	4	26.5	2B0110-03013	03/14/03	06/03/03	3.97
H8790	04/04/03	3.86	4	24.75	2B0110-03014	03/21/03	06/06/03	4.5
H8797	04/07/03	3.97	3.9	21.4	2B0110-03022	03/20/03	06/09/03	4.3
H8792	04/14/03	3.97	4	24	2B0110-03021	04/08/03	06/16/03	4.65
<b>Mean ± Std Dev</b>		<b>3.79±0.3</b>	<b>4±0.1</b>	<b>23.9±1.9</b>				<b>4.46±0.4</b>
<i>Etidronate Treated</i>								
H9085*	05/05/03	3.75kg	3.9	24	2B0110-03022	05/05/03	05/30/03	3.6kg
H9086	04/28/03	3.86	3.9	24.2	2B0110-03002	03/05/03	06/30/03	3.4
H9087	04/29/03	3.86	4	24	2B0110-03015	03/12/03	07/01/03	3.4
H9084	04/30/03	3.75	4	21	2B0110-03013	03/14/03	07/02/03	3.5
H9081	05/06/03	4.4	3.9	29	2B0110-03021	04/08/03	07/8/03	3.5
<b>Mean ± Std Dev</b>		<b>3.97±0.3</b>	<b>3.95±0.1</b>	<b>24.5±3.3</b>				<b>3.48±0.1</b>

\*Sacrificed at 25 days

Table 12: The sacrifice dates are listed for all rabbits, as is the duration of the graft implantation. All rabbits were sacrificed at 63 days except for H9085 which was sacrificed at 25 days.

Table 12: Sacrifice Dates

Rabbit #	Cause of Death	Duration
<b>Saline Control</b>		
H8542	Sacrificed	63 days
H8541	Sacrificed	63 days
H8538	Sacrificed	63 days
H8536	Sacrificed	63 days
H8540	Sacrificed	63 days
<b>indomethacin Treatment</b>		
H8535	Sacrificed	63 days
H8794	Sacrificed	63 days
H8790	Sacrificed	63 days
H8797	Sacrificed	63 days
H8792	Sacrificed	63 days
<b>Etidronate Treatment</b>		
H9085	Euthanized	25 days*
H9086	Sacrificed	63 days
H9087	Sacrificed	63 days
H9084	Sacrificed	63 days
H9081	Sacrificed	63 days

### Literature Cited

1. Newby AC, Zaltsman AB. Molecular mechanisms in intimal hyperplasia. *J Pathol.* 2000;190:300-9.
2. Schwartz RS, Henry TD. Pathophysiology of coronary artery restenosis. *Rev Cardiovasc Med.* 2002;3:S4-9.
3. Hoch JR, Stark VK, van Rooijen N, Kim JL, Nutt MP, Warner TF. Macrophage depletion alters vein graft intimal hyperplasia. *Surgery.* 1999;126:428-37.
4. Bojakowski K, Religa P, Bojakowska M, Hedin U, Gaciong Z, Thyberg J. Arteriosclerosis in rat aortic allografts: early changes in endothelial integrity and smooth muscle phenotype. *Transplantation.* 2000;70:65-72.
5. Faries PL, Marin ML, Veith FJ, Ramirez JA, Suggs WD, Parsons RE, Sanchez LA, Lyon RT. Immunolocalization and temporal distribution of cytokine expression during the development of vein graft intimal hyperplasia in an experimental model. *J Vasc Surg.* 1996;24:463-71.
6. Watanabe T, Haraoka S, Shimokama T. Inflammatory and immunological nature of atherosclerosis. *Int J Cardiol.* 1996;54 Suppl:S51-60.
7. Blum A, Miller HI. The role of inflammation in atherosclerosis. *Isr J Med Sci.* 1996;32:1059-65.
8. Libby P, Ridker PM, Maseri A. Inflammation and atherosclerosis. *Circulation.* 2002;105:1135-43.
9. Freestone T, Turner RJ, Coady A, Higman DJ, Greenhalgh RM, Powell JT. Inflammation and matrix metalloproteinases in the enlarging abdominal aortic aneurysm. *Arterioscler Thromb Vasc Biol.* 1995;15:1145-51.



10. Freestone T, Turner RJ, Higman DJ, Lever MJ, Powell JT. Influence of hypercholesterolemia and adventitial inflammation on the development of aortic aneurysm in rabbits. *Arterioscler Thromb Vasc Biol.* 1997;17:10-7.
11. Wassef M, Baxter BT, Chisholm RL, Dalman RL, Fillinger MF, Heinecke J, Humphrey JD, Kuivaniemi H, Parks WC, Pearce WH, Platsoucas CD, Sukhova GK, Thompson RW, Tilson MD, Zarins CK. Pathogenesis of abdominal aortic aneurysms: a multidisciplinary research program supported by the National Heart, Lung, and Blood Institute. *J Vasc Surg.* 2001;34:730-8.
12. Campbell JH, Campbell GR. The macrophage as an initiator of atherosclerosis. *Clin Exp Pharmacol Physiol.* 1991;18:81-4.
13. Babaev VR, Bobryshev YV, Sukhova GK, Kasantseva IA. Monocyte/macrophage accumulation and smooth muscle cell phenotypes in early atherosclerotic lesions of human aorta. *Atherosclerosis.* 1993;100:237-48.
14. Libby P, Geng YJ, Aikawa M, Schoenbeck U, Mach F, Clinton SK, Sukhova GK, Lee RT. Macrophages and atherosclerotic plaque stability. *Curr Opin Lipidol.* 1996;7:330-5.
15. Galis ZS, Sukhova GK, Kranzhofer R, Clark S, Libby P. Macrophage foam cells from experimental atheroma constitutively produce matrix-degrading proteinases. *Proc Natl Acad Sci U S A.* 1995;92:402-6.
16. Petrinc D, Liao S, Holmes DR, Reilly JM, Parks WC, Thompson RW. Doxycycline inhibition of aneurysmal degeneration in an elastase- induced rat model of abdominal aortic aneurysm: preservation of aortic elastin associated with suppressed production of 92 kD gelatinase. *J Vasc Surg.* 1996;23:336-46.

17. Thompson RW, Parks WC. Role of matrix metalloproteinases in abdominal aortic aneurysms. *Ann N Y Acad Sci.* 1996;800:157-74.
18. Wesley RB, 2nd, Meng X, Godin D, Galis ZS. Extracellular matrix modulates macrophage functions characteristic to atheroma: collagen type I enhances acquisition of resident macrophage traits by human peripheral blood monocytes in vitro. *Arterioscler Thromb Vasc Biol.* 1998;18:432-40.
19. Dannhardt G, Kiefer W. Cyclooxygenase inhibitors--current status and future prospects. *Eur J Med Chem.* 2001;36:109-26.
20. Warner TD, Mitchell JA. Cyclooxygenase-3 (COX-3): Filling in the gaps toward a COX continuum? *Proc Natl Acad Sci U S A.* 2002;99:13371-3.
21. Mitchell JA, Akarasereenont P, Thiemermann C, Flower RJ, Vane JR. Selectivity of nonsteroidal antiinflammatory drugs as inhibitors of constitutive and inducible cyclooxygenase. *Proc Natl Acad Sci U S A.* 1993;90:11693-7.
22. Green GA. Understanding NSAIDs: From Aspirin to COX-2. *Clin Cornerstone.* 2001;3:50-59.
23. Botting RM. Mechanism of Action of Acetaminophen: Is There a Cyclooxygenase 3? *Clin Infect Dis.* 2000;31 Suppl 5:S202-10.
24. Jouve R, Juhan-Vague I, Aillaud M, Serment-Jouve M, Payan H. Comparison of the effects of aspirin and indomethacin on aortic atherogenesis induced in rabbits. *Atherosclerosis.* 1982;42:319-21.
25. Stoller DK, Grorud CB, Michalek V, Buchwald H. Reduction of atherosclerosis with nonsteroidal anti-inflammatory drugs. *J Surg Res.* 1993;54:7-11.

26. Miralles M, Wester W, Sicard GA, Thompson R, Reilly JM. Indomethacin inhibits expansion of experimental aortic aneurysms via inhibition of the cox2 isoform of cyclooxygenase. *J Vasc Surg.* 1999;29:884-92; discussion 892-3.
27. Holmes DR, Petrincec D, Wester W, Thompson RW, Reilly JM. Indomethacin prevents elastase-induced abdominal aortic aneurysms in the rat. *J Surg Res.* 1996;63:305-9.
28. Belton O, Fitzgerald DJ. Cyclooxygenase isoforms and atherosclerosis. *Expert Reviews in Molecular Medicine.* 2003;5:1-18.
29. Martin TJ, Grill V. Bisphosphonates-Mechanisms of Action. *Australian Prescriber.* 2000;23:130-132.
30. Compston JE. The therapeutic use of bisphosphonates. *Bmj.* 1994;309:711-5.
31. Ylitalo R, Monkkonen J, Urtti A, Ylitalo P. Accumulation of bisphosphonates in the aorta and some other tissues of healthy and atherosclerotic rabbits. *J Lab Clin Med.* 1996;127:200-6.
32. Frith JC, Monkkonen J, Blackburn GM, Russell RG, Rogers MJ. Clodronate and liposome-encapsulated clodronate are metabolized to a toxic ATP analog, adenosine 5'-(beta, gamma-dichloromethylene) triphosphate, by mammalian cells in vitro. *J Bone Miner Res.* 1997;12:1358-67.
33. Fleisch H. Bisphosphonates: mechanisms of action. *Endocr Rev.* 1998;19:80-100.
34. Van Rooijen N, Sanders A. Liposome mediated depletion of macrophages: mechanism of action, preparation of liposomes and applications. *J Immunol Methods.* 1994;174:83-93.

35. Maksymowych WP. Bisphosphonates - Anti-Inflammatory Properties. In:  
<http://www.bentham.org/sample-issues/cmcaiaa1-1/maksymowych/maksymowych-ms.htm>.
36. Reszka AA, Halasy-Nagy JM, Masarachia PJ, Rodan GA. Bisphosphonates act directly on the osteoclast to induce caspase cleavage of mst1 kinase during apoptosis. A link between inhibition of the mevalonate pathway and regulation of an apoptosis-promoting kinase. *J Biol Chem.* 1999;274:34967-73.
37. Fisher JE, Rodan GA, Reszka AA. In vivo effects of bisphosphonates on the osteoclast mevalonate pathway. *Endocrinology.* 2000;141:4793-6.
38. Pennanen N, Lapinjoki S, Urtti A, Monkkonen J. Effect of liposomal and free bisphosphonates on the IL-1 beta, IL-6 and TNF alpha secretion from RAW 264 cells in vitro. *Pharm Res.* 1995;12:916-22.
39. Ylitalo R, Monkkonen J, Yla-Herttuala S. Effects of liposome-encapsulated bisphosphonates on acetylated LDL metabolism, lipid accumulation and viability of phagocytosing cells. *Life Sci.* 1998;62:413-22.
40. Monkkonen J, Taskinen M, Auriola SO, Urtti A. Growth inhibition of macrophage-like and other cell types by liposome- encapsulated, calcium-bound, and free bisphosphonates in vitro. *J Drug Target.* 1994;2:299-308.
41. Monkkonen J, Heath TD. The effects of liposome-encapsulated and free clodronate on the growth of macrophage-like cells in vitro: the role of calcium and iron. *Calcif Tissue Int.* 1993;53:139-46.

42. Ylitalo R, Oksala O, Yla-Herttuala S, Ylitalo P. Effects of clodronate (dichloromethylene bisphosphonate) on the development of experimental atherosclerosis in rabbits. *J Lab Clin Med.* 1994;123:769-76.
43. Rosenblum IY, Flora L, Eisenstein R. The effect of disodium ethane-1-hydroxy-1,1-diphosphonate (EHDP) on a rabbit model of athero-arteriosclerosis. *Atherosclerosis.* 1975;22:411-24.
44. Zhu BQ, Sun YP, Sievers RE, Isenberg WM, Moorehead TJ, Parmley WW. Effects of etidronate and lovastatin on the regression of atherosclerosis in cholesterol-fed rabbits. *Cardiology.* 1994;85:370-7.
45. DiCesare PE, Nimni ME, Peng L, Yazdi M, Cheung DT. Effects of indomethacin on demineralized bone-induced heterotopic ossification in the rat. *J Orthop Res.* 1991;9:855-61.
46. Yazdi M, Cheung DT, Cobble S, Nimni ME, Schonfeld SE. Effects of non-steroidal anti-inflammatory drugs on demineralized bone-induced bone formation. *J Periodontal Res.* 1992;27:28-33.
47. Kreitmann B, Riberi A, Zeranska M, Novakovitch G, Metras D. Growth potential of aortic autografts and allografts: effects of cryopreservation and immunosuppression in an experimental model. *Eur J Cardiothorac Surg.* 1997;11:943-52.
48. Kazama S, Miyoshi Y, Nie M, Imai H, Lin ZB, Kurata A, Machii M. Protection of the Spinal Cord with Pentobarbital and Hypothermia. *Ann Thorac Surg.* 2001;71:1591-5.

49. Zaltsman AB, Newby AC. Increased secretion of gelatinases A and B from the aortas of cholesterol fed rabbits: relationship to lesion severity. *Atherosclerosis*. 1997;130:61-70.
50. Senior RM, Griffin GL, Fliszar CJ, Shapiro SD, Goldberg GI, Welgus HG. Human 92- and 72-kilodalton type IV collagenases are elastases. *J Biol Chem*. 1991;266:7870-5.
51. Clancy R, Varenika B, Huang W, Ballou L, Attur M, Amin AR, Abramson SB. Nitric oxide synthase/COX cross-talk: nitric oxide activates COX-1 but inhibits COX-2-derived prostaglandin production. *J Immunol*. 2000;165:1582-7.
52. Chinetti G, Griglio S, Antonucci M, Torra IP, Delerive P, Majd Z, Fruchart JC, Chapman J, Najib J, Staels B. Activation of proliferator-activated receptors alpha and gamma induces apoptosis of human monocyte-derived macrophages. *J Biol Chem*. 1998;273:25573-80.
53. Delerive P, Fruchart JC, Staels B. Peroxisome proliferator-activated receptors in inflammation control. *J Endocrinol*. 2001;169:453-9.
54. Human P, Zilla P. Inflammatory and immune processes: the neglected villain of bioprosthetic degeneration? *J Long Term Eff Med Implants*. 2001;11:199-220.
55. Courtman DW, Errett BF, Wilson GJ. The role of crosslinking in modification of the immune response elicited against xenogenic vascular acellular matrices. *J Biomed Mater Res*. 2001;55:576-86.
56. Allaire E, Guettier C, Bruneval P, Plissonnier D, Michel JB. Cell-free arterial grafts: morphologic characteristics of aortic isografts, allografts, and xenografts in rats. *J Vasc Surg*. 1994;19:446-56.

57. Allaire E, Bruneval P, Mandet C, Becquemin JP, Michel JB. The immunogenicity of the extracellular matrix in arterial xenografts. *Surgery*. 1997;122:73-81.
58. Lehmann JM, Lenhard JM, Oliver BB, Ringold GM, Kliewer SA. Peroxisome Proliferator-activated Receptors alpha and gamma Are Activated by Indomethacin and Other Non-steroidal Anti-inflammatory Drugs. *J. Biol. Chem*. 1997;272:3406-3410.
59. Cotran RS, Kumar V, Robbins SL. Inflammation and Repair. In: *Robbins Pathologic Basis of Disease, 5th Edition*. 5th ed. Philadelphia, PA: W.B. Saunders Company; 1994:51-92.
60. Jaradat MS, Wongsud B, Phornchirasilp S, Rangwala SM, Shams G, Sutton M, Romstedt KJ, Noonan DJ, Feller DR. Activation of peroxisome proliferator-activated receptor isoforms and inhibition of prostaglandin H(2) synthases by ibuprofen, naproxen, and indomethacin. *Biochem Pharmacol*. 2001;62:1587-95.
61. Hebert MJ, Takano T, Holthofer H, Brady HR. Sequential morphologic events during apoptosis of human neutrophils. Modulation by lipoxygenase-derived eicosanoids. *J Immunol*. 1996;157:3105-15.
62. Marx N. PPARgamma and vascular inflammation: adding another piece to the puzzle. *Circ Res*. 2002;91:373-4.
63. Lucas AD, Greaves DR. Atherosclerosis: role of chemokines and macrophages. *Expert Reviews in Molecular Medicine*. 2001;5 November:1-18.
64. Shu H, Wong B, Zhou G, Li Y, Berger J, Woods JW, Wright SD, Cai TQ. Activation of PPARalpha or gamma reduces secretion of matrix metalloproteinase

- 9 but not interleukin 8 from human monocytic THP-1 cells. *Biochem Biophys Res Commun.* 2000;267:345-9.
65. Delerive P, De Bosscher K, Besnard S, Vanden Berghe W, Peters JM, Gonzalez FJ, Fruchart JC, Tedgui A, Haegeman G, Staels B. Peroxisome proliferator-activated receptor alpha negatively regulates the vascular inflammatory gene response by negative cross-talk with transcription factors NF-kappaB and AP-1. *J Biol Chem.* 1999;274:32048-54.
66. Porter KE, Turner NA. Statins for the prevention of vein graft stenosis: a role for inhibition of matrix metalloproteinase-9. *Biochem Soc Trans.* 2002;30:120-6.
67. Gueddari-Pouzols N, Duriez P, Chomienne C, Trussardi A, Jardillier JC. Interaction Between Mevalonate Pathway and Retinoic Acid-Induced Differentiation. *J Biomed Biotechnol.* 2001;1:108-113.
68. Barbier O, Torra IP, Duguay Y, Blanquart C, Fruchart JC, Glineur C, Staels B. Pleiotropic actions of peroxisome proliferator-activated receptors in lipid metabolism and atherosclerosis. *Arterioscler Thromb Vasc Biol.* 2002;22:717-26.